



City Research Online

City, University of London Institutional Repository

Citation: Duncanson, P. (1991). Synthesis of novel dyes and a study of the photochemistry N-formylated aromatic amines and indoles. (Unpublished Doctoral thesis, City, University of London)

This is the accepted version of the paper.

This version of the publication may differ from the final published version.

Permanent repository link: <https://openaccess.city.ac.uk/id/eprint/28498/>

Link to published version:

Copyright: City Research Online aims to make research outputs of City, University of London available to a wider audience. Copyright and Moral Rights remain with the author(s) and/or copyright holders. URLs from City Research Online may be freely distributed and linked to.

Reuse: Copies of full items can be used for personal research or study, educational, or not-for-profit purposes without prior permission or charge. Provided that the authors, title and full bibliographic details are credited, a hyperlink and/or URL is given for the original metadata page and the content is not changed in any way.

City Research Online:

<http://openaccess.city.ac.uk/>

publications@city.ac.uk

SYNTHESIS OF NOVEL DYES AND A STUDY OF THE PHOTOCHEMISTRY

N-FORMYLATED AROMATIC AMINES AND INDOLES

by

PHILIP DUNCANSON

A thesis submitted for the Degree of
DOCTOR OF PHILOSOPHY
in the Chemistry Department of the
City University, London.

May, 1991.

STATEMENT

The experimental work in this thesis has been carried out by the author in the Department of Chemistry at the City University, London and in the laboratories of the International Wool Secretariat, Technical Centre, Ilkley, between November 1986 and August 1989. The work has not been presented and is not being presented for any other degree.

I grant powers of discretion to the University Librarian to allow this thesis to be copied in whole or in part without further reference to me. This permission covers only single copies made for study purposes, subject to normal conditions of acknowledgement.

P. Duncanson

P. DUNCANSON

May, 1991

Dedicated
to
my parents

ACKNOWLEDGEMENTS

I would like to express my appreciation to the following :-

Professor R.S Davidson and P. Duffield for their invaluable guidance and encouragement.

The International Wool Foundation for financial assistance.

The past and present members of the Photochemistry Group at the City University who have made my time there so enjoyable. It is not possible to name everyone but special mention must go to G.Yearwood, Dr. P.Moran, D.Chappell, Miss E.Cockburn, T.Gilby, Dr. M.Walker R.Bowser, N.Khan, A.Taylor, Miss A.O'Donnell, G.Abrahams and S.Collins

Mr A. Murphy for the prompt elemental analysis results and the 'advice' when experiments did not go according to plan.

Mr A. Bell who has answered my many simple questions on the use of a Word Processer with great forbearance and patience.

Last but not least my wife, Linda, without whose support, encouragement, good humour and extreme patience the writing of this thesis would not have been possible.

ABSTRACT

The basic concepts of Photochemistry and the phenomena of colour are outlined.

The chemical nature of wool is briefly described and a review of its photochemistry presented. For convenience the photochemical reactions are separated into two main categories which are free radical reactions and processes leading to the photoyellowing of wool. The photochemistry of Fluorescent Brightening Agents (FBA's) is discussed with reference to oxidative and reductive reactions. Processes leading to the prevention of wool photoyellowing are outlined.

A reactive FBA has been synthesised and coupled with various polyamines. These adducts were found to be a complex mixture when analysed by HPLC. Nevertheless they were applied to wool by a standard exhaustion method and crosslinked with formaldehyde and a thiourea/formaldehyde (TUF) precondensate. These adducts were not as fluorescent as a commercial FWA due to the presence of the amine groups. Extraction experiments showed that more FBA was bound to the wool after crosslinking with formaldehyde and TUF than uncrosslinked FBA. Use of high thiourea concentrations in the TUF treatment gave the wool good lightfastness even though the fluorophore was destroyed.

A reactive azo dye was synthesised and reacted with diethylenetriamine. This adduct was applied to wool at 60 C and 100 C and crosslinked with formaldehyde, TUF and phosphorous reducing agents. When applied and crosslinked at the lower temperature of 60 C the dye was almost completely extracted with organic solvents. However, when the dye was applied and crosslinked at 100 C only 50% was removed by extraction with the same organic solvents. In the presence of reducing agents the dye photodegradation was accelerated.

N-Formylkynurenine and several N-formylated indoles and aromatic amines were synthesised and their photochemistry studied. Simple N-formyl indoles and amines were readily decarbonylated at 254 and 300 nm irradiation. Compounds with a ketone carbonyl conjugated to the chromophore underwent decarbonylation when irradiated at 254 nm but only degraded to give unidentified products on 300 nm irradiation. Oxygen and water did not affect the reaction rate which followed first order kinetics. A reaction mechanism which fits the experimental observations is proposed.

The use of azlactones as coloured compounds has been investigated. Thus three different classes have been synthesised with respect to the aromatic substituents. The classes are donor - acceptor, polycyclic and

organometallic azlactones. Their spectroscopic properties have been studied and the transitions leading to the long wavelength Uv / Vis absorption assigned. It is possible to explain why some azlactones are fluorescent and others are not. Reaction with nucleophiles such as amines, thiols and water leading to ring opened products and other heterocycles are described. The changes in photophysical properties are discussed and compared to the parent compounds. A fluorescent azlactone containing an isothiocyanate reactive group was found to be unsuitable to label proteins because of undesired side reactions. A series of heterocycles was used to dye polyester. The solid state fluorescence spectra were compared to the solution spectra. The light fastness of the dyes were discussed with reference to their structures.

CONTENTS

Page Number

CHAPTER 1 - INTRODUCTION TO PHOTOCHEMISTRY

1.1	Preface	2
1.2	Electronic Structure of Molecules	2
1.3	Absorption of Radiation	5
	1.3.1 The Beer-Lambert Law	5
	1.3.2 Molecular Absorption	5
	1.3.3 Types of Transition	6
	1.3.4 Effect of Conjugation on Absorption Wavelength	10
	1.3.5 Solvents Effects on Absorption Maxima	10
	1.3.6 Identification of (π, π^*) and (n, π^*) States	12
	1.3.7 Spin Multiplicity	13
1.4	Excited States and their Deactivation	14
	1.4.1 The Excited State	14
	1.4.2 Non-Radiative Deactivation Pathways	16
	1.4.3 Radiative Emissions	17
1.5	Quenching of Excited States	21
	1.5.1 Kinetics of Quenching	21
	1.5.2 Electron Transfer Quenching	22
	1.5.3 Concentration Quenching	23
	1.5.4 Heavy Atom Quenching	24
	1.5.5 Quenching by Energy Transfer	24
	1.5.6 Photosensitised Processes	28
1.6	The Phenomena of Colour	28
	1.6.1 Additive Colour Mixing	29
	1.6.2 Subtractive Colour Mixing	30
1.7	References	31

CHAPTER 2 - PHOTOCHEMISTRY OF WOOL PROTEIN AND FLUORESCENT BRIGHTENING AGENTS

2.1	Chemical Structure of Wool	34
2.2	Photochemistry of Wool Protein	36
	2.2.1 Ultraviolet Absorption	36
	2.2.2 Luminescence of Wool	38
	2.2.3 Photochemical Reactions	40
	2.2.3.1 Radical Reactions	40
	2.2.3.2 Photoyellowing of Wool	43
2.3	Photochemistry of Fluorescent Brightening Agents (FBA's)	50
2.4	Protection of Wool Against Photoyellowing	54
	2.4.1 Ultraviolet Absorbers	54
	2.4.2 Antioxidants and Reducing Agents	56
2.5	References	57

**CHAPTER 3 - SYNTHESIS AND APPLICATION TO WOOL OF
A FLUORESCENT BRIGHTENING AGENT AND AN
AZO DYE CONTAINING POLYAMINE SIDECHAINS**

3.1	Introduction	63
3.2	Results	68
	3.2.1 Synthesis of the FBA's	68
	3.2.2 Application of the FBA's to Wool	72
	3.2.3 Synthesis of the Polyamine-Azo Dye	76
	3.2.4 Application of the Polyamine-Dye to Wool	78
3.3	Discussion	83
	3.3.1 Synthesis and HPLC Analysis of the FBA's	83
	3.3.2 Application of the FBA -Polyamine to Wool	87
	3.3.3 Synthesis and Application of the Azo Polyamine-Dye	92
3.4	Conclusion	96
3.5	Experimental	97
	3.5.1 Synthesis of the Stilbene-FBA's	98
	3.5.2 HPLC Conditions	102
	3.5.3 Application of FBA's to Wool	103
	3.5.4 Synthesis of Azo-Polyamine Dye	107
	3.5.5 Application of Dye-Polyamine to Wool	110
3,6	References	115

**CHAPTER 4 - SYNTHESIS AND PHOTODECARBONYLATION OF
N-FORMYLATED AROMATIC AMINES AND INDOLES**

4.1	Introduction	119
4.2	Results	122
4.3	Discussion	130
4.4	Conclusion	132
4.5	Experimental	133
	4.5.1 Synthesis of N-formylated Compounds	133
	4.5.2 Photolysis Experiments	140
	4.5.3 Chromatographic Conditions	141
	4.5.4 Kinetic Studies	143
4.6	References	145

**CHAPTER 5 - SYNTHESIS, REACTIONS AND PHOTOPHYSICAL
STUDIES OF AZLACTONES**

5.1	Introduction	148
5.2	Results	150
5.2.1	Aroylglycine and Aldehyde Synthesis	150
5.2.2	Azlactone Synthesis and Structure	153
5.2.3	Azlactone Spectral Properties	156
5.2.4	Reactions of Azlactones	164
5.2.4.1	Hydrolysis	164
5.2.4.2	Reaction With Nucleophiles	167
5.2.5	Application of Azlactones	173
5.2.5.1	Protein Labelling	173
5.2.5.2	Dyes for Polyester	175
5.3	Discussion	179
5.3.1	Azlactone Synthesis and Structure	179
5.3.2	Reaction With Nucleophiles	189
5.3.3	Application of Azlactones	193
5.3.3.1	Labelling Proteins With Azlactones	193
5.3.3.2	Dying Polyester with Azlactones and Related Compounds	195
5.4	Conclusion	196
5.5	Experimental	199
5.5.1	Synthesis of Starting Compounds	200
5.5.2	Azlactone Synthesis	206
5.5.3	Donor-Acceptor Azlactones	207
5.5.4	Fused Ring Azlactones	212
5.5.5	Heterocyclic Organometallic Azlactones	218
5.5.6	Hydrolysis of Azlactones	221
5.5.7	Reaction of Azlactones With Nucleophiles	224
5.5.8	Conversion of Azlactones to Imidazolin-5-ones	226
5.6	References	233

CHAPTER 1

INTRODUCTION TO PHOTOCHEMISTRY

1. Preface

We see it here, we see it there, we see it everywhere, yet who takes any notice of the plethora of colours that surrounds us in our daily activities. There is hardly one aspect of our lives which remains untouched by colour. From photosynthesis to watching Thunderbirds on TV we are dependent on light and colour. Light can initiate a wide variety of photophysical and photochemical phenomena for the chemist to study. A vast number of investigations have been carried out with a view to understanding the action of light on matter. There are many textbooks which provide excellent reviews on photochemistry ^{1,2,3,4} and this chapter will give only a basic introduction to photochemistry and the phenomenon of colour.

1.2 Electronic Structure of Molecules

Molecular orbitals (MO's) probably afford the clearest understanding of the electronic structure of molecules and of the changes in electronic structure brought about by the absorption of light ^{5,6}. Molecular orbitals are formed by a combination of atomic orbitals (AO's), the most common being a linear combination of atomic orbitals (LCAO). A given number of atomic orbitals always gives rise to the same number of molecular orbitals. For example, the interaction of two identical atomic orbitals

ϕ_A and ϕ_B gives rise to two molecular orbitals given in equation 1.

$$\Psi_1 = \phi_A + \phi_B \quad \text{eq 1}$$

$$\Psi_2 = \phi_A - \phi_B$$

One molecular orbital is bonding (ie. more stable and lower in energy than the initial AO) and the other is antibonding (of higher energy than the initial AO). The situation is represented in Figure 1.1

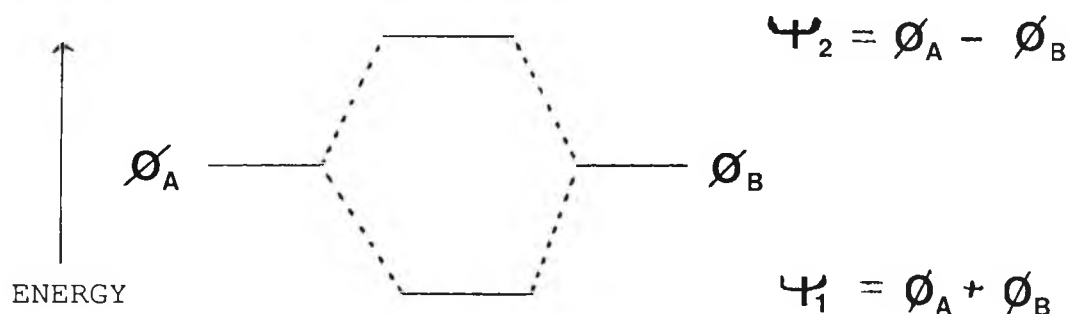


Figure 1.1 Interaction of two identical atomic nuclei.

Those orbitals which are completely symmetrical about the internuclear axis are designated sigma σ (bonding) and σ^*

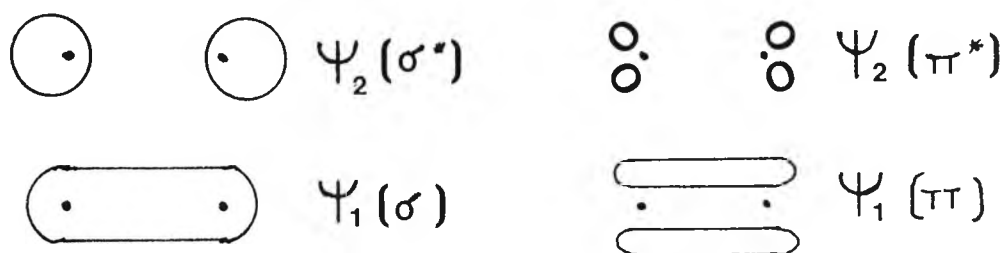


Figure 1.2 Representation of two interacting identical AO's to give end on and parallel overlap.

(sigma-star, antibonding). Molecular orbitals derived by mixing two parallel p-orbitals are called π (pi) and π^* (pi-star). Both possibilities are given in Figure 1.2. Molecular orbitals can encompass more than two atomic centres and this leads to delocalisation. A common example is 1,3-butadiene shown in Figure 1.3.

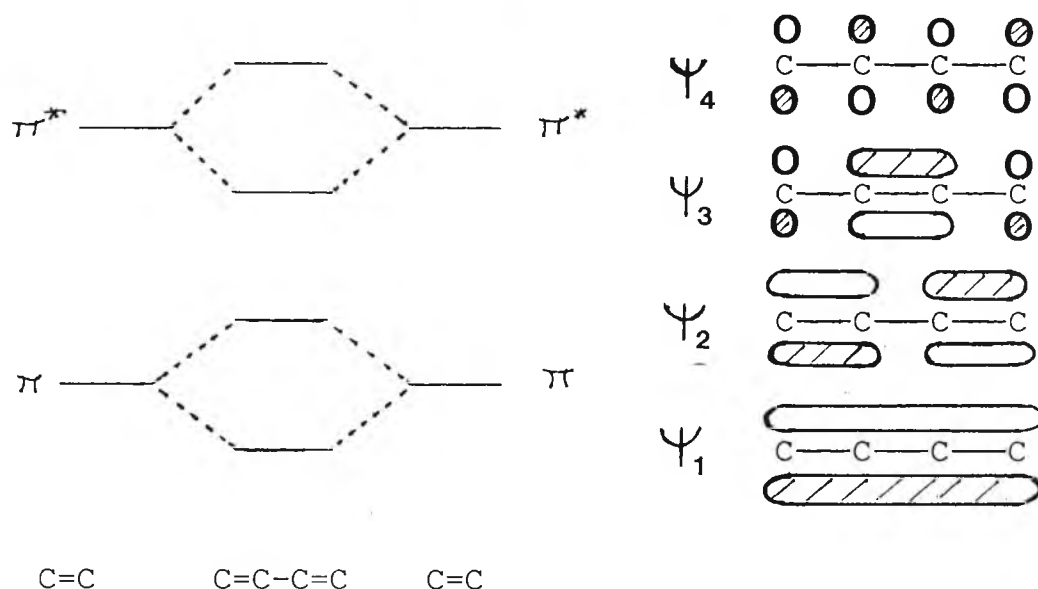


Figure 1.3 π - molecular orbitals and energies for 1,3-butadiene.

Two electrons are assigned to each MO such that their spins are paired and, in general, a molecule in its ground state (GS) has all its electrons spin paired.

In certain compounds, notably those containing elements of Group V, VI and VII there are non bonding valence shell electrons (designated n) which are not involved in bonding and can be regarded as being localised on their atomic nuclei. The energy of such electrons is much the

same as that of electrons occupying the corresponding atomic orbitals on the isolated atom.

1.3 Absorption of Radiation

1.3.1 The Beer-Lambert Law

The bulk absorption characteristics of a solution can be represented by the following equation -

$$\text{Log } \frac{I_0}{I} = A = Ecl$$

I_0 - is the intensity of the monochromatic radiation.

I - is the intensity of transmitted radiation.

c - concentration (in units of mol / L)

l - path length (in units of cm)

A - absorbance

E - molar extinction coefficient (in units of L / mol cm) and is a measure of the absorption intensity for a single wavelength.

The equation is not valid when concentrations of the solute are greater than 0.01 mol / l and very high intensity radiation ie laser light is employed.

1.3.2 Molecular Absorption

When a photon passes close to a molecule there is an interaction between the electric field associated with the molecule and that associated with the radiation. If the photon is absorbed by the molecule it ceases to exist and its energy is transferred to the molecule whose electronic structure changes. In simple terms an electron is promoted from one molecular orbital to another of higher energy.

1.3.3 Types of Transitions

The types of electronic transition usually between the orbitals described above are given in Figure 1.4.

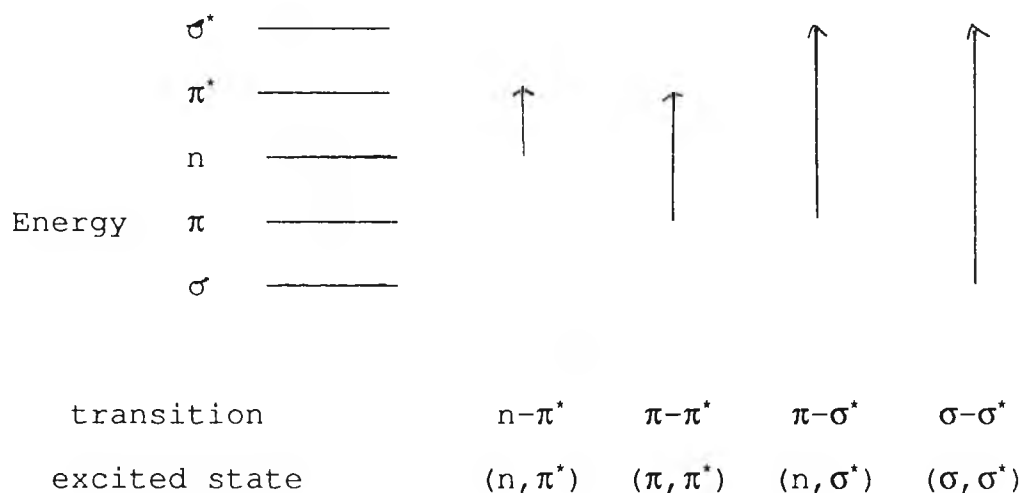


Figure 1.4 Electronic molecular energy levels and the electron transitions between these levels that are found in organic compounds.

$\sigma-\sigma^*$ Here an electron in a bonding σ orbital is excited

to the corresponding antibonding orbital. Relative to other possible transitions the energy required to induce this transition is large, corresponding to radiant frequencies in the vacuum ultraviolet. Absorption maxima due to $\sigma\text{-}\sigma^*$ transitions are never observed in the ordinary accessible UV region.

$n\text{-}\sigma^*$ Saturated compounds containing nonbonding electrons are capable of $n\text{-}\sigma^*$ transitions. In general these transitions require less energy than the $\sigma\text{-}\sigma^*$ type and can be brought about by radiation in the region between 150 and 250 nm. The transition is partly forbidden, hence the molar absorptivities (ϵ) associated with this type of absorption are low and range between 100 and 3000 L / mol cm. An example is the first absorption band of an alkyl halide which is due to the promotion of a non-bonding p-electron into the σ^* antibonding C-X bond⁷. Other compounds with hetero-atoms singly linked to carbon also show this type of absorption but this tends to occur at wavelengths lower than 200 nm. Many of these compounds absorb in a region of the spectrum which is not readily accessible.

$n\text{-}\pi^*$ and $\pi\text{-}\pi^*$ The energies required to induce a transition for a n or π electron to the π^* state bring the absorption wavelengths into a convenient spectral region (200 - 700 nm). Both transitions require the presence of an unsaturated functional group to provide the π^* orbitals. The lowest energy transition whether $n\text{-}\pi^*$ or

$\pi-\pi^*$, will depend on the structure of the molecule.

The molar absorptivities associated with $\pi-\pi^*$ transitions generally have a value of 10^4 l / cm mol. The simplest example of a compound showing this type lowest energy transition is ethylene.

On the other hand, molar absorptivities associated with peaks responsible for $n-\pi^*$ transitions are low and have values from 10 - 100 l / cm mol. Such a low range arises from the transition being symmetry forbidden. Molecules with doubly bonded heteroatoms (eg. C=O, C=N, C=S, N=N, N=O) exhibit characteristic $n-\pi^*$ absorption.

Charge Transfer Transitions This type of transition cannot be represented by reference to Figure 1.4. When both an electron donor group and an electron acceptor group are connected with an electron system it is not possible to consider the transition to the excited state as the movement of one electron between two orbitals. Several kinds of one electron transition have to be regarded as contributing to the transition that actually occurs. Porter and Suppan⁸ have classified the excited state of lowest energy that result from such transitions as Charge-Transfer. The ground state and excited state of a Donor - Acceptor Complex (DAC) can be described by the wavefunctions -

$$\Psi_{(S_0)} = a \Psi_{(DA)} + b \Psi_{(D+A^-)}$$

$$\Psi_{(S_1)} = a \Psi_{(A+D^-)} + b \Psi_{(DA)}$$

$\Psi_{(DA)}$ corresponds to a structure in which no electron transfer takes place and $\Psi_{(D+A^-)}$ represents a structure in which an electron has been totally transferred from donor to acceptor. For the majority of DAC's $b \ll a$, so that $\Psi_{(S_0)} \approx \Psi_{(DA)}$ and $\Psi_{(S_1)} \approx \Psi_{(D+A^-)}$. Thus the spectroscopic transition corresponds approximately to the light induced transfer of an electron from the donor to the acceptor. The energy diagram in Figure 1.5 adequately describes this process. In the ground state

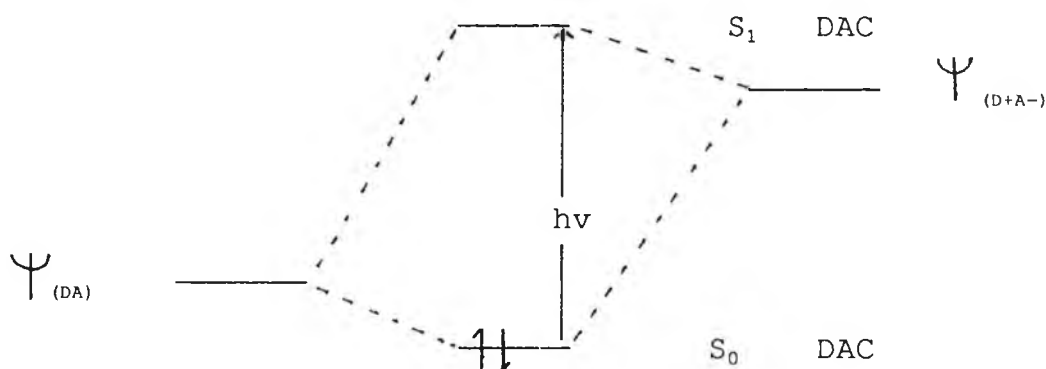


Figure 1.5 Light induced electron transition in DAC complexes.

there is very little charge transfer. The absorption maximum moves to longer wavelength as the donor and acceptor powers increase⁹. The extinction coefficient for DAC complexes is high (10,000 L / cm mol).

1.3.4 Effect of Conjugation on the Absorption Wavelength

In the MO treatment, π - electrons are considered to be further delocalised by conjugation. The orbitals now involve several atomic centres and this effect is to lower the energy between the highest occupied molecular orbital (HOMO) and the lowest unoccupied molecular orbital (LUMO). Hence the transition energy is lowered and the absorption peak is moved to longer wavelengths. This behaviour is realised for both $n-\pi^*$ and $\pi-\pi^*$ transitions. For example, the bathochromic shift on moving from 1,3-butadiene (217 nm) to 1,3,5-hexatriene (250 nm) is 33 nm. Similarly, the $n-\pi^*$ transitions of aldehydes and ketones (280 nm) is moved by 40 nm or more when conjugated as an α,β -unsaturated compound (325 nm)¹⁰.

1.3.5 Solvent Effects on Absorption Maxima

When absorption spectra are measured in solvents of increasing polarity it is found that $\pi-\pi^*$ and charge transfer systems under go a bathochromic shift of their long wavelength peak. Conversely, $n-\pi^*$ systems undergo an absorption peak movement to a shorter wavelength (hypsochromic shift). A solute having an excited state much more polar than the ground state will be stabilized more by solvents of increasing polarity than the ground state. Therefore the transition energy will be lowered leading to a red shift. The hypsochromic effect ($n-\pi^*$

systems) arises from the increased solvation of the unbonded electron pair, which lowers the energy of the n-orbital. In very polar solvents such as water or alcohols hydrogen bonding between solute and solvent is extensive. Promotion of the non bonding electron into the π -electron system reduces the hydrogen bonding in the excited state but does not significantly alter the solvation energy. Thus change to a polar solvent reduces the energy of the ground state to a greater degree than that of the excited state. Therefore as the solvent polarity increases hypsochromic shifts become more marked and the most dramatic effects are seen with polar protic solvents.

Polar solvents stabilize (π - π^*) and destabilize (n - π^*) states with respect to the situation in hydrocarbon

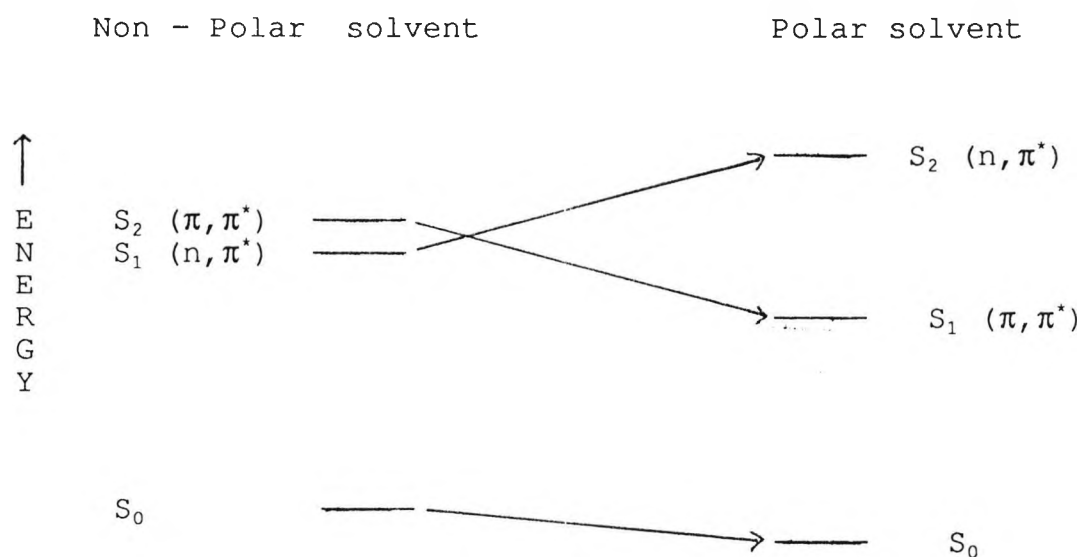


Figure 1.6 The effect of solvent polarity on the ordering of (n, π^*) and (π, π^*) states.

solvents. Thus if the two states mutually have similar energies then changing the solvent can invert the order of the states based on their energies. A scenario is given in Figure 1.6. Anthracene-9-carboxaldehyde provides a dramatic example since it is fluorescent in ethanol and non fluorescent in heptane¹.

1.3.6 Identification of (n, π^*) and (π, π^*) States

The course of a photochemical reaction is dependent upon the multiplicity (see next section) of the excited state and is usually a function of the lowest singlet or triplet energy level. Therefore it is necessary to be

	$^1(n, \pi^*)$	$^1(\pi, \pi^*)$
Intensity of absorption	weak	strong
solvent effects	blue shift in polar solvents	red shift in polar solvents

Table 1.1 Properties of singlet (n, π^*) and (π, π^*) states.

able to identify this state. The differences between the two states discussed above are set out in Table 1.1.

1.3.7 Spin Multiplicity

Nearly all molecules have an even number of electrons in the ground state which occupy orbitals in pairs. When one of the electrons is promoted to an upper orbital its spin may be orientated parallel or opposite to the remaining electron. The arrangement with the spins paired is termed a singlet state and that with parallel spin, a triplet state. Such states are distinct species with different chemical and physical properties. This nomenclature follows the multiplicity (M) which is defined as $2S+1$, where S is the total spin of the system. The first excited singlet state is thus termed S_1 and the first excited triplet state is T_1 . The T_1 state is lower in energy than the S_1 state because of the repulsive nature of spin - spin interactions between electrons of the same spin (Hunds Rule). The magnitude of $S_1 - T_1$ energy difference varies according to the degree of spatial interaction between the orbitals involved. Orbitals which occupy 'different' regions of space (for example, (n, π^*) and charge transfer) have little orbital overlap and the singlet - triplet energy splitting is quite small. More overlap occurs for orbitals occupying similar regions of space ($\pi-\pi^*$) and the difference is larger.

One of the selection rules for an electronic transition states that the multiplicity should remain unchanged . Thus singlet - singlet and triplet - triplet transitions

are fully allowed but singlet - triplet transitions are strongly forbidden. Therefore the excited state initially produced is almost always a singlet state. However, singlet - triplet transitions do occur and this is due to spin - orbit coupling.

1.4 Excited States and their Deactivation

Excited states are short lived and lose their electronic energy in a short period of time. There are competing pathways for a molecule to lose its excess energy and return to the ground state. These pathways are time dependent and determine the molecular photochemistry. The relative magnitude of the rate constant for each process determines the contribution made by a particular pathway.

1.4.1 The Excited State

The transitions between the ground state and excited states in a molecule are best described by reference to an energy level, or 'Jablonski' diagram ¹¹.

It should be noted that each electronic state has a series of vibrational and rotational energy levels associated with it. The rotational energy levels are not shown for clarity. When a transition takes place there is

also a change in these levels and so the absorption

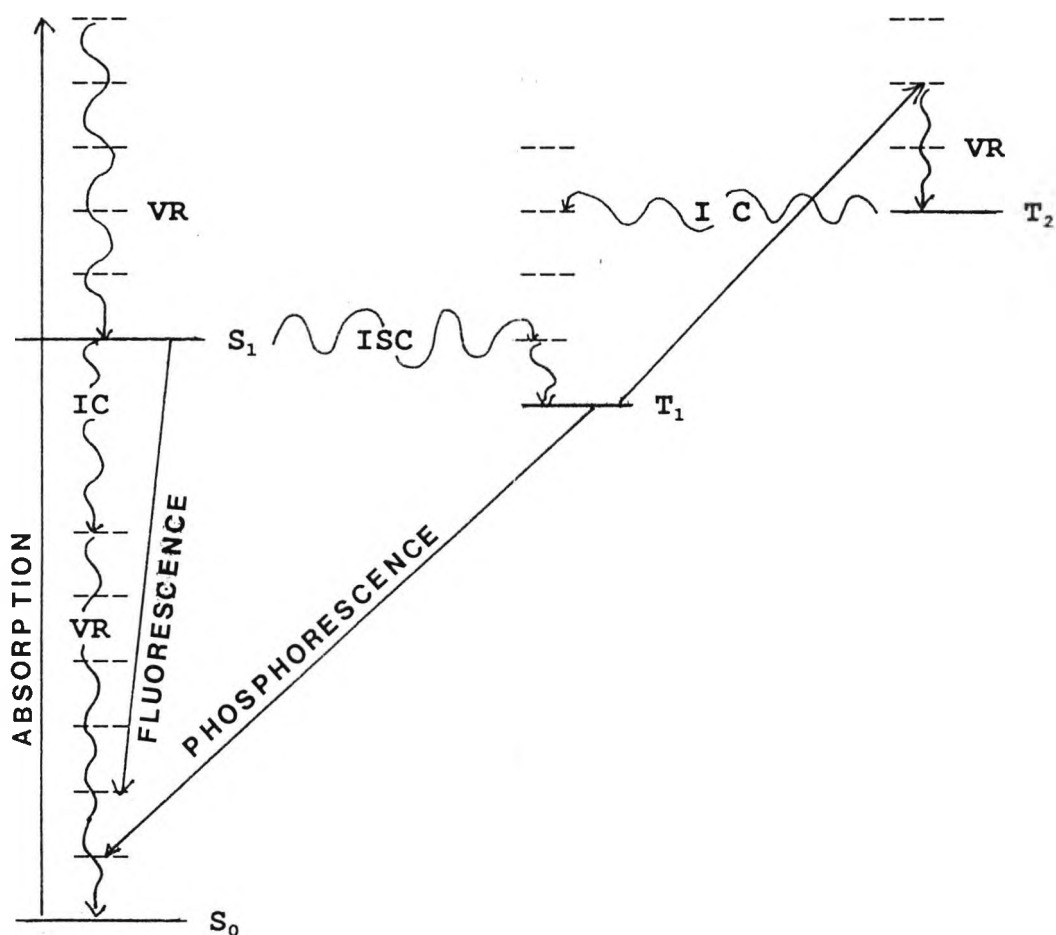


Figure 1.7 Jablonski diagram showing some of the radiative and non-radiative processes between energy levels. (IC = internal conversion, ISC = intersystem crossing, VR = vibrational relaxation)

spectra of molecules consists of bands rather than lines. After excitation the promoted electron can either undergo radiative or non-radiative decay.

1.4.2 Non-Radiative Deactivation Pathways

There are four non-radiative pathways:-

(i) Vibrational Relaxation (VR) The molecule may be promoted to any of several vibrational levels during the excitation process. In solution however this excess vibrational energy is lost in collision with the solvent. The relaxation process is very efficient and the average lifetime of a vibrationally excited molecule is 10^{-12} s, a period much shorter than the average lifetime of an excited state. Consequently, fluorescence, phosphorescence or chemical reaction will occur from the lowest vibrational level of an excited state.

(ii) Internal Conversion (IC) describes the process by which a molecule passes from a higher electronic state to a lower one without a change of multiplicity (singlet - singlet or triplet -triplet transitions). IC is efficient when two electronic energy levels are sufficiently close for vibrational overlap. Thus the transition S_2 to S_1 is rapid (10^{-14} - 10^{-11} s), whilst the S_1 to S_0 is slower (10^{-6} - 10^{-10} s). Consequently any photochemical processes in solution are likely to occur from the lowest excited electronic state.

(iii) External Conversion is the deactivation of an electronically excited state by energy transfer between the excited molecule and the solvent or other solutes.

(iv) Intersystem Crossing (ISC) is the process in which the spin of an excited electron is reversed and a change of multiplicity results. As with IC the probability of a transition is enhanced when similar vibrational levels of the two states overlap. The time for such a transition is of the order $10^{-4} - 10^{-12}$ s

It is clear from the above discussion that an excited molecule will be rapidly converted to its lowest excited state which can either be the singlet or triplet. From this lowest excited state several processes compete, which can be radiative or non-radiative. The non-radiative pathways are IC and VR which have been discussed above. Chemical reactions can also occur from the singlet and triplet state.

1.4.3 Radiative Emissions

The radiative pathway from the singlet state is termed fluorescence and that from the triplet state is called phosphorescence. Both are discussed below-

(i) Fluorescence is caused by a radiative transition between states of the same multiplicity and it is a rapid process. This type of emission is seldom observed from the $\sigma^*-\sigma$ transition, instead it is confined to the less energetic $\pi^*-\pi$ and $\pi^*-\pi$ processes. Experimentally, it has been observed that the stronger fluorescers are molecules

which have (π, π^*) rather than (n, π^*) states and this has been rationalised in two ways. First, the molar absorptivity of a (π, π^*) state is usually 100-1000 times greater than the (n, π^*) state and this quantity represents a measure of transition probability in either direction. Hence, the rate constant for fluorescence will be large for the (π, π^*) state ($10^7 - 10^9$ s) compared to to the (n, π^*) state ($10^5 - 10^7$ s). Secondly, the singlet - triplet energy difference is larger for the (π, π^*) state and the probability of intersystem crossing is smaller.

The most intense fluorescence is found in compounds containing aromatic functional groups with low energy $\pi-\pi^*$ transition levels. Substitution on the aromatic system can affect the fluorescence efficiency. Halogens decrease the fluorescence by a mechanism called the heavy atom effect which increases the probability of ISC to the triplet state. Nitro groups have easily ruptured bonds which can absorb the excitation energy, but more importantly they can undergo $n-\pi^*$ transitions. If the (n, π^*) state is lower in energy than the (π, π^*) state then the fluorescence will be quenched. Carboxylic acids or carbonyl groups generally inhibit the emission because they also introduce (n, π^*) states of less energy than the (π, π^*) state.

Fluorescence is favoured in molecules that possess a rigid structure. For example the quantum efficiencies of fluorene and biphenyl are nearly 1.0 and 0.2 respectively

under similar conditions of measurement ¹². Enhanced fluorescence frequently results when fluorescing dyes are adsorbed on a solid surface. The added rigidity provided by the solid surface is thought to account for the observed effect.

The fluorescence emission of a molecule can be decreased by several other factors. An increase in temperature imparts more energy to the system and the solute undergoes a greater number of collisions with the solvent. Movement to less polar solvents may also decrease the fluorescence efficiency (see section 1.3.5). Solvents containing heavy atoms such as carbon tetrabromide or ethyl iodide promote intersystem crossing to the triplet state. Dissolved oxygen can photochemically oxidise the fluorescing species, but of fundamental importance is the paramagnetic property of molecular oxygen which causes intersystem crossing to the triplet state. Other paramagnetic species such as rare earth ions exert similar effects.

The following equation defines the quantum yield and it is a measure of the efficiency of a photochemical process.

$$\phi_{\text{product}} = \frac{\text{number of moles of product formed}}{\text{number of photons absorbed}}$$

$$= \frac{\text{rate of formation of product}}{\text{intensity of absorbed radiation}}$$

This definition is readily modified to give an expression for the fluorescence quantum yield.

$$\phi_f = \frac{\text{rate of emission by } S_1}{\text{rate of absorption of photons by } S_0}$$

Phosphorescence is the result of a transition between states of different multiplicity, usually $T_1 \rightarrow S_0$. A triplet - singlet transition is much less probable than a singlet - singlet conversion and the average lifetime of the excited triplet with respect to emission ranges from 10^{-4} to several seconds.

The photophysical pathways and their respective timespans available to a molecule are summarised in Table 1.2

Process	Time (s)
Absorption	$10^{-15} - 10^{-16}$
Vibrational Relaxation	10^{-12}
Internal conversion (S_2-S_1)	$10^{-11} - 10^{-14}$
Internal Conversion (S_1-S_0)	$10^{-6} - 10^{-10}$
Fluorescence	$10^{-7} - 10^{-9}$
Intersystem Crossing (S_1-T_1)	$10^{-4} - 10^{-12}$
Intersystem Crossing (T_1-S_0)	$10^{-2} - 10^2$
Phosphorescence	$10^{-4} - 10^2$

Table 1.2 Timespan for the photophysical pathways available to a molecule.

1.5 Quenching of Excited States

When an electronically excited state undergoes accelerated decay to a lower excited state or the ground state it is said to have been quenched. The substance that brings about this effect is a quencher. Other than certain electron energy transfer mechanisms quenching processes seem to be collisional and are often bimolecular events. The entity in which the quenching occurs can be either an encounter complex or an excimer/exciple. Encounter complexes have random relative orientations and the components are separated by 7Å or more, the only requirement being some orbital overlap. Excimer / exciplexes are excited states and have definite geometries¹³.

1.5.1 Kinetics of Quenching

The kinetics of quenching is given by the Stern - Volmer¹⁴ equation below -

$$\frac{\phi_0}{\phi_q} = 1 + k_q \cdot \tau \cdot (Q)$$

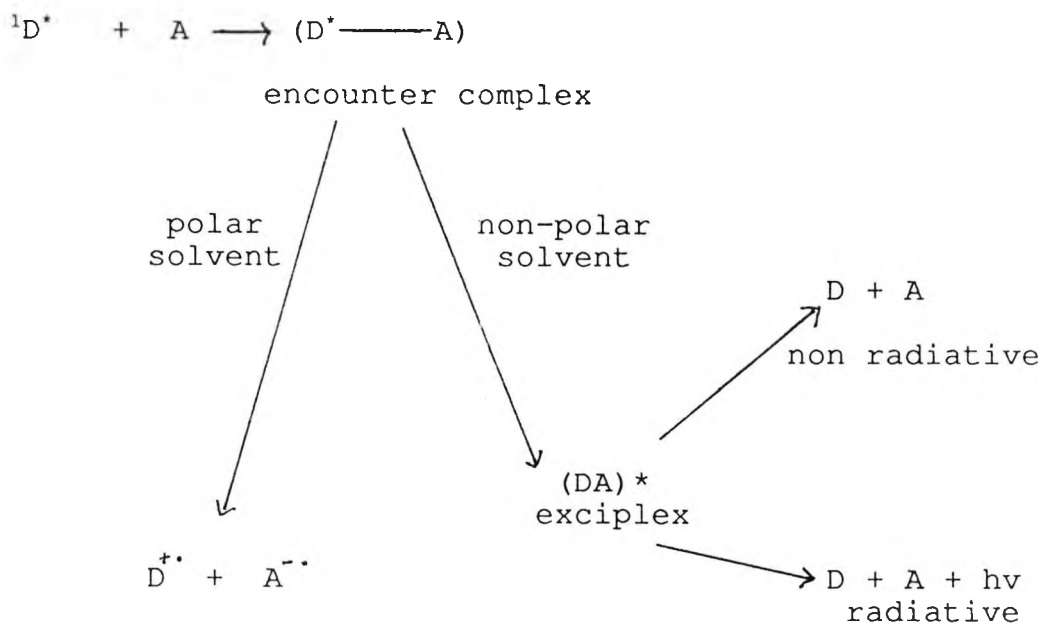
where

- ϕ_0 - fluorescence quantum yield in the absence of quencher
- ϕ_q - fluorescence quantum yield in the presence of quencher
- k_q - rate constant for quenching
- τ - fluorescent lifetime in the absence of quencher
- (Q) - quencher concentration.

For many systems the rate constants are in the order of $10^9 - 10^{10}$.

1.5.2 Electron Transfer Quenching

The quenching of excited states by electron transfer is well documented¹⁵. In polar solvents complete electron transfer occurs leading to the formation of solvent separated radical ion pairs. In non-polar solvents incomplete electron transfer may occur to form an intermolecular charge-transfer complex in an excited state, which may relax by either a radiative or non-radiative pathway. The possible processes are depicted in Scheme 1.1. Weller provided excellent evidence from

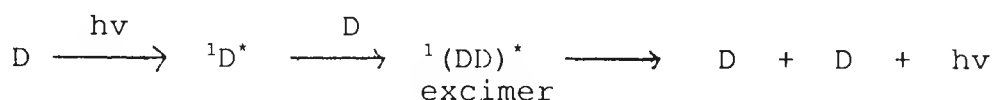


Scheme 1.1 Pathways available for the deactivation of an excited state by electron transfer.

flash photolysis experiments of aromatic hydrocarbons with amines to show the transient generation of a hydrocarbon radical anion and the amine radical cation ¹⁶. Since this pioneering work intermolecular ¹⁷ and intramolecular ¹⁸ electron transfer have been widely studied.

1.5.3 Concentration Quenching

As the concentration of a fluorescing solute increases then its emission signal decreases. One factor responsible is 'self absorption' when an emission wavelength overlaps the absorption wavelength. A second factor is 'self quenching' which commonly involves the interaction of excited molecules with ground state molecules. It has been found that such quenching is often accompanied by the appearance of new emission at longer wavelength. For example, the quenching of pyrene fluorescence on increasing the concentration of pyrene has been shown to follow the Stern-Volmer law and the quenching was accompanied by an increased intensity in the fluorescent band attributed to excited dimer formation ^{19,20}. That is an excited singlet state pyrene molecule interacts with a ground state pyrene molecule to form an excited transient intermediate which decays back to the ground state by radiative decay by the following reaction scheme.

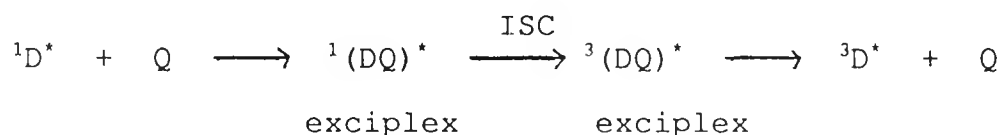


1.5.4 Heavy Atom and Oxygen Quenching

The quenching of molecular fluorescence by compounds containing heavy atoms and the presence of paramagnetic species, namely oxygen was briefly mentioned in section 1.4.2. This phenomenon is now discussed in slightly more detail. It seems that an excited complex of definite stoichiometry (usually 1:1) is formed between an excited solute species and one or more different molecules in the ground state. The excited complex is called an exciplex.

In this excited species the magnetic moment of the spinning electron couples with the orbital magnetic field to induce a change of electron spin. The interaction is known as spin-orbit coupling.

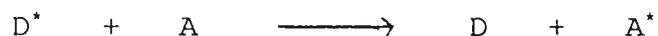
The result is enhanced intersystem crossing to the triplet exciplex which then dissociates into its components. A simplified scheme for this process is given below.



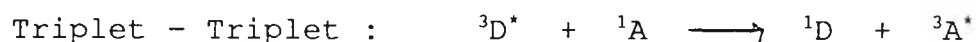
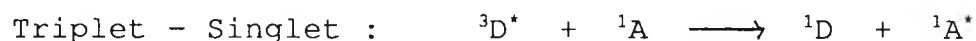
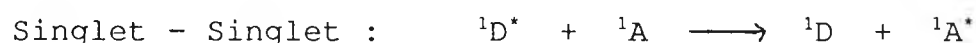
1.5.5 Quenching by Energy Transfer

An excited molecule (donor) can be quenched by transferring its electronic energy to a ground state species (acceptor). Consequently, the donor is returned to the ground state and the acceptor is promoted to an excited state. The acceptor must have lower lying singlet or triplet energy levels than the donor. The

situation can be represented by the following equation -



The process can either be considered as a donor sensitising an excited state of the acceptor, or the acceptor quenching the donor excited state. There are only three common modes of energy transfer in organic photochemistry and these are given below-



The three modes of energy transfer and the formation of singlet oxygen are now discussed in more detail.

(i) Singlet - singlet A donor in an excited singlet state radiatively decays to the ground state and the emitted photons are preferentially reabsorbed by the acceptor promoting it to an excited singlet state. This form of radiative energy transfer is frequently described as the 'trivial' mechanism because of its conceptual simplicity. Deactivation of the donor and excitation of the acceptor are independently spin allowed. The rate of energy transfer depends on :-

- (i) fluorescence efficiency of the donor,
- (ii) the light absorbing power of the acceptor

(iii) the extent of overlap between the donor's emission spectrum and the absorption spectrum of the acceptor.

This kind of energy transfer can occur over short and immense distances

(ii) Triplet - singlet A donor in an excited triplet state transfers its energy via dipole-dipole interactions to a ground state acceptor thus promoting it to an excited singlet state. The transition $^3D^* \rightarrow ^1D$ is spin forbidden and so reduces the rate of energy transfer and consequently this phenomena is rarely observed.

(iii) Triplet - triplet A donor in an excited triplet state interacts over a distance comparable to collisional diameters with a ground state acceptor, subsequently promoting it to the triplet state. Because of the intervention of a bimolecular intermediate the process is allowed. An effective triplet sensitiser should absorb all the irradiated light and have a triplet energy higher than the substrate. Such conditions are satisfied when the energy levels are disposed as in Figure 1.8.

For experimental observation of the phenomena a filter is used to remove the short wavelength light that would excite the acceptor to its singlet state. Substances with small singlet - triplet splitting but a triplet energy level between the lowest excited states (S_1 and T_1)

of the acceptor are ideal sensitisers. The importance of

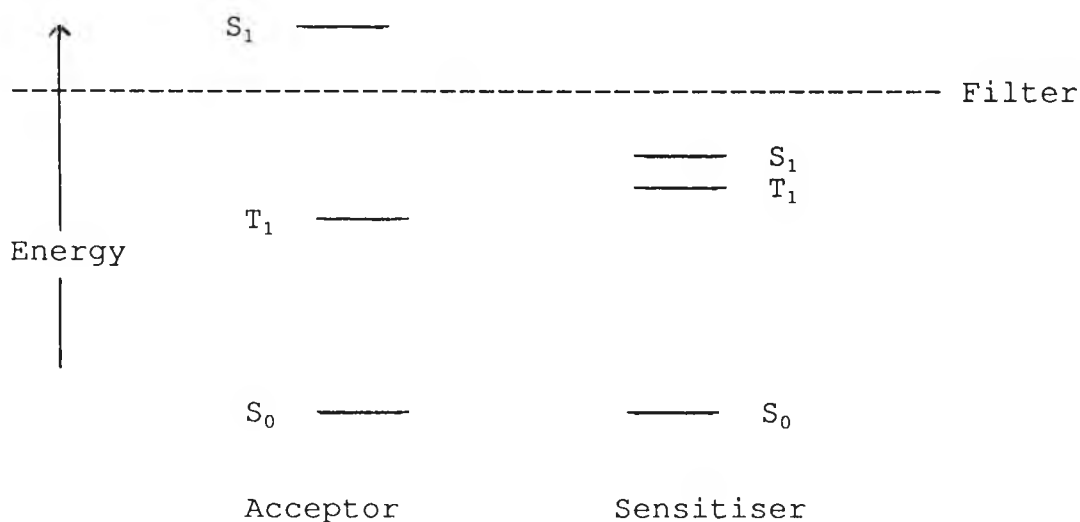


Figure 1.8 Energy levels for a sensitiser and acceptor system that would exhibit triplet energy transfer.

this process should not be overlooked as it provides a method of exclusively populating the triplet state.

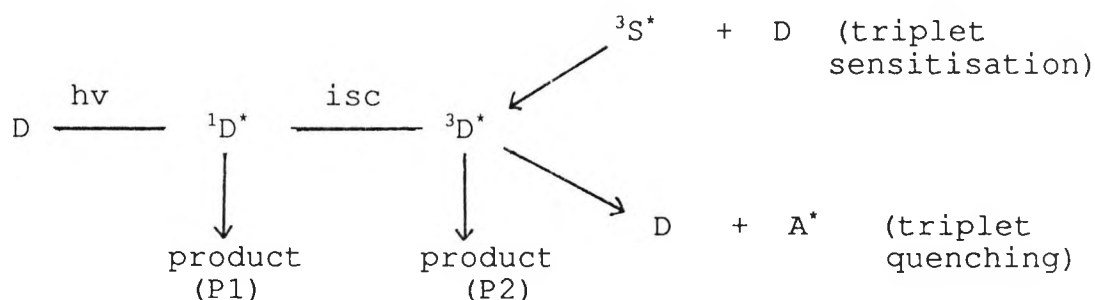
(iv) Formation of Singlet Oxygen Oxygen in its ground state has a triplet electronic configuration. If it collides with an excited triplet species energy transfer may take place promoting the oxygen molecule to an excited singlet state. This state is very reactive and photo - oxidises a variety of organic substrates ^{21,22,24}. The reaction route is known as the Type II mechanism and is important in the next chapter when the photochemistry of proteins is discussed.

1.5.6 Photosensitised Processes

It often happens that the singlet and triplet states of a molecule undergo different chemical reactions.

Therefore to drive the reaction in a particular direction it is necessary to preferentially populate the desired excited state. Control of the products can be maintained by sensitisation and quenching techniques.

The idea is readily seen by reference to Scheme 1.2



Scheme 1.2 Product selection by controlled population of a desired excited state.

Hence the exclusive formation of product P1 can be obtained by addition of a triplet quencher whose energy is less than that of ${}^3D^*$. The formation of product P2 is maximised by specifically producing ${}^3D^*$ by triplet transfer from a photosensitizer ${}^3S^*$ of higher triplet energy, thereby bypassing the singlet state.

1.6 The Phenomena Of Colour

Most average humans are receptive to light between 400

and 700 nm and this range is known as the visible spectrum. The wavelength of light is responsible for the sensation of colour and the visible spectrum can be divided into nine broad spectral regions. Each region is readily distinguishable from the others and these can be depicted in the form of a colour circle ²³ (Figure 1.9).

It should be noted that each sector has another sector diametrically opposite to it and the colour purple is not represented by a wavelength region. The circle can now

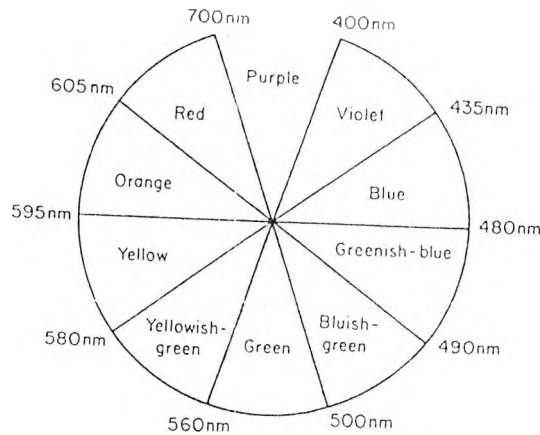


Figure 1.9 The colour circle.

be used to discuss additive and subtractive colour mixing.

1.6.1 Additive Colour Mixing

If all the circle colours are mixed in the correct amounts then white light is produced. Similarly if two monochromatic wavelengths from any pair of opposite

sectors are mixed the eye perceives white. Such pairs of colours are said to be complementary. The colour of a zone can be duplicated by mixing light from both adjacent sectors. For example, if red and yellow are mixed then orange is formed.

The vast majority of colours that pervade our environment are not formed in this manner but arise from subtractive colour mixing.

1.6.2 Subtractive Colour Mixing

This phenomena is essentially the opposite of additive mixing. If one of the components from white light is removed then the eye will perceive the complementary colour of the radiation removed. This is in spite of the fact that the remaining radiation is a complex mixture of wavelengths. To take one example, if a molecule absorbs a band of wavelengths in the region 490 - 500 nm bluish-green light is removed and the colour registered by the eye is red. The emergence of green requires the removal of purple light which does not exist monochromatically but is a mixture of red and violet radiation. Thus filtration of the two wavelengths (ca 650 and 420 nm) produces the desired effect. Dyes and pigments appear coloured because molecules selectively absorb certain wavelengths from daylight. The electronic structure of molecules and the absorption of light has been discussed in earlier sections.

1.7 REFERENCES

1. J.A. Barltrop and J.D. Coyle. 'Excited States in Organic Chemistry', John Wiley, New York, (1975).
2. N.J. Turro. 'Modern Molecular Photochemistry', Benjamin/Cummings, San Fransisco, (1978).
3. J. Calvert and J. Pitts. 'Photochemistry', John Wiley, New York, (1965).
4. J.M. Coxon and B. Halton. 'Organic Photochemistry', William Clowes and Sons Ltd, Cambridge Univesity Press, (1974).
5. A. Streitweiser. 'Molecular Orbitals Theory for Organic Chemists', Wiley, London, (1961), Chapter 1.
6. H.H. Jaffe and M. Orchin. 'Theory and Application of U.V Spectroscopy', Wiley, London, (1963), Chapter 3.
7. Ref 3, p. 522.
8. G. Porter and P.Suppan. Trans. Faraday Soc. 61 , (1965), 1664.
9. G. Briegleb. 'Elektronen - Donator - Acceptor Komplexes', Springer, Berlin, (1961).
10. D.A. Skoog and D.M. West. 'Principles of Instrumental Analysis', Holt - Saunders, Japan, (1981) p. 174 - 175.
11. A. Jablonski. Z-Physik, 94 , (1935), 38 - 46.
12. Ref 10, p.287.
13. B. Stevens. Adv Photochem, 8, (1971), 161.
14. O. Stern and M. Volmer. 'Z-Physik, 20 , (1919), 183.

15. R.S. Davidson. 'Advances in Physical Organic Chemistry', Vol 19, Academic Press, London, (1983). p 1 - 130
16. A. Weller. Pure and Applied Chem. 16 , (1968), 115.
17. M. Gordon and W.R. Ware. 'The Exciplex', Academic Press, New York, (1975).
18. J.W. Verhoeven. Pure and Applied Chem. Vol 62 (8), (1990) , 1585 - 1596.
19. T.H. Forster and K. Kasper. Z. Electrochem , 59, (1955), 977.
20. C.A. Parker and C.G. Hatchard. Trans Faraday Soc. 59, (1963), 284.
21. K.Gollnick and G.O. Schenck. '1,4-Cycloaddition Reactions - The Diels-Alder Reaction in Organic Synthesis', Academic Press, New York, (1967).
22. K.Gollnick. Advances in Photochemistry Vol 6, Interscience, New York, (1968), p. 1.
23. J. Griffith. 'Colour and Constitution of Organic Molecules' Academic Press, London, (1976), p. 5.
24. S.Patai. 'The Chemistry of Functional Groups, Peroxides' John Wiley and Sons Ltd, (1983), Chapter 7, p 201

CHAPTER 2

**PHOTOCHEMISTRY OF WOOL PROTEINS AND FLUORESCENT
BRIGHTENING AGENTS**

2.1 Chemical Structure of Wool

Wool which has been cleaned is essentially 'pure' protein and so exhibits the chemistry associated with its constituent amino acids ¹. Hydrolytic degradation and chromatographic analysis has shown the presence of the eighteen amino acids commonly found in the hydrolysates of most proteins. The residues are given in table 2.1 ². As with other proteins, wool contains both acidic and basic groups and is therefore amphoteric. There is an approximate balance between the acidic and basic groups. The acidic properties are from aspartic, glutamic, c-terminal residues and the basic character is due to arginine, lysine, and histidine sidechains. The amino acid composition of wool is dependent upon several factors. Alterations in the diet and health of a sheep and its external environment are particularly important. Cystine residues are vital crosslinking agents which bridge different protein chains. It has been suggested that all of the polypeptide chains in wool may be crosslinked, so that the whole wool fibre is one giant protein molecule ³. Disulphide reduction and capture of the thiols with iodoacetate allows the extraction of soluble proteins ⁴. The isolated proteins can be separated into three fractions dependent on the sulphur content. One group contains a group of 'low sulphur' proteins, so called because their sulphur content is less than that of wool. Another fraction contains two groups, the 'high sulphur' and 'ultrahigh sulphur' proteins

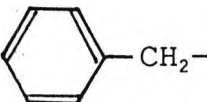
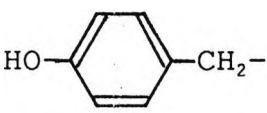
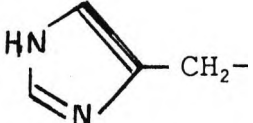
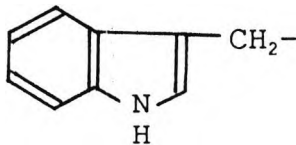
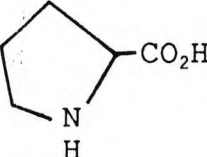
Name	Structure (H ₂ N-CH-CO ₂ H)	Abreviation
Glycine	H-	Gly
Alanine	CH ₃ -	Ala
Valine	(CH ₃) ₂ CH-	Val
Leucine	(CH ₃) ₂ CHCH ₂ -	Leu
Isoleucine	CH ₃ CH ₂ (CH ₃)CH-	Ile
Methionine	CH ₃ SCH ₂ CH ₂ -	Met
Serine	HOCH ₂ -	Ser
Threonine	CH ₃ (HO)CH-	Thr
Aspartic acid	HO ₂ CCH ₂ -	Asp
Glutamic acid	HO ₂ CH ₂ CH ₂ -	Glu
Lysine	H ₂ N(CH ₂) ₄ -	Lys
Arginine	$\begin{array}{c} \text{H}_2\text{NCNH}(\text{CH}_2)_3- \\ \\ \text{NH} \end{array}$	Arg
Phenylalanine		Phe
Tyrosine		Tyr
Histidine		His
Tryptophan		Try
Proline		Pro

Table 2.1 Amino acids in Wool

whose sulphur content is higher than the original wool. A third fraction, found to be especially rich in glycine and tyrosine is called high-Gly/Tyr protein.

2.2 Photochemistry of Wool Protein

The photoactive residues in proteins include disulphide bonds, and the aromatic sidechains tyrosine, tryptophan and phenylalanine. The chemical constitution of the protein is important as this will influence the photochemical properties. In general light affects proteins in three different ways ;-

- in the early stages of exposure new crosslinks may be formed

- prolonged irradiation brings about photodegradation due to main chain amide and disulphide bond rupture

- photodiscolouration accompanies the above reactions.

The significance and extent of the above reactions depend on the intensity and energy of the irradiation source, temperature and humidity.

2.2.1 Ultraviolet Absorption

The uv absorption spectrum of wool between 250 and 300 nm

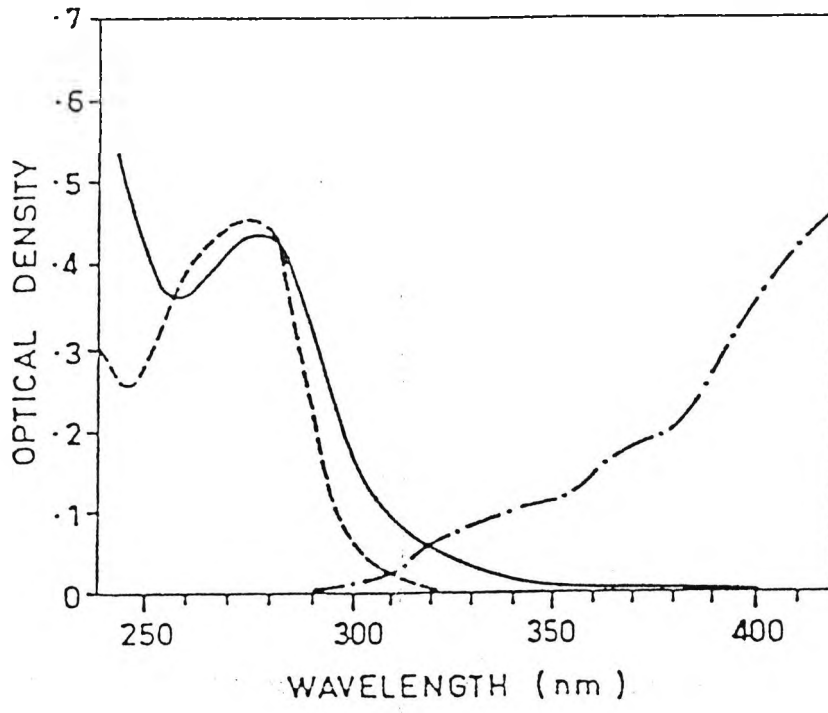


Figure 2.1 The ultraviolet absorption spectrum of

- (i) a 6 μm radial section of merino wool keratin (-----),
- (ii) the absorption spectrum calculated from the amino acid composition (—),
- (iii) the relative spectral intensity of Sydney south light at noon (-.-.-.)

(Extracted from ref 5)

is due essentially to the presence of the amino acids tyrosine and tryptophan with minor contributions from phenylalanine and cystine. At wavelengths above 290 nm the wool fibre has a much higher absorption than can be accounted for by amino acid absorption indicating the presence of other species which absorb in this region (Figure 2.1) ⁵. Although wool absorption in the 300 - 380 nm region is small, the amount of energy reaching the earth in this wavelength range is much greater than that below 300 nm. Therefore the photochemistry of the unknown species must be taken into consideration when discussing the interaction of wool proteins with radiation in the region 300 - 380 nm. This 'non protein' species has not been identified but it is postulated as photodecomposition products ⁶ or natural pigment precursors ⁷.

2.2.2 Luminescence of Wool

Irradiation of wool in the 280 - 290 nm wavelength region leads to a fluorescence signal which is largely attributable to tryptophan even though tyrosine absorbs strongly in the same range ⁸. The lack of tyrosine emission is attributed to an energy migration from tyrosine to tryptophan via an acceptor-donor mechanism ⁹. Electron transfer between the aromatic residues also occurs. Laser flash photolysis (265 nm) of Trp-Tyr leads to an observation of the radical cation $\text{Trp}^{\bullet+}$ -Tyr, and a

phenoxy radical due to proton and electron loss from the tyrosine residue ¹⁰. Reduction of the disulphide bonds in wool by treatment with tributyl phosphine was found to double the original fluorescence ¹¹. The fluorescence quenching by the disulphides is in part, via an electron transfer mechanism ¹². Thus flash photolysis of tryptophan in the presence of cystine gave the radical anion of cystine¹³. Bent and Hayon showed that the triplet state of tyrosine was quenched by disulphides with the formation of radical anions of the disulphide ¹⁴. Singlet energy transfer from tyrosine to dithioglycollic acid was proposed after similar products were found from the direct and tyrosine sensitised photolysis of the disulphide ¹⁵.

Following the recognition that the fluorescence of wool was due essentially to emission from tryptophan it was soon recognised that the room temperature phosphorescence was also essentially due to tryptophan. Konev ¹⁶ found an intense short lived emission which was assigned to the tryptophan triplet and a longer lived signal which was proposed to occur from the recombination of a photoejected electron with the tryptophan radical cation. A study by Ghiggino concluded that under dry nitrogen the phosphorescence (excitation at 280 nm) decay was apparently second order and the rate-determining step was a radiationless tryptophan - tryptophan triplet quenching. However in the presence of oxygen and/or moisture the triplet state of tryptophan is quenched by

oxygen with the possible formation of singlet oxygen ¹⁷. A second phosphorescence decay study with the sample under dry nitrogen (excitation at 290 nm) invoked the participation of an unknown species absorbing at 330 - 350 nm and the triplet state of tryptophan ¹⁸.

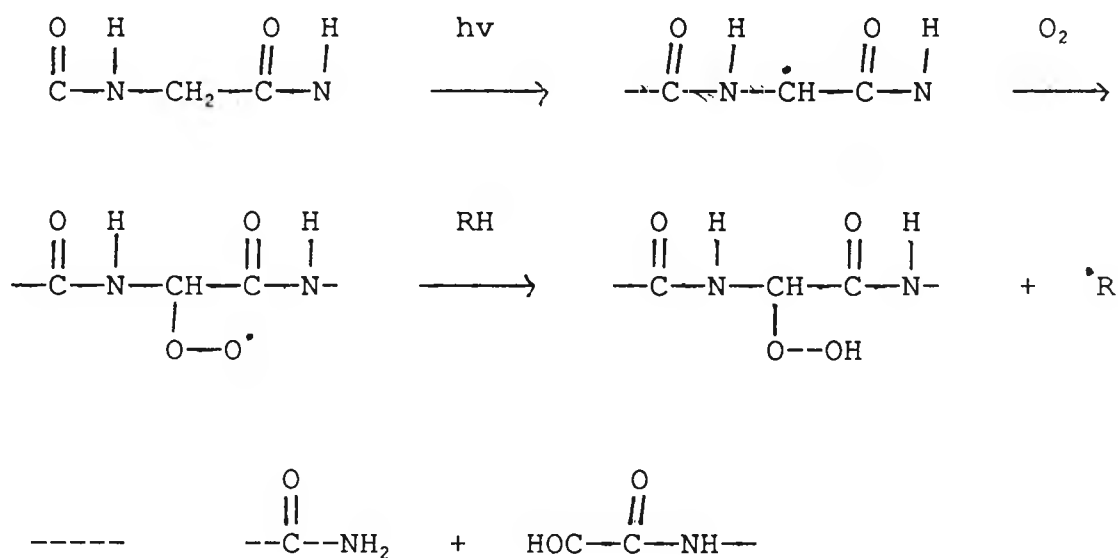
2.2.3 Photochemical Reactions

Upon irradiation the wool protein can undergo many photochemical processes. These processes are dependent on parameters such as irradiation wavelength, presence or absence of oxygen, and frequently compete with each other. In order to simplify the multitude of photochemical reactions they are classified into two categories - (i) free radical and (ii) reactions leading to the yellowing of wool. This classification is only for convenience and is not absolutely strict. For example, the formation of dityrosine is proposed to occur by a radical mechanism but it is thought to influence the photoyellowing of wool and is therefore discussed in this section.

2.2.3.1 Radical Reactions

The identification of small amounts of pyruvic and glyoxylic acids in the protein hydrolysate of simple model peptides indicate amide bond fission at the glycine

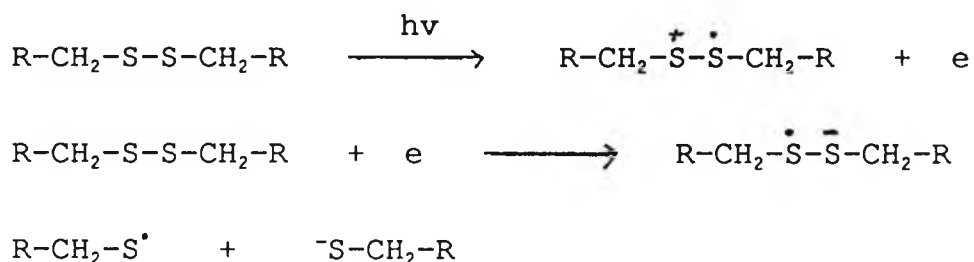
and alanine residues ¹⁹. It was also found that free phenylalanine increased the photolysis of these derivatives. The catalytic activity of an aromatic amino acid was proposed to occur by photoionisation of the phenyl group. The mechanism suggested that peptide radicals are formed which then react with oxygen to form α -ketoacetyl groups. The reaction pathway can be envisaged by the following equations -



The identification of other α -keto acids suggests that main chain breakdown is not confined to glycine and alanine but can occur adjacent to many amino acid residues ²⁰. In fact, it has been suggested that electron donors such as aromatic amino acids will sensitise acceptors such as peptide bonds by energy transfer without actually releasing electrons ²¹.

Irradiation of cystine can lead to a plethora of products depending on the irradiation wavelength ²². Both C-S and

S-S bond fission have been observed. In proteins, cystine is believed to form thiyl radicals by homolytic fission of the disulphide bond or by the rearrangement of a cystinyl radical anion via the following reaction scheme ²³ -



Photoexcited tyrosine can cleave disulfides via an electron transfer process ^{14,15,24,25}.

Evidence for the participation of thiyl radicals was obtained by electron spin resonance spectroscopy (e.s.r) ²³. The spectrum has not been satisfactorily assigned and conflicting designations remain. One proposal is the formation of a glyciny radical and alanyl radical ²⁶ which agrees with the chemical evidence. A second suggestion is that the unpaired electron is associated with peptide carbonyl carbon ²⁷, but no chemical evidence supports this designation.

Tryptophan also forms a free radical species which has been identified as the 3-indolyl radical. It is formed by rearrangement of the 1-indolyl radical following N-H bond fission ²⁸ and/or photoejection of an electron and subsequent deprotonation ²⁹. The formation is wavelength

dependent in aqueous media with only N-H bond fission occurring at >275 nm ³⁰. Studies of the radical forming properties of tryptophan in poly(vinyl alcohol) films indicates that this pathway appears to play only a minor role with irradiation wavelengths >300 nm, and so by deduction in wool under the same radiation conditions ³⁰. Wool has been irradiated in the presence of tritiated water with the idea that the free radicals produced on irradiation will abstract tritium and so radiolabel the original amino acid residue. After reduction /carboxymethylation and enzymatic degradation radiolabelled tryptophan, tyrosine, phenylalanine, histidine and s-carboxymethylcysteine were identified ³¹.

It appears that free radical reactions are mainly responsible for the rupture of disulphide bonds and polypeptide backbone breakdown.

2.2.3.2 Photoyellowing of Wool

The formation of α - keto acids was first proposed to account for the increased wool yellowness because of their visible light absorption ¹⁹. However, Holt and Milligan have provided evidence to refute this suggestion ²⁰. Tryptophan is the amino acid most susceptible to sunlight yellowing in aqueous media ³². A strong correlation was found for the rates of yellowing of 29 different keratin samples with their initial

concentration of tryptophan and with the destruction of tryptophan ³³. The incorporation of tryptophan into wool causes a significant increase in yellowing ³⁴. Some yellow products from photodegraded wool have been isolated, but only kynurenine, a recognised oxidation product of tryptophan could be identified ³⁵. Furthermore it was found that the photoproducts were covalently bound to the protein. To avoid the problems associated with the isolation of peptide-bound products from an insoluble wool substrate, the photochemistry of tryptophan and its derivatives has been widely investigated. The studies have either involved direct photolysis or reaction of the amino acid residue with singlet oxygen formed by dye sensitisation ³⁶. Following prolonged irradiation of tryptophan (i) the following products have been isolated and identified : N-formylkynurenine (NFK, vi) ³⁷, kynurenine (vii) ³⁸, 3a-hydroperoxypyrrolidinoindole (iv) ³⁹ and 3a-hydroxypyrrolidinoindole (v) ³⁹. To account for the products Sun and Zigman ³⁹ have devised the reaction scheme shown in Figure 2.2. The initial reaction involves the interaction of the indole nucleus with oxygen to give a short lived indolenine hydroperoxide (ii). It is not clear if this species is formed via a 3-indolyl radical and radical cation, a process involving Trp (S₁), Trp (T₁) or reaction of singlet oxygen with tryptophan. Presumably, at wavelengths greater than 300 nm the singlet oxygen mechanism is in sole operation but

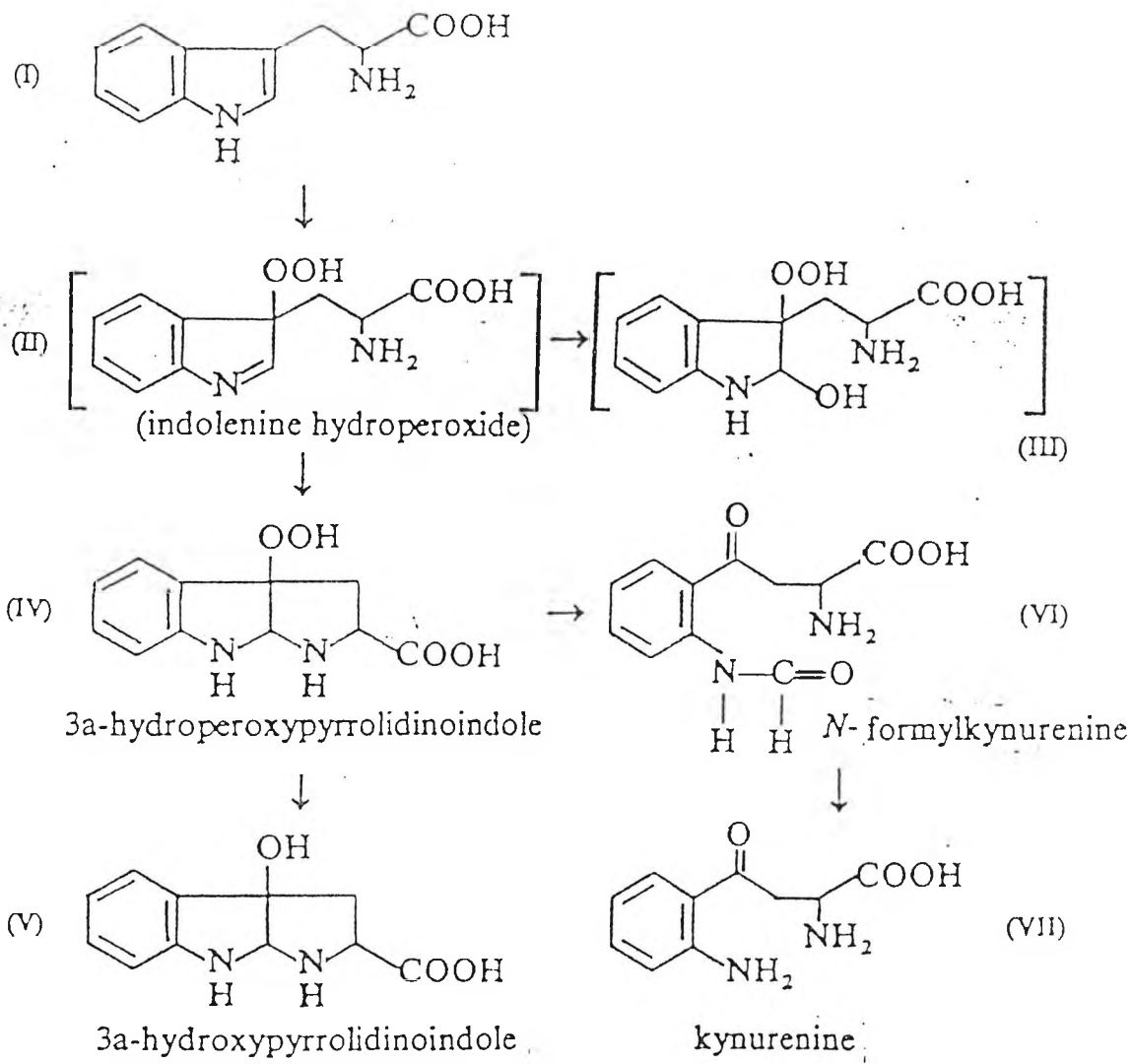
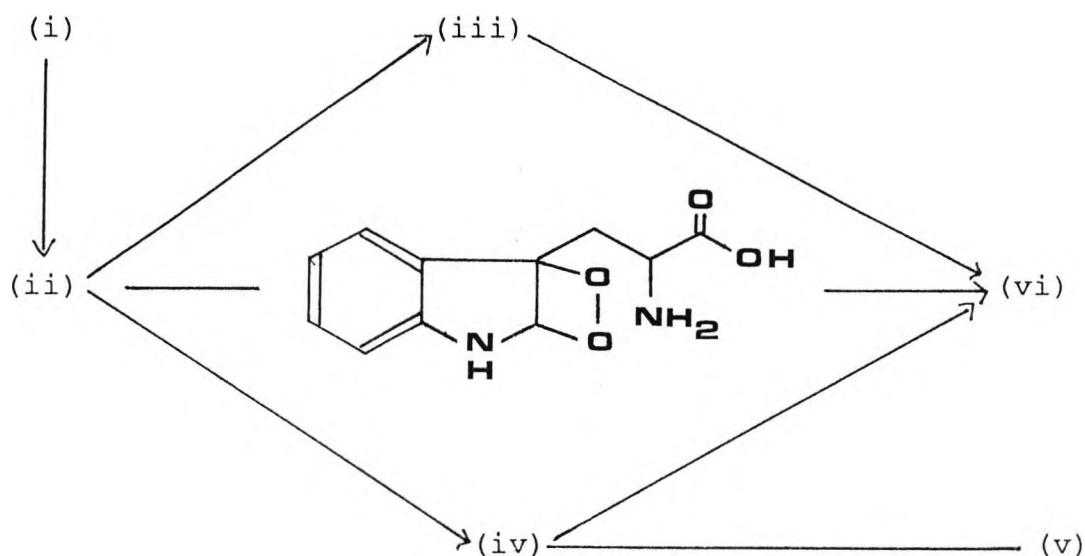


Figure 2.2 The direct photolysis of tryptophan in aerated aqueous solution (Sun and Zigman³⁹).

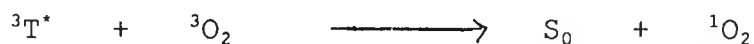
at higher energy irradiation then other pathways may contribute to the intermediate formation. Intramolecular attack by the α -nitrogen lone pair of electrons or intermolecular addition of water is possible, but isolation of (iv) indicates this is a more stable product. It is likely that (iv) plays only a minor part in the photochemistry of protein bound tryptophan. The steric factors and loss of nucleophilic activity associated with the amide bond will retard its formation. In fact, N-acetyltryptophan yellows more slowly than free tryptophan in aqueous solution ⁴⁰ .

The products obtained by the dye sensitised photo-oxidation of tryptophan have included NFK (vi) ⁴¹, (iv) ⁴² and (v) ^{43,44}. Parallel to the direct photolysis, an indolenine hydroperoxide was formulated as the initial product which converts to NFK or (iv) by alternate pathways. The following reaction scheme has been proposed -



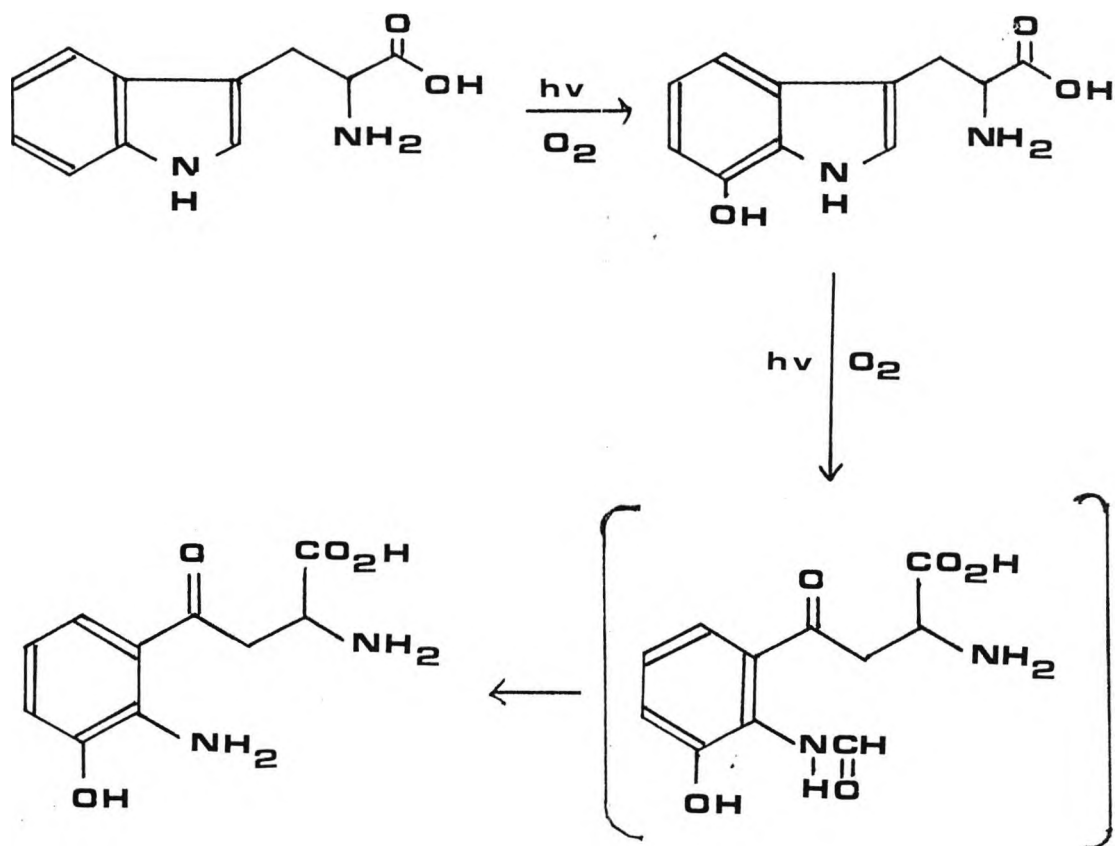
The reaction scheme is very similar to that proposed by Sun and Zigman and the restrictions for protein bound tryptophan are also applicable. One of the photoproducts would be NFK formed via the energetically unfavourable dioxetane and this compound is intensely yellow coloured ⁴⁴.

A phosphorescence quantum yield of 0.13 for the tryptophan emission of wool at 77 K indicates that considerable intersystem crossing to the tryptophan triplet occurs ⁵. It has been proposed that the triplet excited state of tryptophan and an unidentified species absorbing at 340 nm react with ground state oxygen to produce singlet excited oxygen by energy transfer -



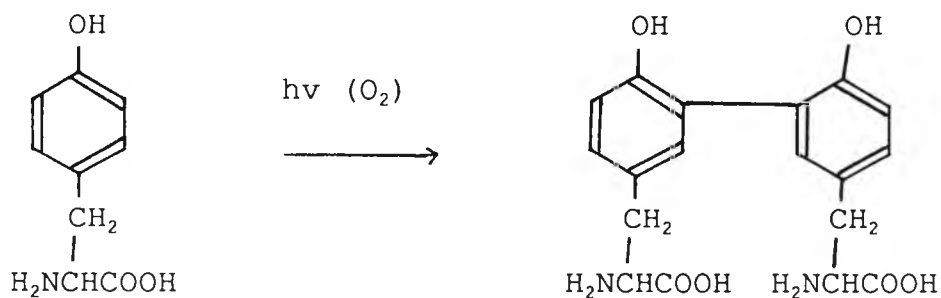
The singlet excited state oxygen then diffuses through the wool keratin to react with the amino acids histidine, tryptophan and methionine ⁴⁵. Application of a known singlet oxygen quencher, sodium azide, to wool reduced the rate of tryptophan degradation ⁵.

Lennox ⁴⁶ suggests that oxidation can take place on the benzene ring of tryptophan to give a hydroxytryptophan which on rupture of the indole ring would yield 3-hydroxykynurenine presumably via 3-hydroxyNFK. The 3-hydroxykynurenine is a yellow pigment isolated from butterfly wings ^{47,48}. Aminophenols such as



3-hydroxykynurenine and dihydroxytryptophan readily give deeply coloured tarry products and polymers related to melamin ^{49,50}.

Tyrosine can be photooxidised to dityrosine (and possibly tri and poly tyrosines) in proteins ⁵¹. A possible mechanism is the coupling of phenoxy radicals ⁵². The reaction is shown schematically below-



Dityrosine may be the unknown absorbing species at

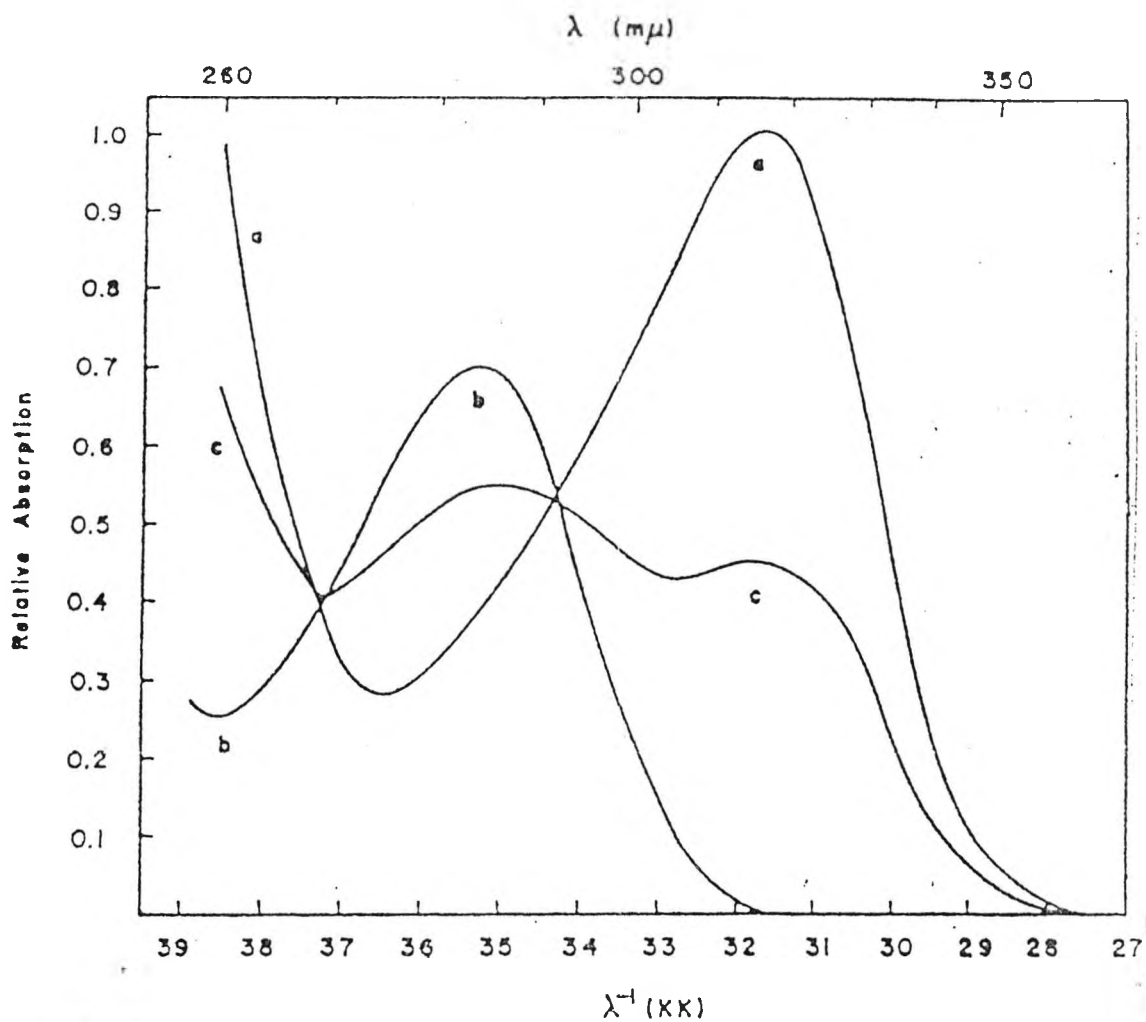


Figure 2.3 Absorption spectra of bityrosine at different pH values (a) pH 11
 (b) pH 3
 (c) pH 7

(Lehrer and Faxman ⁶¹)

340 nm. Its UV spectrum is pH dependant having a longwavelength maximal absorption at pH 7 and 11 and a higher energy absorption at pH 3 ⁶¹. The spectra are given in Figure 2.3. Dityrosine was found to be produced on heating wool as well as by irradiation ⁶⁸. When dityrosine was applied to wool and irradiated the same rate of photoyellowing as an untreated sample resulted. From this evidence it appears that dityrosine does not initiate secondary photochemical reactions ⁶⁸.

While there is considerable evidence to support the theory that singlet oxygen is involved in the yellowing of wool it must be stressed that the photochemical reactions are very complex and other reactions may be contributing to the discoloration.

2.3 Photochemistry Of Fluorescent Brightening Agents

Fluorescent Brightening Agents (FBA's) are essentially colourless fluorescent dyes used for whitening the natural cream colour of wool, paper and plastics. They absorb in the near UV and re-emit the absorbed energy as visible light. Unfortunately, their incorporation into natural protein fibres such as wool invariably promotes photodegradation and discolouration of these fibres ^{53,54}. Undoubtedly, the most popular type of FBA for wool contains the stilbene chromophore ⁵⁵. There is good evidence that stilbenes on the surface of

wool can sensitise the formation of singlet oxygen which then reacts with tryptophyl residues located some distance from the FBA ⁵⁶. A further study showed that stilbenes can both sensitise and quench singlet oxygen. The conclusion, however, was that stilbene FBA's will photosensitise the yellowing of wool and will degrade upon irradiation irrespective of whether they sensitise or quench singlet oxygen ⁵⁷.

The photolysis at wavelengths > 295 nm of a pure commercial Stilbene FBA was studied in an aqueous solution and on wool. Three main products were identified in both cases. The reaction is given by the following scheme in Figure 2.4.

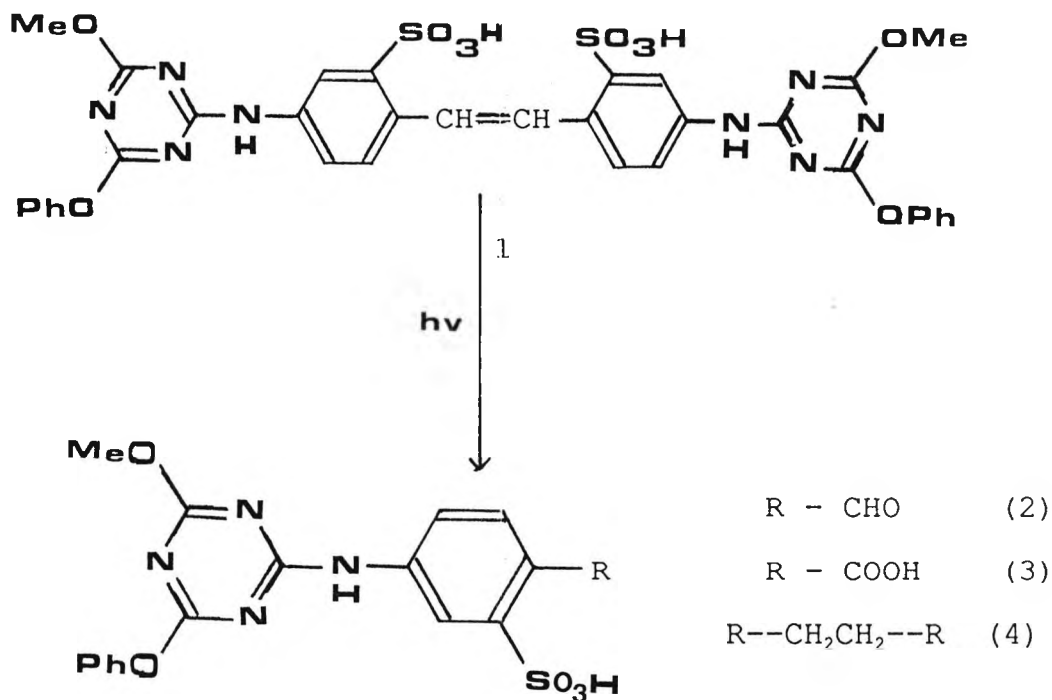


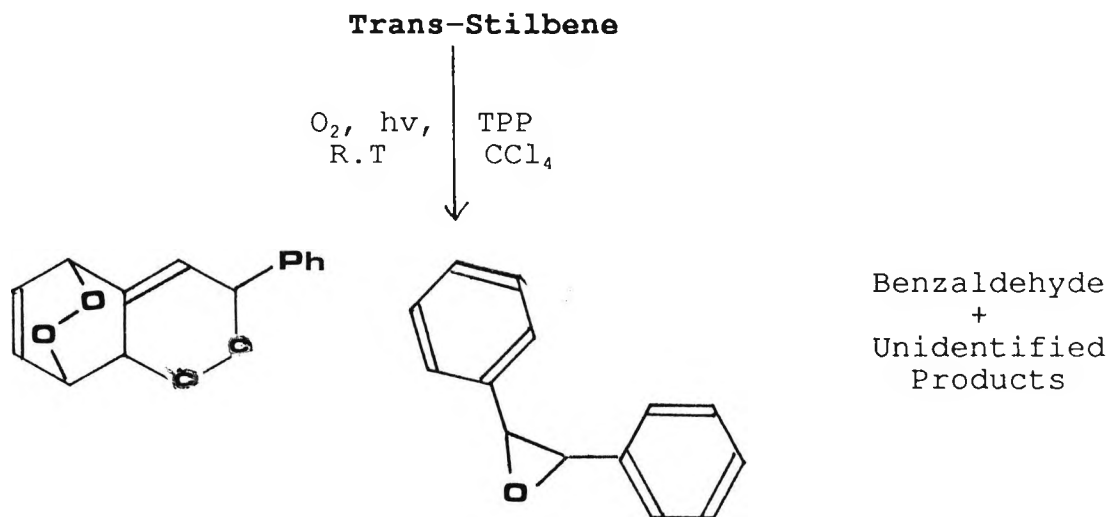
Figure 2.4 Photolysis of Stilbene FBA in aqueous solution and on wool.

The results from photolysis of aqueous solutions are discussed first. Isomerisation from the fluorescent trans to the non fluorescent cis configuration gives the main reaction product (65 %) after short irradiation times (30 minutes). The yield of the cis isomer decreases as the reaction proceeds. To a much smaller extent the aldehyde (2) is formed (0.1 % after 30 mins irradiation). It is postulated to arise from the photo-oxidation of the alkene bond presumably via a (2 + 2) cycloaddition with singlet oxygen to give a dioxetane, which then rearranges to the aldehyde. Further aerial oxidation is thought to produce the carboxylic acid (3). Even so, when the irradiation was performed for 2 hours under nitrogen approximately 4 % of the aldehyde was found thus questioning the proposed mechanism. Holt and Milligan have concluded that it was unlikely that the formation of carbonyl groups were responsible for wool yellowing²⁰. However they will undoubtedly act as a triplet sensitisers. Photoreduction of stilbenes in the presence of secondary amines has been reported to give 1,2-diphenylethanes⁵⁸ and it has been shown to occur by an electron - transfer mechanism^{59,60}. It was found that the formation of (4) from (1) transpires equally well in the presence or absence of oxygen.

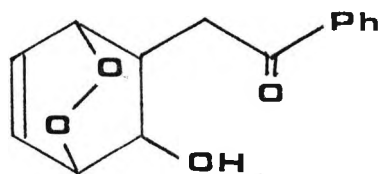
When compound (1) was applied to wool and irradiated the same photolysis products were extracted albeit in different proportions. It was noticeable that a significant proportion of the FWA became resistant to

extraction presumably due to covalent binding to the wool. In fact, the dihydro derivative (4) and nonextractable material constituted 77 % of the photolysis products after 24 hours irradiation.

With respect to the number and diversity of stilbene FWA's ⁶² it seems appropriate to discuss the reaction of singlet oxygen with this chromophore. In organic solvents the products isolated from the irradiation of trans-stilbene using tetraphenylporphyrin as sensitiser yielded a diendoperoxide, trans-stilbene oxide, cis stilbene and benzaldehyde ⁶³. The reaction scheme is given below-



A further product isolated from the base catalysed rearrangements of the diendoperoxide was the hydroxy ketone-



To explain the formation of some products the reaction was proposed to proceed through a zwitterion. An addition compound was proposed as the solvent addition product. It would be of interest to study the reaction of singlet oxygen with a commercial FBA in order to ascertain the primary reaction products. The possible reaction of these photoproducts with amino acids can be studied and evaluated. Thus the mechanism by which the FBA is bound to the protein may be further elucidated.

2.4 Protection of Wool Against Photoyellowing

A number of attempts have been made to devise treatments to protect wool from photoyellowing. These have included UV absorbers, antioxidants and reducing agents.

2.4.1 Ultra-Violet Absorbers

Ultra-violet absorbers are applied to absorb the damaging u.v. radiation and dissipate the excess energy harmlessly, usually in radiationless decay (heat for example). Three classes of compound have been investigated as potential absorbers under normal aqueous processing conditions ⁶³. The structures of the most promising compounds are given below -

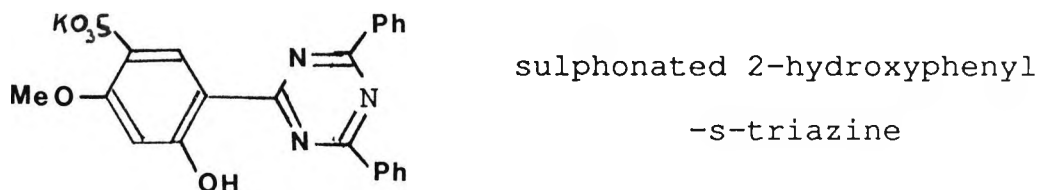
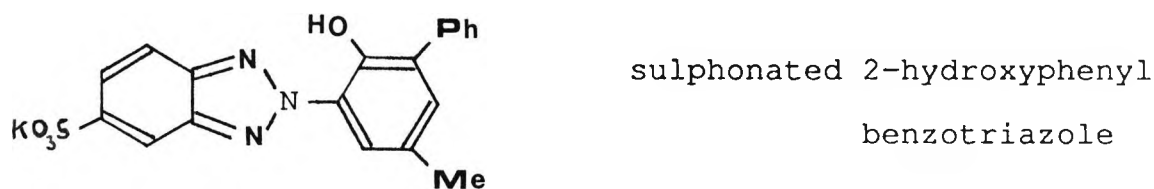
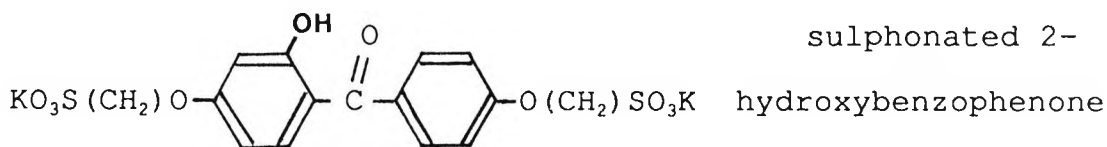


Table 2.2 summarizes the various advantages and disadvantages. These compounds have been prepared only

Property	Benzophenone	Benzotriazole	Triazine
Ease of Synthesis	***	**	*
Solubility	***	*	*
Substantivity	**	***	***
Initial Colour	**	*	***
Washfastness	**	**	***
Effectiveness			
phototendering	**	***	***
photoyellowing	*	***	***

Table 2.2 Merits of sulphonated UV absorbers.

Superiority is indicated by additional dots.

on a small scale and there is as yet no commercial production. Commercially available UV absorbers do not impart much protective effect and in fact do not usually contain the important sulphonate group which confer water solubility and protein substantivity under acidic conditions.

Unfortunately UV absorbers cannot be used to protect FWA's since they compete with the agent for UV light and thus reduce its whitening effect.

2.4.2 Antioxidants and Reducing Agents

The yellowing of wool is predominantly an oxidation reaction and so many treatments include the use of reducing agents or compounds which react with the fibre to give reducing agents. A wide range of compounds have been employed including methyl isothiocyanate ⁶⁴, thiocarboxylic acids ⁶⁵ and bisulphite ⁶⁶. Thiourea-formaldehyde has proved a more effective anti yellowing agent than other reducing agents ⁶⁷. The process minimises the photoyellowing of fluorescently whitened, as well as unwhitened wool. Unfortunately the protective effect is considerably reduced when the wool is first rinsed, but no further reduction occurs on further laundering.

2.5 REFERENCES

1. J.A. Maclaren and B. Milligan. 'Wool Science. The Chemistry and Reactivity of the Wool Fibre', Marrickville, Science Press, (1981).
2. Wool Science Review, No. 21.
3. H. Lindley and R.W. Cranston, *Biochem J*, 139, (1974), 515.
4. D.R. Goddard and L. Michaelis. *J. Biol Chem*, 112, (1935), 361.
5. C.H. Nicholls and T.M. Pailthorpe, *J.Text Inst*, 67, (1976), 397.
6. E.G. Bendit, *J.Text Inst* 51, (1960). 546.
7. C.H.Nicholls and J.I.Dunlop, *Nature*, 205, (1965), 1310.
8. S.V.Konev, 'Fluorescence and Phosphorescence of Proteins and Nucleic Acids', Plenum Press, New York, (1967).
9. J.W.Longworth, 'Excited States of Proteins and Nucleic Acids', Pleniem Press, New York, (1971).
10. J.F.Baughner and L.I.Grossweiner, *J. Phys Chem*, 81, (1977), 1249-1254.
11. I.H.Leaver, *Photochem. Photobiol*, 21, (1975), 197.
12. J.W.Longworth and C.Helini, 'Excited states of Biological Molecules', Wiley, London, (1976), p468-476.
13. L.I.Grossweiner and Y.Usui, *Photochem. Photobiol* 11, (1970), 53-56.

14. B.V.Bent and E.Hayon, J.Am Chem Soc 97, (1975), 2955-2606.
15. A.Shafferman and G.Stein, Photochem. Photobiol, 20, (1974), 399-406.
16. S.V. Konev, 'Fluorescence and Phosphorescence of Proteins and Nucleic Acids', Plenum Press, New York, (1967).
17. K.P.Ghiggino, C.H.Nicholls and M.T.Pailthorpe, J.Photochemistry 4, (1975), 155.
18. J.H.Lever, Photochem .Photobiol 27, (1978), 439.
19. A.Beybeck and J.Maybech, Photochem. Photobiol, 6, (1967), 355.
20. L.A.Holt and B.Milligan, Text Res J. 47, (1977) 620.
21. R.F.Steiner and E.P.Kirby, J. Phys Chem, 73, (1969) 4130.
22. W.F.Forbes and W.E.Savage, Photochem. Photobiol, 1, (1962), 1-13.
23. M.T.Pailthorpe and C.H.Nicholls, Photochem. Photobiol 1, (1972), 465.
24. J.Feitelson and E.Hayon, J.Phys Chem, 77, (1973), 10-15.
25. J.Feitelson and E.Hayon, Photochem. Photobiol, 17, (1973), 265-271.
26. W.Gordy and H.Shields, Rad Res, 9, (1958), 611.
27. B.C.Barkakaly and J.H.Keighley, Proc. Int. Wool Text. Res. Conf, Aachen, 11, (1976), 194.
28. M.T.Pailthorpe and C.H.Nicholls, Photochem. Photobiol, 14, (1971), 135.

29. R.Santus and L.I.Grossweiner, Photochem. Photobiol, 15, (1972), 101.
30. E.Amorizel, A.Bernan, and D.Grand, Photochem. Photobiol, 29, (1979), 1071.
31. L.A.Holt and B.Milligan, Biochem Biophys Acta, 264, (1979), 1071.
32. A.S.Inglits, I.H.Leaver and F.G.Lennox, '3rd International Wool Textile Research Conf' Paris, Section 2, 121.
33. F.G.Lennox and R.J.Rowlands, Photochem. Photobiol, 9, (1969), 359.
34. L.A.Holt and B.Milligan, J Text Inst, 67, (1976), 269.
35. L.A.Holt and B.Milligan, Aust J Biol Science, 26, (1973), 871.
36. D.Creed, Photochem. Photobiol, 39, (1984), 537-562.
37. R.S.Asquith and D.Rivett, Biochem Biophys Acta, 252, (1971), 111.
38. G.Matsuda and Nagusaki Zgakkai Zasshi, 28, (1953) 438.
39. M.Sun and S.Zigman, Photochem. Photobiol, 29, (1979), 893.
40. I.H.Leaver and F.G.Lennox, Photochem. Photobiol, 4, (1965) 491.
41. W.C.Savige, Aust J.Chem, 24, (1971), 1285.
42. M.Nakeganera, H.Watamube, S.Kudato, H.Okjima, H.Hino, J.L.Flippers and B.Withop, Proc Natl Acad Sci. U.S.A. 74, (1977), 4730.

43. W.E.Savige, Proc. Intl. Wool Text. Res. Conf. Aachen ii, (1976), 570.
44. M.Nakagawa, T.Kaneko, H.Yoshikawa and T.Hino, J. Am Chem Soc, 96, (1974), 624.
45. C.B.I.Matheson and J.Lee, Photochem. Photobiol, 29, (1979), 879.
46. G.Lennox et al. Appl. Polymer Symp 18, (1971), 353.
47. R.S.Brown and D.Becher, Tet Letts, 18, (1967), 1721.
48. T.Tokuyam et al, J. Am Chem Soc, 89, (1967), 1017.
49. H.F.Launer, Tech Wool Conf, San Francisco and Albany, California, 13-15th May, 1964, USDA Ars-74-29 (1964), 71.
50. W.E.Savige, Proc. Vth. Int. Wool. Text. Res. Conf, Aachen, ii, (1975), 570.
51. M.S.Otterburn and P.E.Gargan, J. Chromatog, 303, (1984), 429.
52. G.Dobson and L.I.Grossweiner, Trans. Faraday Soc 61, (1965), 708-714.
53. I.H.Leaver and G.C.Ramsay, Photochem. Photobiol 9, (1969), 531-6.
54. R.S.Davidson, D.King, D.M.Lewis and S.K.Jones, JSDC, 101, (1985), 291-294.
55. M.Zahradnik, 'The Production and Application of Fluorescent Brightening Agents', Chichester, West Sussex, John Wiley and Son, 1982.
56. I.H.Leaver, Photochem. Photobiol, 27, (1978), 451-456.

57. R.S.Davidson, G.M.Ismail and D.M.Lewis, JSDC, 103, (1987), 261.
58. M.Kaivanini and K.Matsunaga, Chem Comm, (1972), 313.
59. F.D.Lewis and T-I Ito, J. Am Chem Soc, 99, (1977), 7991.
60. F.D.Lewis, Acc Chem Res. 12, (1979), 152.
61. S.S.Lehrer and G.D.Faxman, Biochemistry, 6, (1967), 757.
62. A.E.Siegrist, H.Hofti, H.R.Meyer and E.Schmidt, Rev Prog Coloration, 17, (1987), 39-55.
63. L.A.Holt, I.H.Leaver, B.Milligan, P.J.Waters and J.F.K.Wilshire, Proc. 7th Intl. Wool Res. Conf (Tokyo), iv, (1985), 31.
64. B.J.Caldwall and B.Milligan, Text Res Journal, 40, (1974), 23.
65. J.E.Tucker, Text Res Journal 39, (1969), 830.
66. L.A.Holt, B.Milligan and L.J.Wolfram, Text Res Journal, 44, (1974), 846.
67. B.Milligan and J.E.Tucker, Text Res Journal, 34, (1964), 681.
68. K.Roper and E.Finnimore, Proc. 7th Int. Wool Tex. Res. Con, Tokyo, iv, (1985), 21.

CHAPTER 3

SYNTHESIS AND APPLICATION TO WOOL OF A FLUORESCENT BRIGHTENING
AGENT AND AN AZO DYE CONTAINING POLYAMINE SIDECHAINS

3.1 INTRODUCTION

Reactive dyes and Fluorescent Brightening Agents are widely used for dyeing textile fibres ^{1,2}. They are designed to form covalent bonds with the fibre and so augment other bonding forces such as electrostatic, non-polar, Van der Waal and hydrogen bond interactions. Many reactive groups have been developed and those commercially available for dyeing wool are given in Table 3.1.

In practice not all the dye is covalently bound to the fibre. There are two principle reasons for this :- (i) the reactive group is deactivated by hydrolysis in the dye bath, and (ii) some of the original dye may fail to react either with the fibre or with water. Both hydrolysed and unreacted dye are less firmly bound to the wool than the covalently bound dye. Therefore the best reactive dyes are those which react primarily with the fibre. This property is readily quantified by evaluating dye fixation and is easily found by subtracting the amount of unbound dye from the total dye uptake.

Studies with model compounds such as amines , thiols, phenols, alcohols and amino acid derivatives have been used to ascertain which of the functional side chains of wool are capable of reaction with reactive dyes. The general conclusion was that cysteine, lysine, histidine

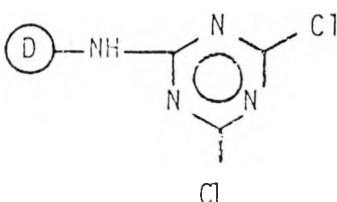
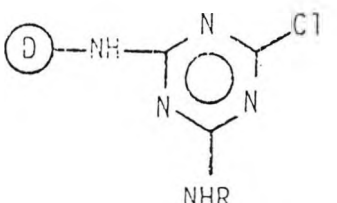
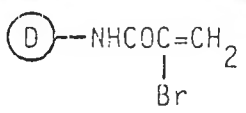
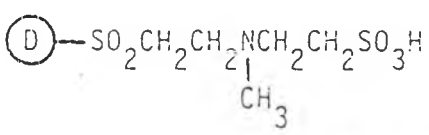
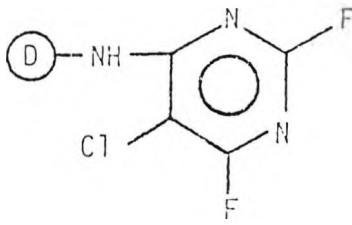
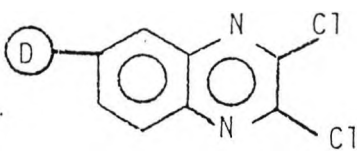
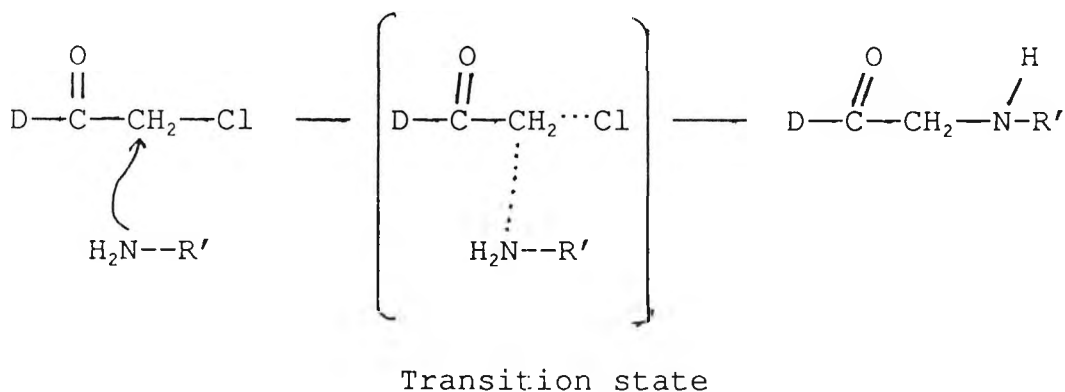
Vinyl sulphone	$\text{D}-\text{SO}_2\text{CH}=\text{CH}_2$	Solidazol N
B-Sulphatoethylsulphone	$\text{D}-\text{SO}_2\text{CH}_2\text{CH}_2\text{SO}_3\text{H}$	Remazol/Remalan
Chloroacetamide	$\text{D}-\text{NHCOCH}_2\text{Cl}$	Cibalan Brilliant
Dichlorotriazine		Procion M
Monochlorotriazine		Procion H Cibacron
Acrylamide	$\text{D}-\text{NHCOCH}=\text{CH}_2$	Procilan
α -Bromoacrylamide		Lanasol
Methyltaurinoethylsulphone		Hostalan
Monochlorodifluoropyrimidine		Verofix Reactolan Drimalan F
2,3-Dichloroquinoxaline		Levafix E

Table 3.1 :- Structure of the reactive group in many of the commercially available reactive dyes which can be applied to wool.
(Maclaren and Milligan ³)

and N-terminal residues were the main sites of reaction regardless of the type of reactive dye used ³. To a lesser extent, threonine, serine and tyrosine can also form covalent bonds ⁴.

The reaction of wool with the reactive dyes in Table 3.1 can be divided into two mechanistic classes. Both reaction mechanisms are discussed below :-

(i) Nucleophilic Substitution Reactions :- These reactions are best described as nucleophilic attack by a lone pair of electrons from an amino acid in the wool on an electron deficient carbon atom in the reactive group. Usually the carbon centre is activated by electron withdrawing moieties adjacent to it such as C=O, SO₂ and direct bonding to a good leaving group. The leaving



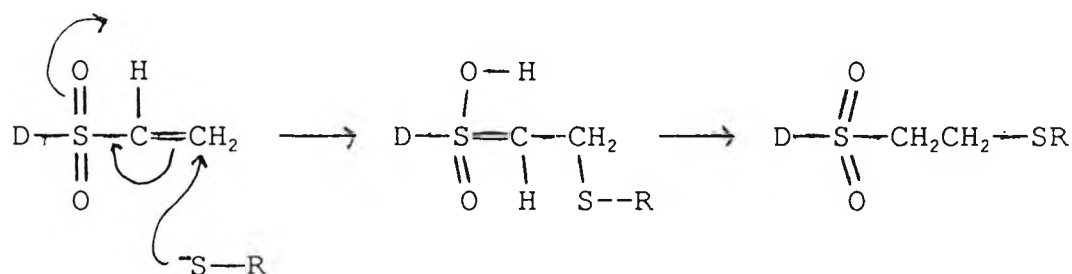
D -- Chromophoric centre

Scheme 3.1 : - Reaction of a chloroacetamide dye with an amine.

group is normally a halide.

For example, such a system is given in Scheme 3.1 which shows the reaction of a chloroacetamide dye with a primary amine. The mechanism is bimolecular and usually named an S_N2 reaction for substitution, nucleophilic, bimolecular.

(ii) Michael Addition :- This is attack by a lone pair of electrons from a nucleophilic site in an amino acid on the end of a conjugated system. The double bond is necessarily activated by the presence of electron withdrawing units such as $C=O$, CN or SO_2 . An example is given in Scheme 3.2 which shows the addition



D -- chromophoric centre

Scheme 3.2 :- Michael addition of a thiolate anion to a vinyl sulphone.

of a thiolate anion to a vinyl sulphone dye. The overall reaction is termed a 1,2 addition.

Reactive dyes for wool have now been available for nearly

twenty years and their use is continuing to increase albeit slowly. Advantages include their brilliance of shade, high wet fastness, reproducibility of shade ⁵ and possible protection of the fibre against hydrolytic damage during dyeing ⁶. Disadvantages are problems of clearing unfixed dyes to achieve maximum fastness in full depths and restrictions due to lack of levelness when dyeing wool in piece form. Most reactive dyes are powders and this introduces hazards for workers handling these compounds. The RSC is in the process of producing a safety booklet regarding the safe use of these dyes ⁷. It is envisaged that the textile industry will become more safety conscious with the use of potentially hazardous chemicals. Dye bath effluent discharges are also coming under stricter control as environmental issues increase in importance. Improvements are needed either by improving the degree of covalent bonding between dye and fibre thus reducing the need for an alkaline after treatment or by designing novel non-damaging after treatments ⁵. However this still does not overcome the hazardous nature of reactive dyes.

We have taken a novel approach in attempting to solve both problems. Our strategy is to take a reactive dye and form dye-polyamine adducts which can be crosslinked to the fibre. Several advantages were predicted :-

- (i) the hazardous nature of the reactive group would be removed.

- (ii) non crosslinked dye can be readily removed by an aqueous wash thus making an after treatment unnecessary.
- (iii) good wash fastness due to high dye - fibre bonding
- (iv) the polyamine will aid dye uptake
- (v) water insoluble dyes can be modified thus increasing the range and type of dyes available to wool.

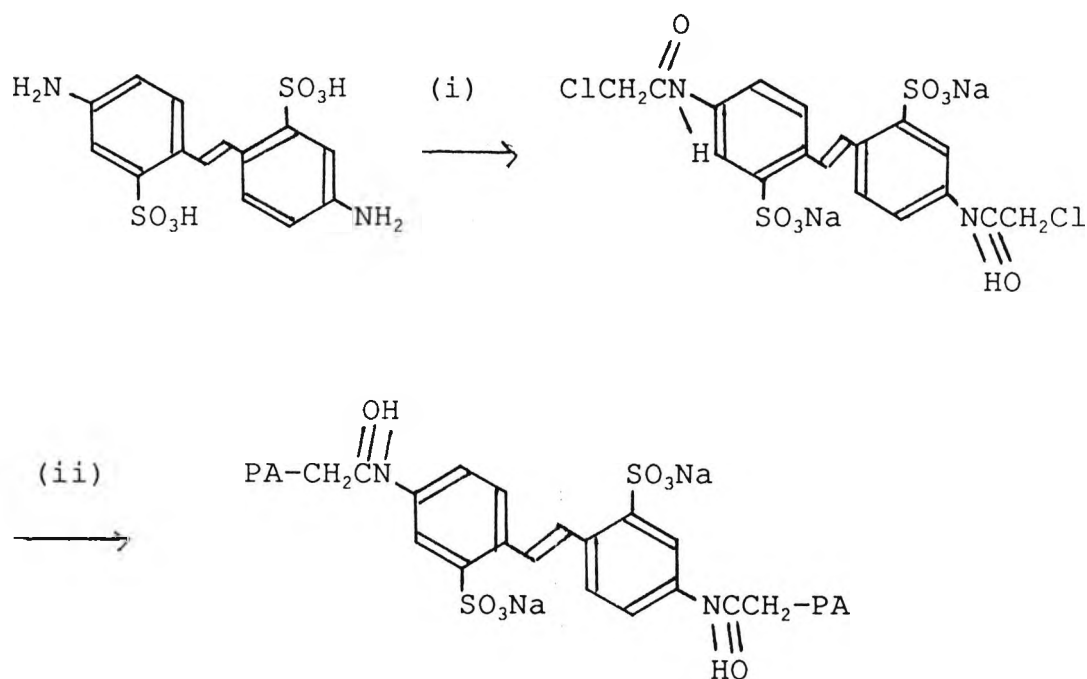
Wool has previously been pretreated with tetraethylpentamine under mild conditions and relatively low add on levels (ca 1 % owf) have been shown to increase significantly the rate of exhaustion of a premetallised dye applied under isothermal conditions. Application of ¹⁴C labelled spermine has shown that a small amount remains fixed to the fibre after extensive extraction ²⁹.

This chapter describes the synthesis of a reactive fluorescent brightening agent and an azo dye. They are then reacted with a series of polyamines, applied to wool and crosslinked with formaldehyde. The dye uptake was measured spectrophotometrically and wash fastness assessed by extraction with solvents of differing severity.

3.2 RESULTS

3.2.1. Synthesis of Fluorescent Brightening Agents

A range of Fluorescent Brightening Agents (FBA's) based on the 4,4'-diaminostilbene-2,2'-disulphonic acid (DAS) were synthesised according to Scheme 3.3. The intermediate 4,4'-dichloroacetamidostilbene-2,2'-disulphonic acid sodium salt (DCDAS) was obtained in 80-90 % yield and characterised by ^1H nmr and ir spectroscopy.



PA- polyamine

Scheme 3.3 :- Synthetic scheme for FBA's containing polyamine sidechains. (i) $\text{ClCH}_2\text{COCl} / \text{NaHCO}_3$

(ii) PA / NaOH

However, acceptable elemental analysis data was difficult to obtain due to the presence of water even after rigorous drying. Analytical Thin Layer Chromatography (TLC) on silica plates and paper strips proved difficult

because of extensive tailing. This tailing was attributed to the compound being present as its sodium salt. Reversed Phase Total Ion Pairing High Performance Liquid Chromatography (RPTIPHPLC) has previously been applied to the analysis of sulphonated compounds⁸. A series of chromatograms showing the power of this technique is given in Figure 3.1. The first two chromatogram shows that the starting material contains no major impurities and that DCDAS was pure (99 %).

The reaction of DCDAS with amines went smoothly under mild conditions. Thus five adducts were formed with the following amines :

$\text{H}_2\text{NCH}_2\text{CH}_2\text{NH}_2$	1,2-diaminoethane
$\text{H}_2\text{NCH}_2\text{CH}_2\text{CH}_2\text{NH}_2$	1,3-diaminopropane
$\text{H}_2\text{N}(\text{CH}_2\text{CH}_2\text{NH})_2\text{H}$	diethylenetriamine
$\text{H}_2\text{N}(\text{CH}_2\text{CH}_2\text{NH})_3\text{H}$	triethylenetetramine
$\text{H}_2\text{N}(\text{CH}_2\text{CH}_2\text{NH})_4\text{H}$	tetraethylenepentamine

Analysis of the reaction mixtures by TIPHPLC indicated that one major ($\approx 95\%$) and several minor products were present. An example of the diaminoethane adduct is given Figure 3.1. As the number of amine groups increased then the number of impurities increased. As before, these adducts could be characterised by ^1H nmr and ir spectroscopy but no reproducible elemental analysis was obtained, possibly because of the presence of inorganic impurities.

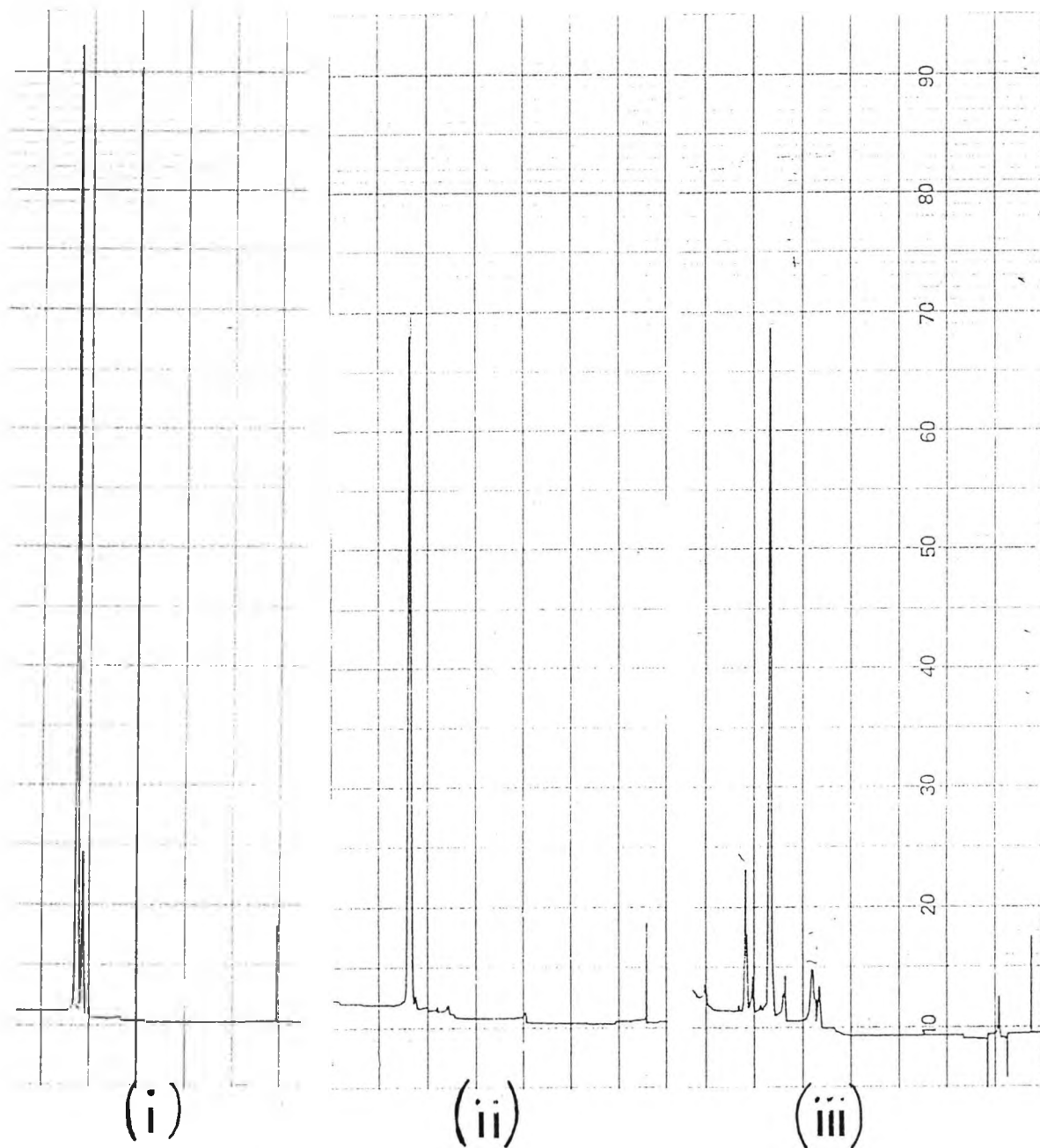


Figure 3.1 :- Chromatograms of :-

- (i) starting material 4,4-diaminostilbene-2,2'-disulphonic acid sodium salt (DAS),
- (ii) 4,4'-dichloroacetylaminostilbene-2,2'-disulphonic acid sodium salt (DCDAS),
- (iii) DCDAS - 1,2-diaminoethane adduct.

3.2.2 Application of FBA's to Wool

The results are very similar and are presented in full in appendix 1. Therefore, rather than present them all, a representative example which gives average values is chosen to illustrate the salient points.

The adducts could be applied to bleached wool by a standard exhaustion method and dye uptakes of 50 - 80 % were recorded. Generally, the treated wool appeared yellower than untreated wool. Total diffuse reflectance spectra of treated and untreated wool shows that the FWA is in some way bound to the wool surface. A typical spectrum is given in Figure 3.2. It can be clearly seen that the dye reflection tails strongly into the visible region of the spectrum and this accounts for the wool's yellow appearance. A more quantitative approach was to compare the yellowness index (Y.I) values and these are given in Table 3.2. Low Y.I numbers are indicative of white wool where as high values represent discoloured wool. Simple observation of the samples under 366nm U.V light showed that they were fluorescent. Solid sample fluorimetry catalogued the emission as a broad structureless signal with a maximum at 440 nm. The fluorescence emission was less intense than that of a commercially available product, Photine HV.

Fixation of the FBA was achieved by crosslinking the polyamine side chains with formaldehyde and a thiourea /

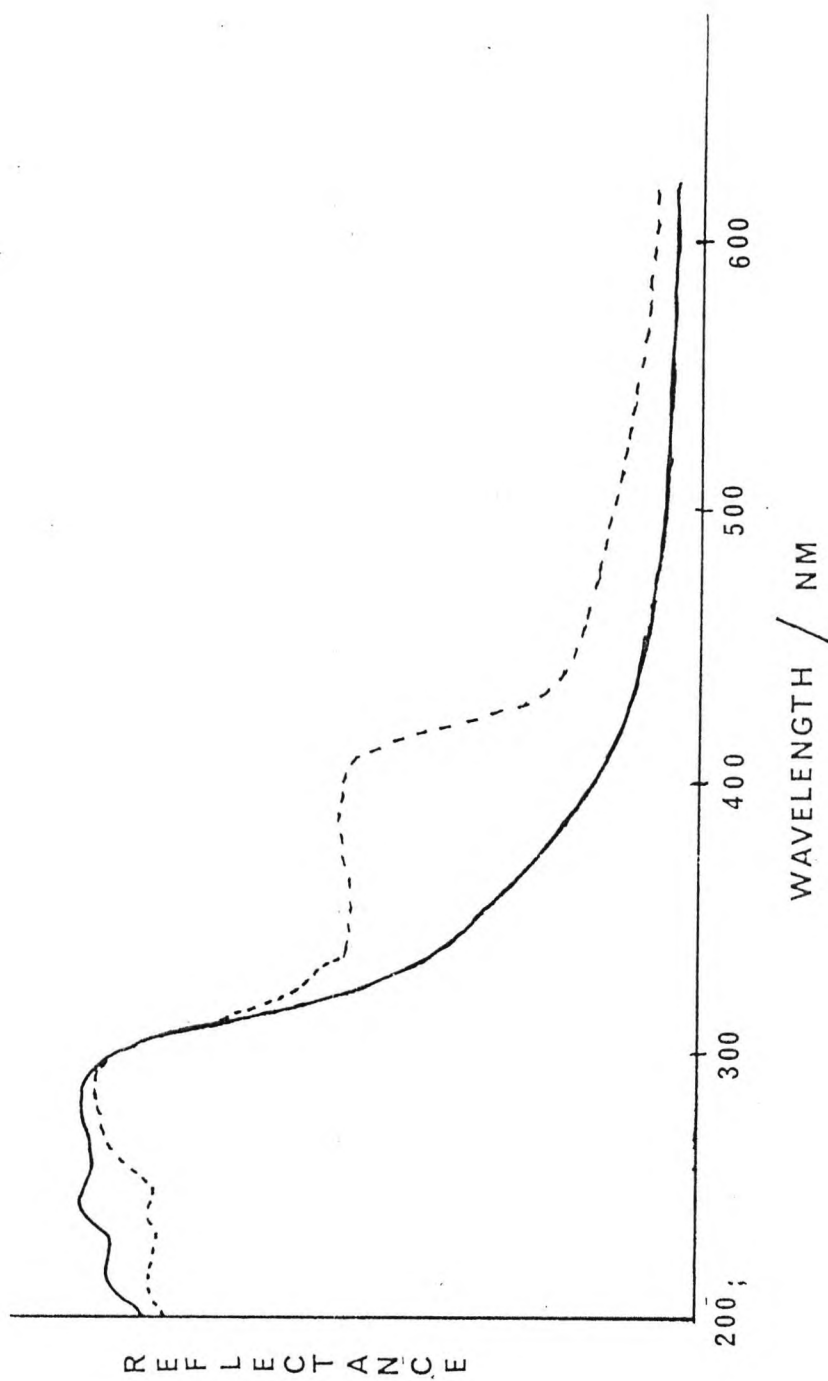


Figure 3.2 :- Total Diffuse Reflectance spectrum of wool (—), and the DCDAS - 1,2-diaminoethane adduct applied to wool (-----).

formaldehyde (TUF) precondensate under Pad - Batch conditions. The crosslinking treatment slightly lowered

Application Conc % O.W.F	Yellowness Index		
	Before Fixation	Formaldehyde Fixation	TUF Fixation
0	10.8	10.2	10.2
0.2	12.4	11.7	11.6
0.4	12.6	12.2	12.5
0.6	12.2	12.2	11.8
0.8	12.9	12.5	12.4
1.0	14.3	13.4	12.3

Table 3.2 :- Y.I results for the diaminoethylene adduct treated wool.

the Y.I values (Table 3.2). Extraction of the FWA was carried out with boiling 25 % aqueous pyridine. Solid sample fluorescence clearly shows the increased amount of crosslinked FBA remaining on the wool surface compared to uncrosslinked FBA. An example of the spectra obtained are given in Figure 3.3. One surprising observation that emerged from the light fastness tests was that FBA-TUF treated wool whitened on irradiation. Usually FBA treated wool discolours very quickly and this was found for the formaldehyde crosslinked adducts. Comparison of the lightfastness results at standard 5 for crosslinked and uncrosslinked diaminoethane FBA are given in Table

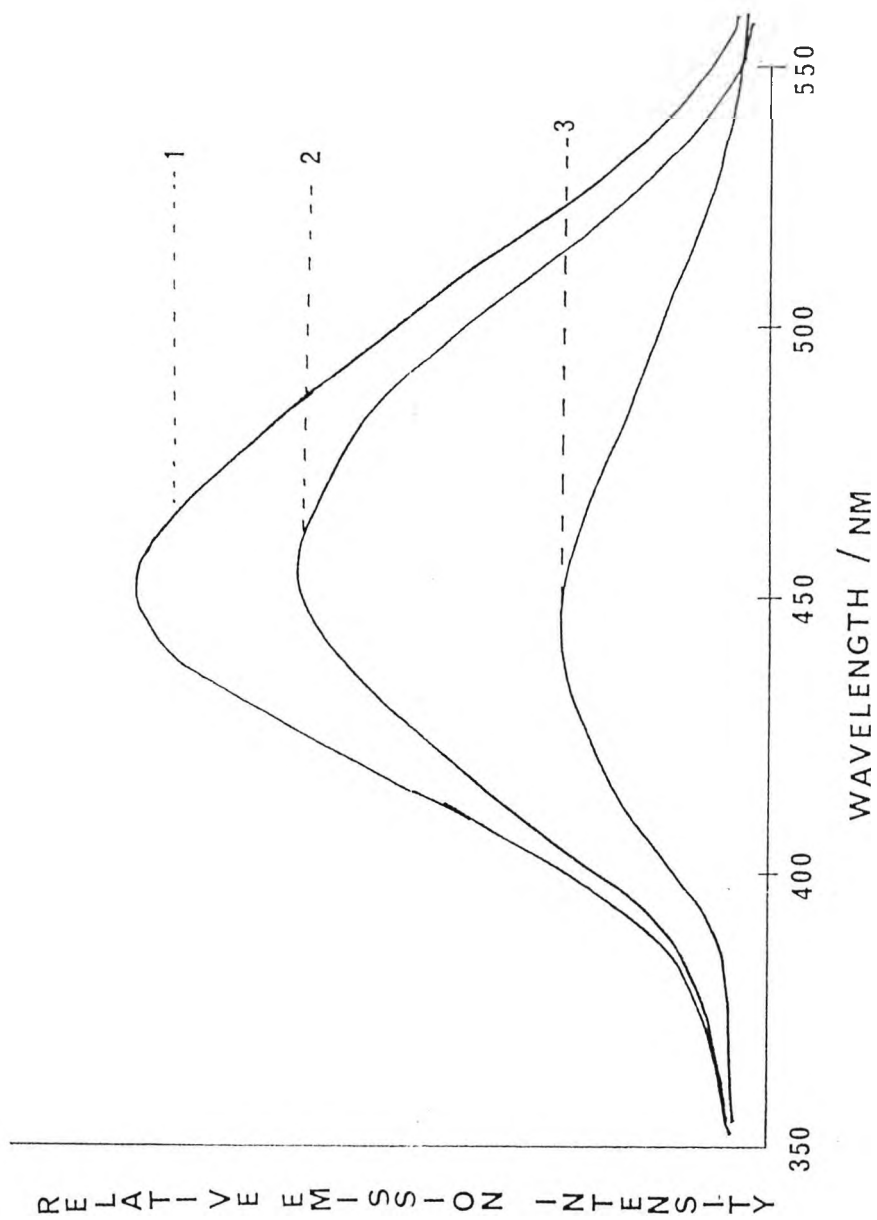


Figure 3.3 :- Solid sample fluorescent spectra of wool treated with DCDAS- 1,2-diaminoethane FBA:

1. uncrosslinked and unextracted,
2. crosslinked with formaldehyde and extracted with aqueous pyridine,
3. uncrosslinked and extracted with aqueous pyridine.

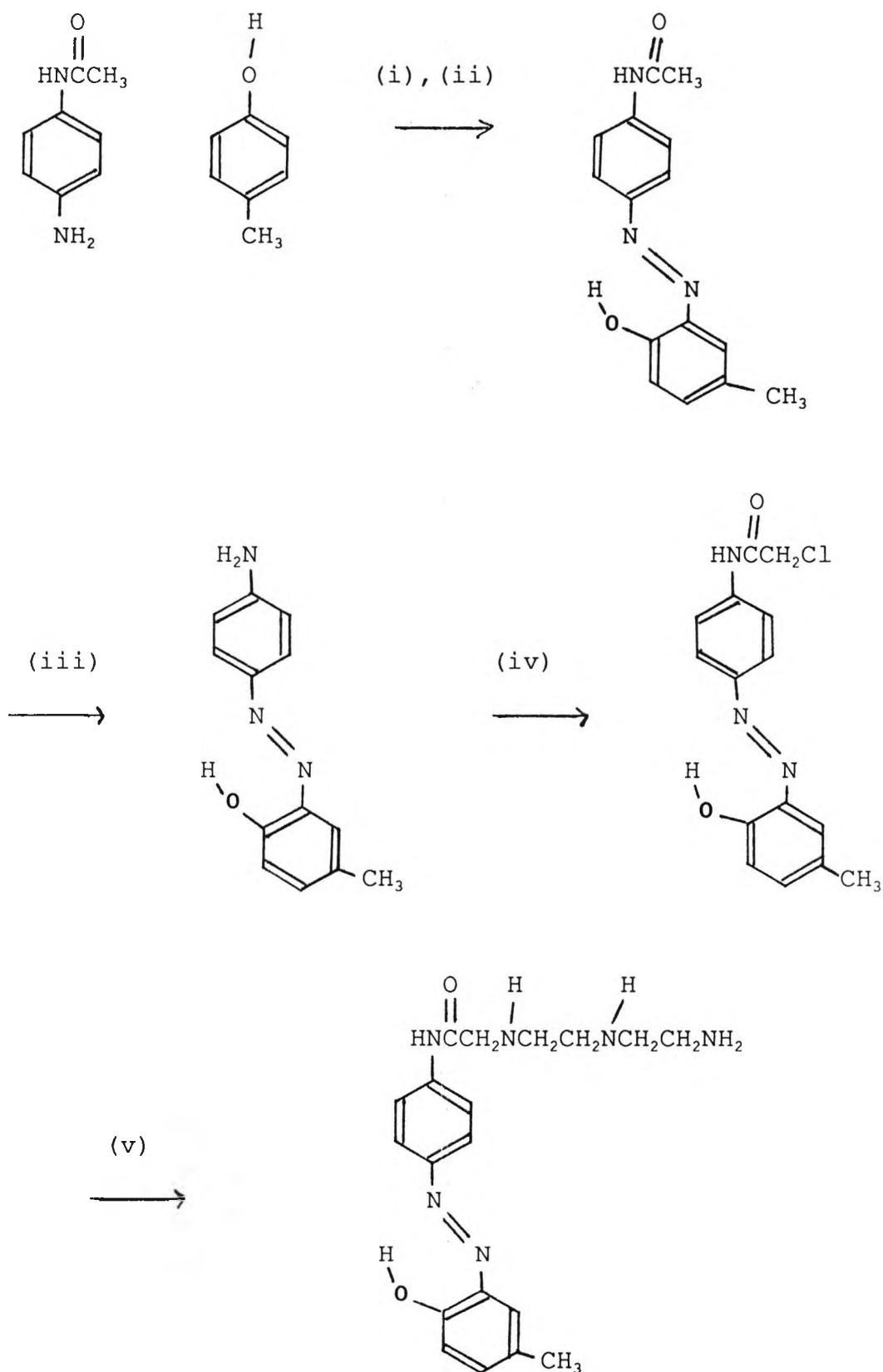
3.3. In both cases no fluorescence was observed when the returned samples were placed under 366 nm light indicating the fluorophore had been destroyed.

FBA Concentration (% O.W.F)	Lightfastness Results		
	FBA	FBA+Form	FBA+TUF
0	4-5	4-5	5
0.2	4-5	4-5	4-5
0.4	4-5	4-5	5
0.6	4	4	5
0.8	4	4	5
1.0	4	4	4-5

Table 3.3 :- Lightfastness results at Standard 5 for the diaminoethane - FBA

The polyamine side chains decreased the fluorescence intensity of the FBA to such an extent that the wool appeared yellow. Thus the object of an FWA had been defeated, however, this property will not affect the absorption characteristics of a dye and so these other chromophores should be readily amenable to this treatment. To test this idea a water insoluble azo dye was synthesised, reacted with diethylenetriamine, applied to wool from an aqueous media and crosslinked with formaldehyde as above.

3.2.3 Synthesis of Polyamine-Azo Dye



Scheme 3.4 :- Synthesis of polyamine-azo dye.

Reagents:- (i) HCl / NaNO₂, (ii) NaOH, (iii) NaOH / H₂O,
 (iv) ClCH₂COCl, (v) Diethylenetriamine

The reactive dye was synthesised in three steps according to Scheme 3.4. Each step gave high crude yields and purification was readily achieved by recrystallisation. Good analytical data was obtained on each product. Alternatively the crude intermediates could be used without purification and the pure reactive dye obtained in 90 % yield. The dye reacted smoothly with a 10 fold excess of diethylenetriamine at room temperature to give a water soluble product. Unfortunately the dye - polyamine adduct proved impossible to isolate in a pure state. No way could be found to remove excess polyamine from the reaction mixture. The polyamine imparted properties to the dye that are characteristic of diethylenetriamine, thus solvent extraction failed because both compounds were soluble in the same solvents. When subjected to column chromatography some diethylenetriamine eluted with the dye - polyamine adduct. Analytical TLC only gave one spot and it was assumed that the reaction mixture contained predominantly the mono alkylated amine. The dye was used as a solution in excess polyamine when applied to wool.

3.2.4 Application of Polyamine-Dye To Wool

The polyamine - azo dye was applied from aqueous media at pH 6 with no dye bath additives under exhaustion conditions at 60 and 100°C. Dye uptake was measured

spectroscopically and found to be 80 % at 60°C and 70 % at 100°C. The dye fixation with formaldehyde (50 and 200% O.W.F) was carried out by exhaustion at the temperature of application. During this process some dye was extracted from the wool as seen by the pale yellow appearance of the remaining bath liquor. Extractions were carried with boiling solvents of differing severity. The three solvents were (i) water (ii) water / methanol / n-butanol, 1:1:1, (iii) water / n-butanol / glacial acetic acid 1:1:1, and the results are summarised in Table 3.4 and 3.5. A gentle solvent such as water

Extraction Solvent	Dye Extracted (%)	
	Uncrosslinked	Crosslinked
H ₂ O	2	2
H ₂ O / n-BuOH / MeOH (1:1:1)	80	80
H ₂ O / n-BuOH / AcOH (1:1:1)	100	100

Table 3.4 :- Extracted dye (%) from wool treated at 60°C

removed a small amount of dye from the wool treated at 60°C. The more organic based solvent water /methanol/ butanol removed approximately 80% of the dye. All the dye was removed when samples were extracted with the most severe solvent water/n-butanol/glacial acetic acid.

When the dyeing and crosslinking was carried out at 100°C then the dye proved more resistant to extraction by

these solvents than the lower temperature application. The data is given in Table 3.5. No dye was removed in boiling water and under more severe conditions a large proportion of the dye remained bound to the wool. This

Extraction Solvent	Dye Extracted (%)	
	Uncrosslinked	Crosslinked
H ₂ O	0	0
H ₂ O / MeOH / n-BuOH (1:1:1)	70	25
H ₂ O / n-BuOH / AcOH (1:1:1)	95	45

Table 3.5 :- Extracted dye from wool treated at 100°C

is readily seen in the diffuse reflectance spectra given in Figure 3.4. The example given is that of wool dyed at 100°C divided into two samples one of which was crosslinked and then extracted with water/ n-butanol/ glacial acetic acid. The uncrosslinked dye is readily removed and its spectrum closely resembles undyed wool. Conversely, a large proportion of the dye remains on the formaldehyde crosslinked sample. An initial experiment showed that the procedure could be performed in one step with excellent dye uptake. No extraction experiments were performed and it is not clear how efficiently the dye was bound.

Following on from the earlier work it was decided to examine the effect of anti yellowing agents on dye

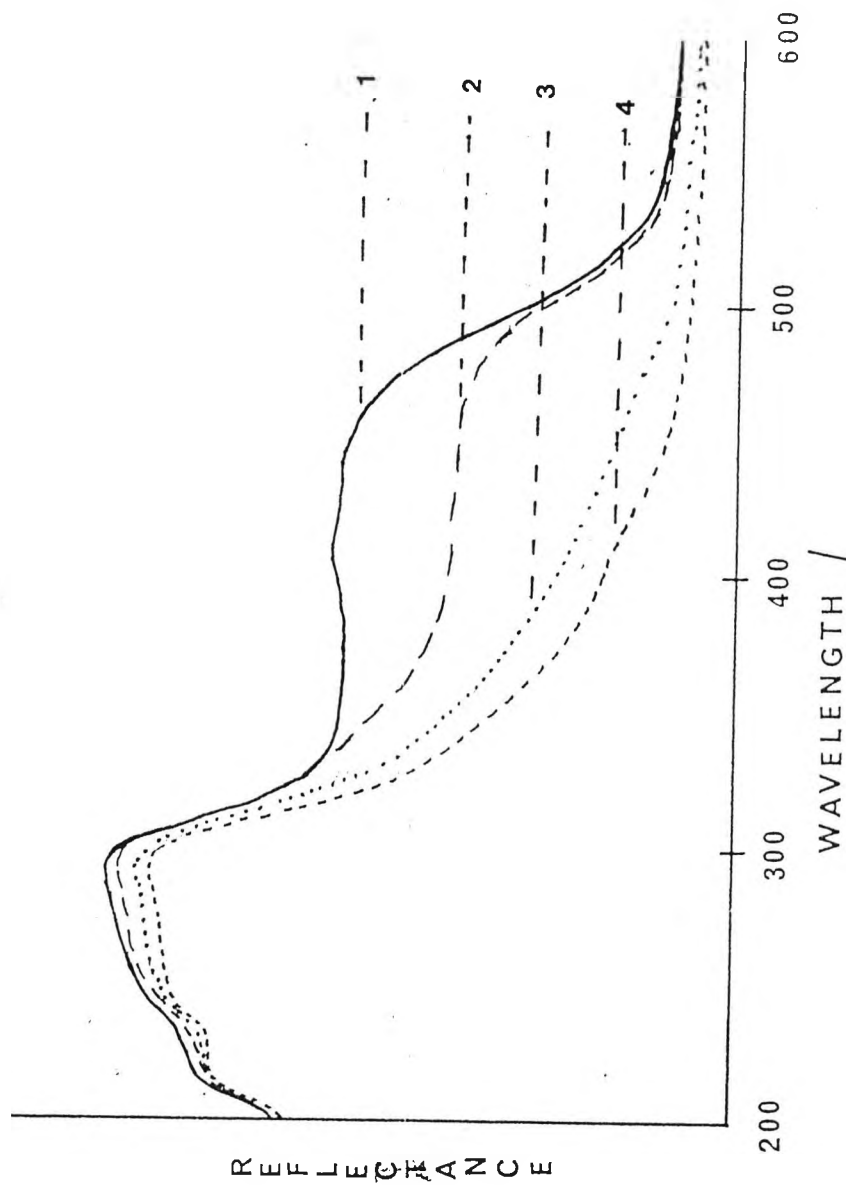


Figure 3.4 :- Total diffuse reflectance spectra of :-

1. wool dyed with the azo-polyamine adduct at 100°C
2. crosslinked adduct which has been extracted with water/methanol/glacial acetic acid 1:1:1
3. uncrosslinked adduct which has been extracted as above
4. wool

stability. Thus the dye - polyamine adduct was treated with TUF precondesates, a phosphonous acid / formaldehyde solution and various mixtures of thiourea/formaldehyde/ phosphonous acid by a Pad - Batch technique and under exhaustion conditions. The samples were submitted to Xenotest light fastness tests at standard 3 and 5. The antiyellowing solutions are given in Table 3.6 together with the lightfastness results. At standard 3 all the treated samples faded slightly more than the untreated.

Antiyellowing Soln conc (% O.W.F)	Application method	Lightfastness test	
		Std 3	std 5
Untreated	Pad-Batch	3+	3-4
Thiourea (50)/Form (40)	Pad-Batch	2	2
Thiourea (10)/Form (8)	Pad-Batch	2-3	3
Thiourea (2) /Form (4)	Pad-Batch	2-3	3
H ₃ PO ₂ (10) / Form (32)	Pad-Batch	2-3	3
Thio (10)/H ₃ PO ₂ (10) / Form (32)	Pad-batch	2-3	3
Thiourea (25)/Form (25)	Exhaustion	2-3	2
Thio (25)/Form (50) / H ₃ PO ₂ (25)	Exhaustion	3	3
H ₃ PO ₂ (25) / Form (25)	Exhaustion	3	3

Table 6 :- Application of antiyellowing solutions to the dye - polyamine treated wool and the lightfastness results. (Form -formaldehyde, Thio- thiourea)

Under the test conditions there seems to be no dependence on the antioxidant concentration, for example, dyed wool treated with thiourea at 50 and 2 % O.W.F fades to the same degree. However a more pronounced effect is observed at standard 5 where the treated dyed wool fades much more than untreated wool. Visually this fading is quite striking at high thiourea concentrations (50, 25 and 10 % O.W.F) as the dye has been completely destroyed and the wool appears white with no tinge of yellow. There are some traces of dye remaining after the other treatments. The dye destruction does not appear to depend on the method of antiyellowing solution application. Both treatments end with the dye being more faded than the blank. Visually and substantiated by the figures, it emerges that higher thiourea concentrations inflict greater dye damage.

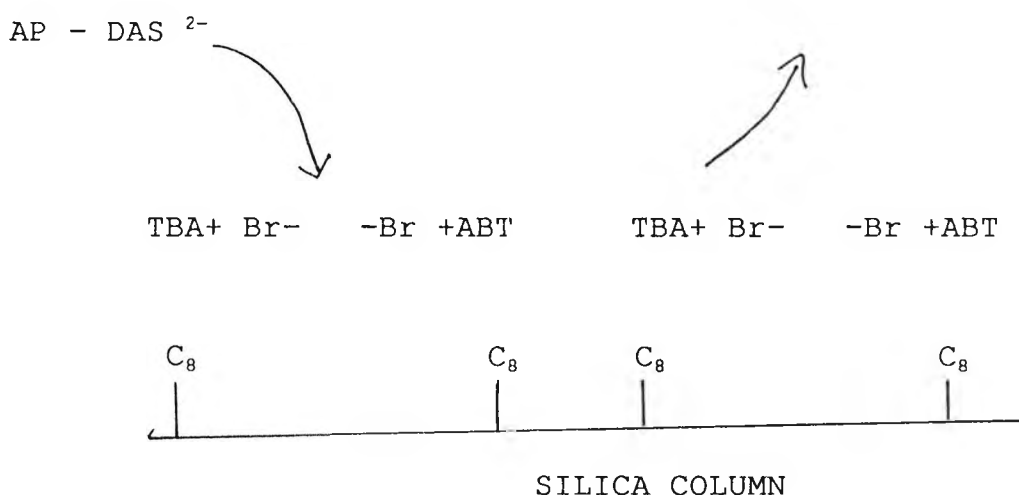
3.3 DISCUSSION

3.3.1 Synthesis and HPLC Analysis Of The FBA's

DAS based dyes have two negatively charged centres and are highly polar entities. The TLC analysis on silica failed to give any separation because of this charged nature. To separate ionic or ionisable molecules Ion-pair partition chromatography is the technique of choice ⁹. Hence, Analytical Reverse Phase Ion Pair Partition chromatography seemed to be advantageous in determining

their purity. This technique uses a chemically bonded silica support with an aqueous phase containing the required basic counter ion. The counter ion used was tetrabutylammonium bromide (TBABr) which is a quaternary ammonium salt. This is attracted to the bonded silica by Van der Waals forces and can become attached. The actual chemistry of the partitioning is complex and has not yet been fully elucidated but it is thought to be due to one or both of the following mechanisms;

(i) Ion Exchange



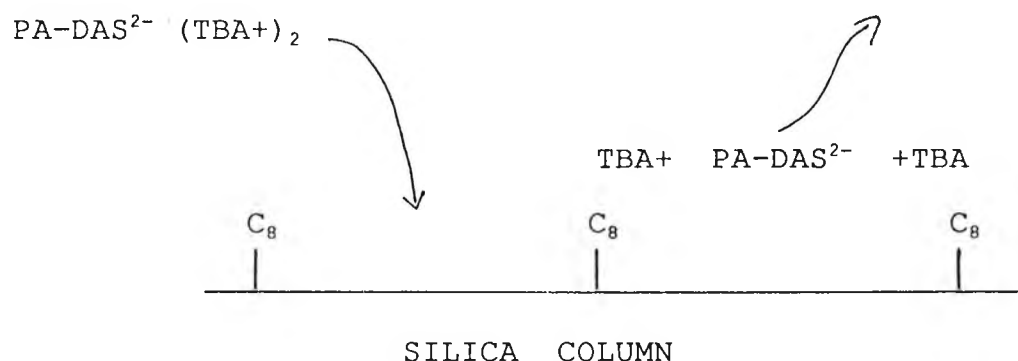
The bonding of TBABr to the C₈ column hydrocarbon phase forms in-situ ion exchange sites. At these sites the DAS dyes undergo ion exchange of two sodium atoms for two tetrabutylammonium cations. Separation is achieved by a dynamic ion exchange mechanism.

(ii) Ion-pair partition

The tetrabutylammonium bromide undergoes ion exchange with the sodium salt of the DAS dyes to give sodium bromide and tetrabutylammonium-DAS adducts in the mobile medium.



The ions can then partition between the stationary and mobile phases.

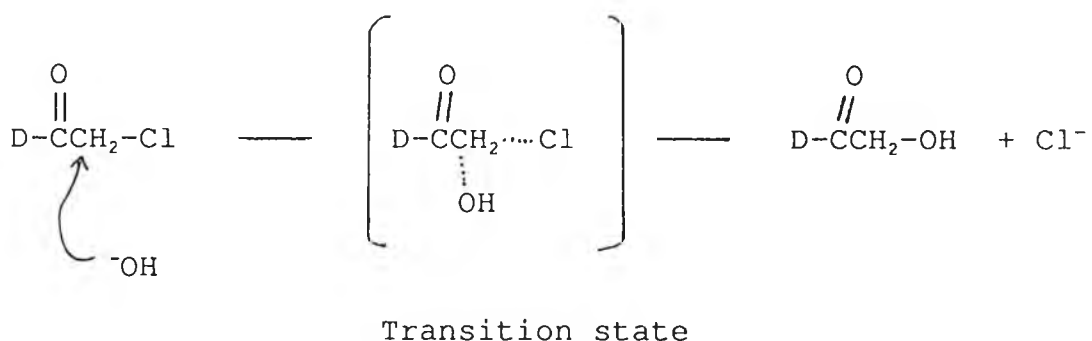


From the above mechanism it is thought that the TBA-DAS ion pair formed in the eluent bonds to the hydrocarbon in the column. This results in a dynamic ion-pair partition mechanism operating.

Reference to the chromatograms in Figure 3.1 illustrates the resolution associated with this technique. The starting material is resolved into one major and minor peak which are postulated as the trans and cis isomers respectively. It is unlikely that impurities are present because the starting material gave a correct elemental analysis.

The expected group frequencies were found in the I.R spectrum for dichloroacetamidostilbene-2,2'-disulphonic acid sodium salt (DCDAS). Most prominent were the C=O and S=O stretches. The ^1H nmr spectrum demonstrated that only one product was present. This was confirmed by HPLC analysis (Figure 3.1).

The same diagnostic I.R peaks as above were found in the FBA-polyamine adducts spectra. The ^1H nmr spectra had several peaks appearing as broad overlapping signals which signifies some impurities. This was confirmed by HPLC. Minor peaks found in the chromatographic analysis of the DCDAS / polyamine reaction mixture can postulated as the products of several competing reactions. For example, one reactive group may undergo hydrolysis or react with the polyamine through a secondary amine group whilst the second group reacts via a primary amine. Dimers and possibly trimers can be formed from two chromophores and a polyamine. The polyamine is present



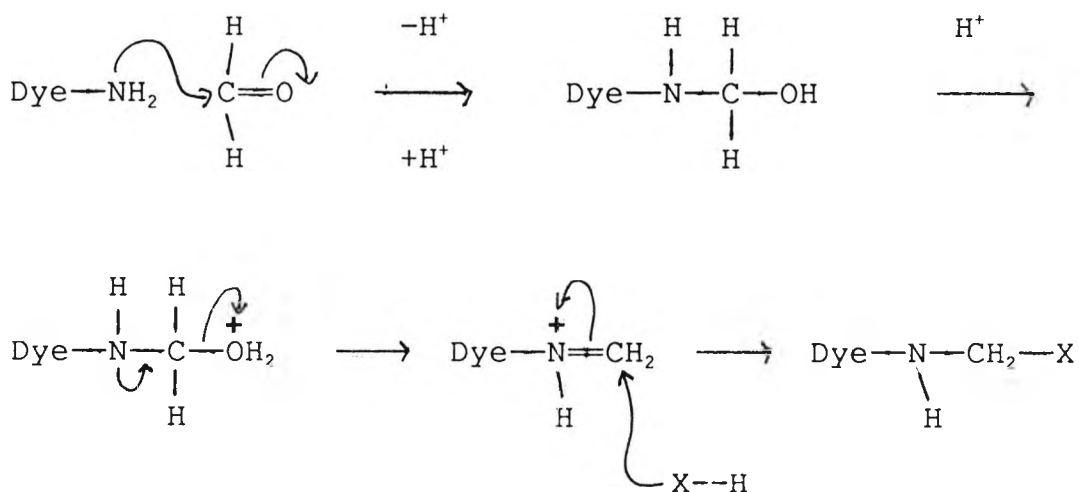
D - Chromophoric centre

Scheme 3.5 : - Base hydrolysis of the chloroacetamide reactive group.

in such a large excess that construction of trimers will be very improbable and dimer formation will only occur to a small extent. Therefore the most probable reaction leading to the impurities is base catalysed hydrolysis of the reactive group. This is hardly surprising considering the number of basic groups present. The mechanism in Scheme 3.5 parallels the one given earlier in Scheme 3.1 and is therefore classified a S_N2 reaction.

3.3.2 Application Of The FBA - Polyamines To Wool

It is not clear if the polyamine side groups are



X -- Nucleophilic centre from either an amino acid or polyamine.

Scheme 3.6 : Crosslinking of a dye with polyamine side chains to either amino acid residues or other dye molecules.

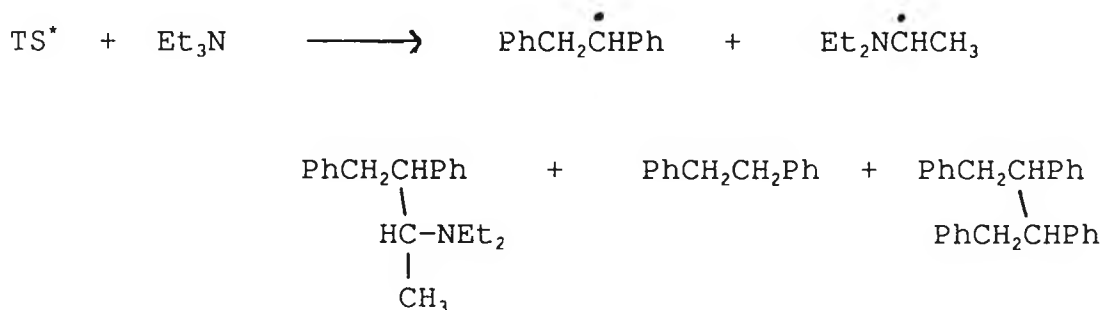
covalently bonded to nucleophilic centres in the polypeptide chain or form a large crosslinked polymer with further FBA molecules. The mechanism of bond formation proposed in Scheme 3.6 allows either possibility. When the polyamine has only a small number of amine groups present then intuitively we can expect the majority of the FBA to be covalently bound to the protein. As the number of polyamine groups increases then the FBA polymer formation becomes more feasible.

Comparison of the FBA - polyamine treated wool with Photine HV treated wool seems to indicate that it is the presence of amine groups which quench the fluorescence. We cannot be sure to what extent the polyamine sidechains react with the crosslinking agent and if any primary or secondary amine groups remain. Neither is it possible to predict whether these amines are in close proximity to the stilbene. Therefore it is prudent to discuss the solution photochemistry and assume that parallel reactions can occur in the protein matrix.

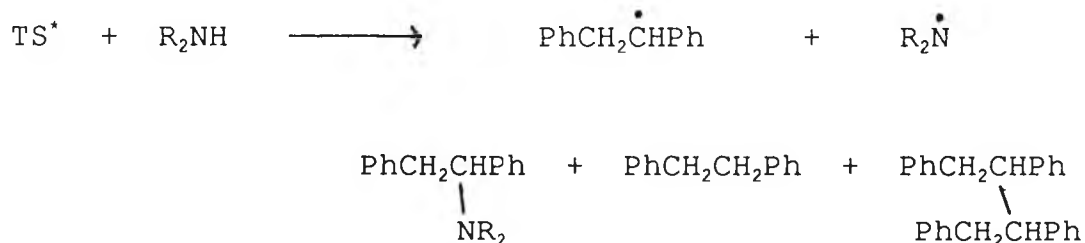
The course of a photochemical reaction between singlet trans-stilbene (TS) and simple alkyl amines depends on the type of amine and solvent polarity ²⁹. An exciplex intermediate has been proposed to explain the experimental observations ³⁰. Only the relevant chemical transformations are presented.

Stilbene does not form products with simple tertiary amines in non polar solvents. In polar solvents addition

of the amine α - C-H bond is accompanied by the formation of diphenylethane and 1,2,3,4-tetraphenylbutane. The reaction is given below -



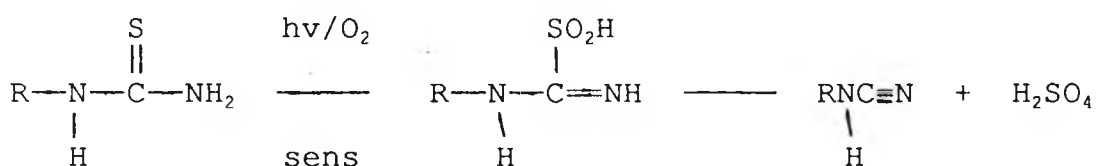
With secondary amines, addition of the N-H bond to stilbene occurs accompanied by the formation of 1,2-diphenylethane and 1,2,3,4-tetraphenylbutane -



Primary amines show similar behaviour to that of secondary amines but are much less reactive.

The TUF treatment originally developed for use with silk¹⁰, has dramatically retarded the photoyellowing of wool treated with FBA's¹¹. Hence the treatment was adapted for commercial application¹², but has the serious disadvantage that the protective effect is greatly diminished when the wool is washed. Thiourea is a good reducing agent and has been used to reduce endoperoxides

to cis diols¹³. Hydroperoxides have similarly been reduced to alcohols¹⁴. Reaction of thiourea with hydrogen peroxide is a convenient method of preparing thiourea dioxide¹⁵. Sensitised photo-oxygenation with chlorophyll has transformed thiourea into cyanamide and sulphuric acid¹⁶ via an intermediate thiourea dioxide¹⁷. A similar reaction is found from the eosin sensitised photo-oxidation of allylthiourea in an ethyl cellulose polymer¹⁸. It has recently been proposed that the intermediate thiourea dioxide is hydrolysed to



R = H, Thiourea

sensitiser = chlorophyll

= CH₂=CH-CH₂-, Allylthiourea

= eosin

Scheme 3.7 : Photosensitised oxidation of thiourea and allylthiourea

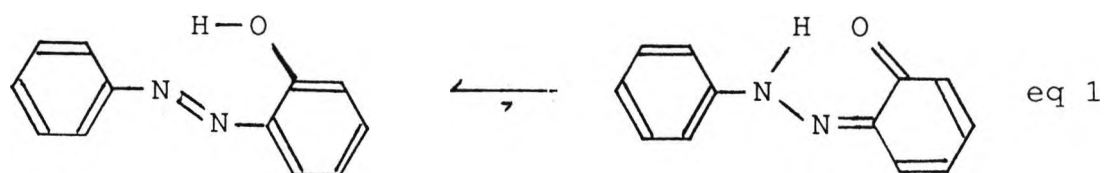
urea and sulphinic acid. The sulphinic acid then acts as a catalyst for photobleaching any yellow species formed during photoyellowing¹⁹. A spectroscopic study of the TUF treatment leads to the proposal that there are three possible processes occurring : - (i) quenching of the excited states of photolabile tryptophyl side chains at the short wavelength threshold of the solar spectrum (290 - 320 nm), (ii) inhibition of photoprocesses that

are initiated at longer wavelengths in the near U.V region (320 - 390 nm) of the spectrum , (iii) sensitisation of the wool to bleaching when it is exposed to visible radiation ²⁰.

The dramatic loss of protective effect upon washing in previous TUF treatments suggests that a large proportion of the thiourea is removed. This extracted thiourea is obviously not bound to the wool and unlikely to be in polymeric form trapped inside the protein structure. Subsequently, it can be argued that there are only a limited number of reactive sites available for the TUF precondensate to bind. A prime site for reaction is the ϵ -amino terminal amino group of lysine. It has been shown that primary alkylamines readily react with thiourea and formaldehyde at room temperature to give tetrahydro-5-alkyl-2-thio-1,3,5-triazines ²¹. Increasing the amine groups by introduction of polyamine side chains therefore expands the reactive sites for the TUF precondensate. The thiourea can be bound by several means between wool / FBA or as FBA / FBA polymers and so more thiourea will be retained in the wool structure. It is impossible to determine the exact thiourea concentration as this can vary depending on the polyamine side chain. Such a high fixed concentration will severely retard the photooxidative processes occurring upon irradiation. The observed loss of fluorescence after the test signifies the FBA chromophore is predominantly destroyed by a reductive mechanism.

3.3.3 Synthesis and Application of The Azo-Polyamine Dye

The choice of 4-methylphenol as coupling component to the diazo salt leads to a regiospecific reaction. The phenolate anion is strongly ortho and para directing, but the 4 position is blocked leaving only the 2 or 6 position available for reaction. Hydroxyazo dyes have been shown by nmr to exist completely as the azo structure in solution ²². In equation 1 the equilibrium between the tautomeric azo and quinone hydrazone forms is over to the left. The hydroxy group at C-2 undergoes intramolecular hydrogen bonding to an azo nitrogen which



reinforces the trans double bond geometry. Base conditions were chosen to hydrolyse the amide to the amine so the phenolate anion formed would aid dissolution ²³. Acylation of the aromatic amine went smoothly and in high yields under Schotten-Baumann conditions. Amination of the activated alkyl halide with diethylenetriamine also proceeded readily at room temperature. Unfortunately a pure sample was not obtained due to the reasons mentioned earlier.

The observed higher dye uptake at 60°C than 100°C was unexpected. It is readily explained by arguing that

some dye is extracted at the same time it is taken up by the wool under the more vigorous application conditions. Hence, a dynamic equilibrium between adsorbed and extracted dye is set up. At 60°C the dye-wool interactions dominate such that more dye remains on the wool. Crosslinking with formaldehyde is expected to follow the mechanism put forward in Scheme 3.6.

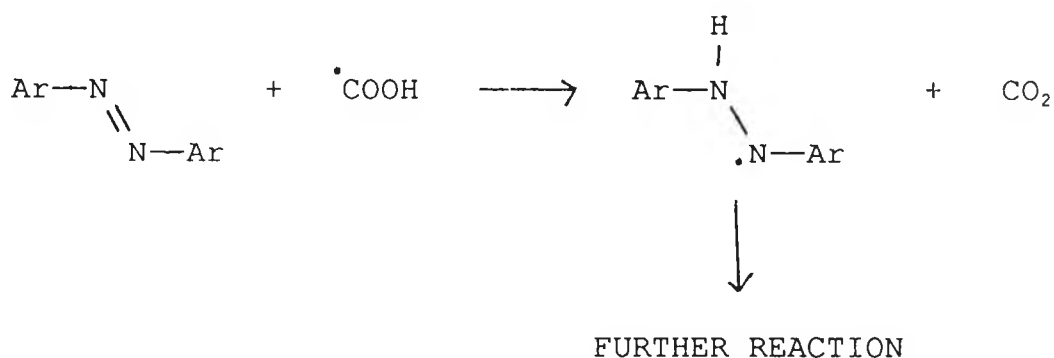
The extraction experiments display evidence that treatment at 60°C only imparts only a surface effect. If the dye had penetrated the fibre then it would be expected that more crosslinked dye would have remained following extraction. Upon extraction each solvent removed similar amounts of dye from the crosslinked and uncrosslinked dyed fibre. The organic based solvents removed a large percentage of the dye showing that very little was bound to the fibre.

Treatment at 100°C imparts a much more permanent effect. No dye was removed with boiling water. Much less dye was removed from formaldehyde treated wool than uncrosslinked wool when treated with organic solvents. This tends to signify that some dye is bound to the wool or is present in polymeric form.

Azo dyes can undergo both oxidative and reductive fading depending mainly on the dye and substrate structure ²⁴. The oxidative mechanism involves both Type I and Type II processes. It has been shown that azo dyes can sensitise

the formation of singlet oxygen although not as efficiently as methylene blue. Thiourea will retard this Type II mechanism by reacting with the singlet oxygen. It is not known if the excited species in the Type I process will be deactivated by thiourea but the intermediate hydroperoxide is readily intercepted and transformed to a photoinactive alcohol.

A reduction mechanism has been shown to involve hydrogen donation to the dye by powerful reductive radical species. In model studies mandelic acid PhCH(OH)COOH was photolysed to give the carboxy radical ($\cdot\text{COOH}$). The hydrogen of this radical adds readily to the dye to form a hydrazyl radical which then undergoes a series of irreversible reactions to destroy the chromophore (Scheme 3.8).

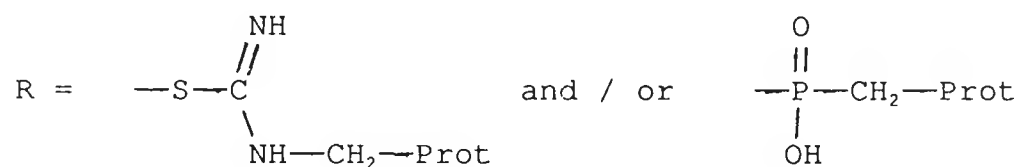
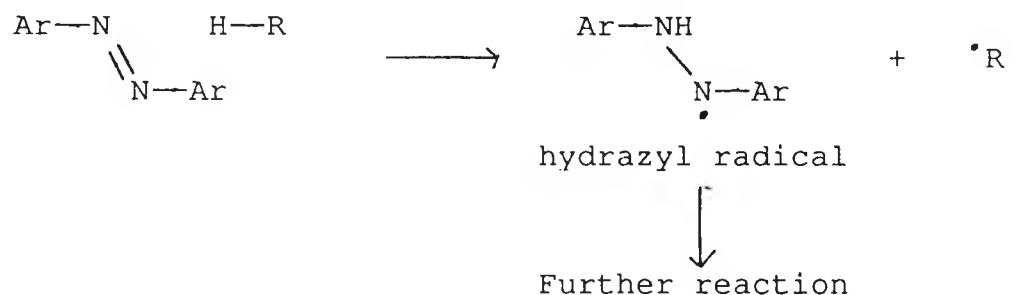


Scheme 3.8 : Reaction of a carboxy radical with an azo dye

Protein fibres readily absorb near UV light to give radical species ²⁶ which will attack the azo linkage

thereby leading to destruction of the dye

The presence of reducing agents increases the rate of dye loss and thiourea seems to have the most dramatic effect. A few speculative answers to the question as to why the dye degradation is quicker in the presence of these compounds are put forward. The reducing agent may attack the dye in its excited state by donating a hydrogen atom. By analogy to the above pathway it is proposed that a hydrogen atom is donated by the reducing agent. Thiourea can tautomerise to the thiol and this is the form which participates in the reaction. The suggested pathway is given -



Phosphonous acid can add to acrylamide by a free radical mechanism ²⁷ and compounds containing a P-H bond are well known to undergo radical reactions ³⁰. The P-H bond may interact with the excited dye leading to reduction of the dye or act as a radical transfer agent from the

polypeptide to the dye. Thiourea dioxide formed from the reaction of thiourea with singlet oxygen may decompose to the sulphinic acid which is the active reducing species.

3.4 CONCLUSION

As expected the reactive group was removed on reaction with polyamines thus making the dyes less hazardous. Excellent washfastness was found for both the FBA and Azo dye - polyamine crosslinked compounds, even under vigorous extraction conditions. It would be interesting to compare the crosslinking reaction efficiency when carried out under exhaustion and pad-batch conditions. The two stage treatment allows an option whether to fix or not. For example, when the dyeing finish is uneven it is possible to remove the dye and start again. This is an obvious advantage over reactive dyes. A disadvantage is that two treatments are required. Even so, it was found that dyeing and crosslinking can be performed in one treatment. A major drawback is the use of formaldehyde as a crosslinking agent. Other than its obnoxious smell, formaldehyde is a possible carcinogen. The azo dye - polyamine was used as a concentrated liquid which overcomes the problems of dust associated with reactive dyes. The initial water insoluble azo - dye was applied from aqueous media after attachment to the polyamine. It is envisaged that many other water insoluble reactive dyes can be solubilised in this manner.

In dye synthesis the need for a sulphonation step may be eliminated.

The use of TUF precondensates with the FBA - polyamine adducts prevents the wool undergoing severe discolouration. However, similar treatments increase the rate of azo dye fading. It is not clear if the reducing agents affect the FBA destruction.

More work is required on the single stage process and an investigation into how efficiently the dye is bound. The reaction of polyamines with other reactive dye classes should be investigated with respect to improving and enlarging the usefulness of these adducts. Less toxic crosslinking agents are a prime target, however, these chemicals by their very nature will be carcinogenic

In summary, this chapter has provided evidence that the novel polyamine adducts are an alternative to reactive dyes. These compounds have some advantages over present reactive dyes and unfortunately, a few disadvantages. There remains much more work to be performed before a complete evaluation of their usefulness in the textile field is ascertained.

3.5 EXPERIMENTAL

The starting chemicals were obtained from Aldrich and

used without further purification. ^1H nmr spectra were recorded with a Jeol JMN-MH 100 instrument using TMS and DSS as internal standards. IR spectra were run on a Perkin-Elmer 983 instrument. Other instrumental techniques are described in the appropriate sections.

3.5.1 SYNTHESIS OF STILBENE FBA 's

3.5.1.1 4,4'-Dichloroacetamidostilbene-2,2'-disulphonic acid sodium salt (DCDAS)

4,4'-Diaminostilbene-2,2'-disulphonic acid (DAS) (3.7 g, 10 mmol) and sodium bicarbonate (3.4 g, 40 mmol) were dissolved in water (50 mls) and cooled to 0-5°C. Chloroacetyl chloride (3.39 g, 30 mmol) in acetone (10 mls) was added dropwise with constant stirring to the DAS solution. The mixture was stirred at 5°C for 30 minutes and then at room temperature for 1 hour. The solid was collected by filtration washed with acetone and air dried to give a yellow powder. Yield 5.0 g (85 %).

Analysis

Melting Point > 200°C

IR (KBr disc) :- 3300 cm^{-1} (N-H str, sec amide), 1670 cm^{-1} (C=O str, amidic carbonyl), 1600 and 1500 cm^{-1} (C-H vib, aromatics), 1330 and 1200 cm^{-1} (SO_3 str, sulphonic acid), 975 cm^{-1} (HC=CH def, trans alkene).

^1H nmr (solvent DMSO d_6 , ref TMS) :- δ 10.5 (1H, b.s,

amidic N-H), δ 8.2 - 7.7 (4H, m, aromatic and alkene protons), δ 4.3 (2H, s, methylene protons).
The signal at δ 10.5 disappears after shaking with D₂O.

3.5.1.2. Formation of FBA - Polyamine Adducts

The procedure for synthesising these adducts is similar, independent of which polyamine is used and therefore only the general method is given. The spectroscopic data for each adduct is recorded.

DCDAS (1.5 g, 2.6 mmol) was dissolved in an aqueous solution containing a 10 molar excess of the polyamine and sodium hydroxide (0.25 g, 6.3 mmol). The solution was warmed to 50°C and stirred for 15 mins. The solution was concentrated to 5-10 mls under reduced pressure and deposited in methanol which precipitated a yellow solid. The solid was collected by filtration and washed with a small amount of acetone and air dried.

DCDAS + 1,2-Diaminoethane

Analysis

IR (KBr disc):- 3400 - 3200 cm⁻¹ (N-H str, sec amide, sec amine, primary amine), 2985 - 2800 cm⁻¹ (C-H str, aliphatic), 1670 cm⁻¹ (C=O str, amidic carbonyl), 1340 - 1200 cm⁻¹ (SO₃ str, sulphonate group), 960 cm⁻¹ (HC=CH def,

trans alkene).

¹H nmr (solvent DMSO d⁶ / D₂O, ref TMS) :- δ 8.5 (1H, s, aromatic), δ 8.4 (1H, s, alkene), δ 8.2 - 8.0 (2H, AB quartet, aromatic), δ 3.5 (2H, s, methylene), δ 3.0 (4H, m, alkyl from diaminoethane).

DCDAS + 1,3-Diaminoethane

Analysis

IR (KBr disc) :- 3400 - 3200 cm⁻¹ (N-H str, sec amide, sec amine, primary amine), 2985-2800 cm⁻¹ (C-H str, alkyl), 1670 cm⁻¹ (C=O str, amidic carbonyl), 1340 - 1210 cm⁻¹ (SO₃ str, sulphonate), 960 cm⁻¹ (HC=CH def, trans alkene).

¹H nmr (solvent DMSO d⁶ / D₂O, ref TMS) :- δ 8.6 (1H, s, aromatic), δ 3.6 (2H, s, methylene on reactive group), δ 3.0 (2H, t, methylene adjacent sec amine), δ 2.8 (2H, t, CH₂ adjacent primary amine), δ 1.8 (2H, t, central CH₂).

DCDAS + diethylenetriamine

Analysis

IR (KBr disc) :- 3400 - 3200 cm⁻¹ (N-H str, sec amide, sec amine, primary amine), 2980 - 2785 cm⁻¹ (C-H str, alkyl), 1670 cm⁻¹ (C=O str, amidic carbonyl), 1350 and 1200 cm⁻¹ (SO₃ str, sulphonate), 970 cm⁻¹ (HC=CH def, trans alkene).

¹H nmr (solvent DMSO d⁶ / D₂O) :- δ 8.6 (1H, s, aromatic),

δ 8.4 (1H, s, alkene), δ 8.0 (2H, m, aromatic), δ 3.5 (2H, s, methylene), δ 3.0 - 2.6 (8H, m, alkyl from diethylenetriamine).

DCDAS + Triethylenetetramine

Analysis

IR (KBr disc):- 3400 - 3200 cm^{-1} (N-H str, sec amide, sec amine, primary amine), 2790 - 2980 cm^{-1} (C-H str, alkyl), 1670 cm^{-1} (C=O str, amidic carbonyl), 1300 and 1190 cm^{-1} (SO_3 str, sulphonate), 965 cm^{-1} (HC=CH def, trans alkene).

^1H nmr (solvent DMSO d^6 / D_2O) :- δ 8.5 (1H, s, aromatic), δ 8.3 (1H, s, alkene), δ 8.0 - 7.9 (2H, m, aromatic), δ 3.5 (2H, s, methylene), δ 3.1 - 2.5 (12H, m, alkyl from polyamine).

DCDAS + Tetraethylenepentamine

Analysis

IR (KBr disc):- 3400 - 3200 cm^{-1} (N-H str, sec amide, sec amine, primary amine), 2795 - 2990 cm^{-1} (C-H str, alkyl), 1670 cm^{-1} (C=O str, amidic carbonyl), 1330 and 1190 cm^{-1} (SO_3 str, sulphonate), 975 cm^{-1} (HC=CH def, trans alkene),

^1H nmr (solvent DMSO d^6 / D_2O) :- δ 8.5 (1H, s, aromatic), δ 8.3 (1H, s, alkene), δ 8.0 - 7.9 (2H, m, aromatic), δ 3.5 (2H, s, methylene), δ 3.1 - 2.5 (12H, m, alkyl from

polyamine).

DCDAS + Tetraethylenepentamine

Analysis

IR (KBr disc) :- 3400 - 3200 cm^{-1} (N-H str, sec amide, sec amine, primary amine), 2795 - 2990 cm^{-1} (C-H str, alkyl), 1670 cm^{-1} (C=O str, amidic carbonyl), 1330 and 1190 cm^{-1} (SO_3 str, sulphonate), 975 cm^{-1} (HC=CH def, trans alkene).

^1H nmr (solvent DMSO d^6 / D_2O , ref TMS) :- δ 8.5 (1H, s, aromatic), δ 8.3 (1H, s, alkene), δ 8.0 (2H, m, aromatic), δ 3.6 (2H, s, methylene), δ 3.0 - 2.5 (16H, m, alkyl from polyamine).

3.5.2 High Performance Liquid Chromatography Conditions

The column was stainless steel (250 x 4.6 mm i.d) packed with 5 μm Hypersil (C_8 MOS). The Cecil UV detector was set at a detection wavelength of 360 nm. A dual pump gradient programmer was fitted to the column and the total flow rate was 2.5 ml min^{-1} . The initial eluent concentration was 10% soln A - 90% soln B which was changed to a final concentration of 85% soln A - 15% soln B at 5% min^{-1} and an injection volume of 20 μl .

Eluent A : Tetrabutylammonium bromide (TBABr) (0.3224 g)

was weighed out and transferred to a 1 litre volumetric flask. To the flask 1 ml of 20 % v/v aqueous glacial acetic acid, 1 ml of 5% w/v aqueous potassium hydroxide were added and the flask was made up to the mark with methanol. The contents were transferred to a round bottomed flask and heated under reflux for 5 minutes. The mixture was allowed to cool slightly and then filtered through a GF/F glass fibre filter.

Eluent B : TBABr (0.3224 g) was weighed out and transferred to a 1 litre volumetric flask. Added to the flask was 1 ml of 20 % v/v glacial acetic acid, 1 ml of 5 % w/v potassium hydroxide solution and the flask made up to the mark with distilled water. The flask was shaken well and the contents transferred to a round bottomed flask. The solution was heated under reflux for 5 minutes, allowed to cool and filtered through a GF/F glass fibre filter.

3.5.3 Application of FBA's to Wool

3.5.3.1 Wool Bleaching

Salt serge wasted fabric (2m, 433 g/m, 2x2 twill construction) was bleached by an exhaustion method at 60°C for 1 hour. The bath contained 6 g/l tetrasodium pyrophosphate and 25 ml/l hydrogen peroxide (30%). This was followed by rinsing in cold water and oven drying at 50°C.

3.5.3.2 Treatment of Wool With FWA's

Application to bleached wool was carried out by an exhaustion method in an Ahiba Process Controller PC 100 on samples 20 \pm 0.1 g with a liquor/wool ratio of 30:1 at pH 4. The pH was altered by the addition of 20 % glacial acetic acid. The FBA concentrations were 0, 0.2, 0.4, 0.6, 0.8, 1.0 % OWF. The bath also contained 2 mls of EDTA (10 % soln). The bath temperature was kept at 30°C for 10 minutes and raised at 1° per min to 80°C and maintained for 1 hour at 80°C. The bath was allowed to cool and the wool washed with copious amounts of cold water and oven dried at 50°C. The commercial FBA was applied by the same procedure.

3.5.3.3 Measurement of FWA Uptake

The optical density at 360 nm of the dye bath liquor was measured before addition of the wool and after the exhaustion procedure. Dye uptake was expressed as a percentage using the following equation -

$$\text{Dye uptake} = \frac{(\text{OD}_{(B)} - \text{OD}_{(A)})}{\text{OD}_{(B)}} \times 100$$

OD_(B) - Optical density of dye bath before exhaustion

OD_(A) - Optical density of dye bath after exhaustion

3.5.3.4 Crosslinking of FBA's

A formaldehyde (50 mls of 40 % solution in 100 mls) solution containing the wetting agent Nonadet SH (1.0 g) was padded on to FBA treated wool (10 ± 0.1 g) until a net pick up of 100 % w/w was achieved. This treatment gives a formaldehyde concentration of 20 % OWF.

In separate experiments a solution containing formaldehyde (50 mls of 40 % solution), thiourea (10 g) and Nonadet SH (1.0 g) made up to 100 mls and padded on to FBA treated wool (10 ± 0.1 g) until a net pick up of 100 % w/w was achieved. This treatment gives a concentration of formaldehyde 20 % OWF and thiourea 10 % OWF.

After the treatments the wool was stored overnight at room temperature before rinsing in cold water and oven drying at 50°C.

3.5.3.5 Extraction of FBA's

Strips of wool (2.0 ± 0.1 g) were extracted for 5 minutes with aliquots (3 x 30 ml) of boiling 25 % aqueous pyridine in a round bottomed flask. The extracted wool was washed with cold water until no trace pyridine remained and oven dried at 50°C.

3.5.3.6 Yellowness Index Measurements

Samples were measured in a computerised I.C.S microphotometer. The lower the yellowness index value the whiter is the wool colour.

3.5.3.7 Lightfastness Measurements

Wool samples were exposed to Blue scale 3 and 5 using the Xenotest according to ISO standard procedure.

3.5.3.8 Total Diffuse Reflectance Spectra

The total diffuse reflectance attachment to a Lamda 5 spectrophotometer was calibrated with standard white barium sulphate plates. Spectra were run with barium sulphate as reference.

3.5.3.9 Solid Sample Fluorescence Spectra

Fluorescence spectra of fabric were obtained using a Perkin-Elmer MPF-4 fluorescence spectrophotometer. The fitment for solids was designed and made at the City University and is similar to that described by McKellar and Allen ²⁸. The samples were placed at 50° to the incident beam to avoid scattering.

3.5.4 SYNTHESIS OF AZO - POLYAMINE DYE

3.5.4.1 2-(4-Acetanilido-azo)-4-methylphenol

Sodium nitrite (2.0 g, 29 mmol) solution (15 mls) was added to 4-aminoacetanilide (4.05 g, 27 mmol) slurried in 50 % hydrochloric acid (16 mls) at 0-5°C. The freshly prepared diazo salt was slowly added to p-cresol (2.92 g, 27 mmol) dissolved in potassium hydroxide (3.16 g, 56 mmol) solution (25 mls) at 0°C. A deep red solution formed and after approximately 2/3 rd diazo salt addition a dark red solid precipitated. Stirring was continued for 30 mins at 5°C and the thick red residue collected by filtration under vacuum. The filter cake was washed with water and recrystallised from ethanol/water 1:1 (≈250 mls). Small brown needle shaped crystals were obtained. Yield 5.60 g (77 %).

Analysis

Melting point 176 - 178°C

IR (KBr disc) :- 3300 cm⁻¹ (N-H str, sec amide), 1696 cm⁻¹ (C=O str, amidic carbonyl), 1277 cm⁻¹ (C-O str, phenolic),

¹H nmr (solvent CDCl₃, ref TMS) :- δ 14.1 (1H, b.s, amidic N-H), δ 7.6 - 6.6 (8, m, aromatic), δ 2.35 (3H, s, aromatic methyl), δ 2.2 (3H, s, acyl methyl).

Uv / Vis :- (solvent EtOH) λ max 395 nm

<u>Elemental Analysis</u>	for $C_{15}H_{15}N_3O_2$		
Calculated	C - 66.90	H - 5.61	N - 15.60
Found	C - 66.62	H - 5.79	N - 15.43

3.5.4.2 2-(p-anilinazo)-4-methylphenol

2-(p-acetanilidoazo)-4-methylphenol (5.35 g, 20 mmol), sodium hydroxide (5.0 g, 125 mmol) and water (100 ml) were heated at $\approx 80^\circ\text{C}$ under reflux conditions for 3 hours. TLC analysis (silica on polyester plates, eluent CHCl_3) showed that the reaction was complete and that only one product remained. After cooling to room temperature concentrated hydrochloric acid was added till the pH dropped to 7. The precipitated solid was collected by filtration under vacuum washed with water and recrystallised from ethanol/water 1:4. The brown needle shaped crystals were oven dried at 50°C . Yield 4.1 g (95 %).

Analysis

Melting point $135-136^\circ\text{C}$

IR (KBr disc) :- 3400 and 3340 cm^{-1} (N-H str, primary aromatic amine), 1590 and 1485 cm^{-1} (C-H vib, aromatic), 1250 cm^{-1} (C-O str, phenolic).

^1H nmr (solvent CDCl_3 , ref TMS) :- δ 7.75 - 7.6 (3H, m, aromatic), δ 7.2 - 6.6 (4H, m, aromatic), δ 4.1 (2H, s, aromatic amine), δ 2.35 (3H, s, aromatic methyl).

Uv / Vis :- (solvent EtOH) λ_{max} 390 nm

Elemental Analysis for $C_{13}H_{13}N_3O$

Calculated	C - 68.70	H - 5.76	N - 18.48
Found	C - 68.47	H - 5.93	N - 18.33

3.5.4.3 2-(p-chloroacetylanilidoazo)-4-methylphenol

Choroacetyl chloride (2.3 g, 20 mmol) was added over a 10 minute period to a 5 % aqueous acetone solution (50 mls) of 2-(p-anilinazo)-4-methylphenol and sodium bicarbonate (2.5 g, 30 mmol) at $0-5^{\circ}C$. The mixture was allowed to warm up to room temperature and stirred for 1 hour. Addition of the mixture into water (500 mls) precipitated a solid which was collected by filtration and recrystallised from ethanol/water 1:1. The pale yellow needle like crystals were oven dried at $50^{\circ}C$. Yield 5.0 g (90 %).

Analysis

Melting point $154-155^{\circ}C$

IR (KBr disc) :- 3300 cm^{-1} (N-H str, sec amide), 1689 cm^{-1} (C=O str, amidic carbonyl), 1595 and 1490 cm^{-1} (C-H vib, aromatic), 1245 cm^{-1} (C-O str, phenolic), 600 cm^{-1} (C-Cl str, reactive group).

1H nmr (solvent $(CD_3)_2CO$, ref TMS) :- δ 8.9 (1H, b.s, amidic N-H), δ 7.2 (4H, s, aromatic), δ 7.1 (1H, s, C-3 proton on phenol), δ 6.7 (1H, d, $J=6\text{ Hz}$, C-5 proton adjacent methyl), δ 6.3 (1H, d, $J=6\text{ Hz}$, C-6 proton adjacent hydroxyl), δ 4.35 (2H, s, methylene), δ 2.4 (3H,

s, aromatic methyl).

Uv / Vis (solvent EtOH) :- λ max 400nm

<u>Elemental Analysis</u>	for	$C_{15}H_{14}ClN_3O_2$		
Calculated	C - 59.31	H - 4.64	N - 13.83	
Found	C - 59.31	H - 4.59	N - 13.67	

3.5.4.4 Azo Dye - Polyamine Adduct

Diethylenetriamine (7.0 g, 70 mmol) and 2-(p-chloroacetanilidazo)-4-methylphenol (2.0 g, 7 mmol), were stirred at room temperature for 24 hours. TLC was performed on silica plates (polyester support) using dichloromethane as eluent. After the designated time only one spot remained and the solution was used in the above form.

3.5.5 Application of Dye-Polyamine to Wool

The adduct was exhausted on to salt serge (20 \pm 0.1 g, 2x2 twill, 200 g/m²) with a liquor / wool ratio of 30:1 at pH 6. The pH was adjusted with 20 % glacial acetic acid. An adduct concentration of 2% OWF was employed. Two different application programs were used :-

Program 1 - The bath was kept at 40°C for 10 minutes, raised at 1° per min to 60°C and kept at 60°C for 1 hour.

Program 2 - The bath was kept at 40°C for 10 minutes, raised at 1° per min to 100°C and kept at 100°C for 1

hour.

The fabric was rinsed in cold water and oven dried at 50°C.

3.5.5.1 Measurement of Dye Uptake

The procedure is the same as that for measuring FWA uptake except that the optical density was monitored at 430 nm.

3.5.5.2 Dye Fixation

The dye was fixed by both exhaust and pad batch methods.

(i) Exhaustion :- Stips of dyed wool (10 ± 0.1 g) were exhausted with solutions of formaldehyde in a liquor / wool ratio of 30:1 at pH 7. The pH was adjusted with ammonium hydroxide. The amount of formaldehyde added was :-

- (i) 0 - blank
- (ii) 12.5 mls of 40 % HCHO which gives a concentration of 50% OWF.
- (iii) 50 mls of 40 % HCHO which gives a concentration of 200 % OWF.

The exhaustion was carried out using the same temperature

programme as for the dyeing. That is, wool dyed at 60°C was crosslinked with the same temperature programme as the 60°C application. Similarly wool dyed at 100°C was crosslinked at 100°C.

Strips of dyed wool (10 ± 0.1 g) were exhausted at 100°C for 1 hour at a liquor / wool ratio of 60:1 with the following reducing reagents. The components in the reducing agent solution were :-

(i) thiourea (2.5 g, ≈ 25 % OWF), formaldehyde (6 mls of 40 % solution, ≈ 25 % OWF).

(ii) thiourea (2.5 g, ≈ 25 % OWF), formaldehyde (12.5 mls of 40 % solution, ≈ 50 % OWF), phosphonous acid (5 mls of 50 % solution, ≈ 25 % OWF)

(iii) phosphonous acid (5 mls of 50 % solution, ≈ 25 % OWF), formaldehyde (6 mls of 40 % solution, ≈ 25 % OWF).

After the treatment the wool was washed with cold water and oven dried at 50°C.

(ii) Pad - batch :- The following solutions were padded onto dyed wool (10 ± 0.1 g) until a net pick up of 100 % was achieved :-

(i) thiourea (25.0 g, ≈ 50 % OWF) dissolved in formaldehyde (50 mls of 40 % solution, ≈ 40 % OWF).

(ii) thiourea (5.0 g, ≈ 10 % OWF) formaldehyde (10 mls of 40 % solution, ≈ 8 % OWF) made up to 50 mls.

(iii) thiourea (1.0 g, ≈ 2 % OWF), formaldehyde (5mls of 40 % solution, ≈ 4 % OWF) made up to 50 mls.

- (iv) phosphonous acid (10 mls of 50 % soln, \approx 50 % OWF), and formaldehyde (40 mls of 40 % soln, \approx 32 % OWF).
- (v) thiourea (5.0 g, \approx 10 % OWF), formaldehyde (40 mls of 40 % soln, \approx 32 % OWF), phosphonous acid (10 mls of 50 % soln, \approx 10 % OWF).

The padded samples were stored overnight, washed with water and oven dried at 50°C.

3.5.5.3 Extraction and Fixation of the Dye-Polyamine Adduct

Wool (2.0 \pm 0.1 g) exhaustively crosslinked with formaldehyde (0, 50, 200 % OWF) was extracted for 5 minutes per aliquot (3 x 30 ml) of boiling solvent. The solvents were water ; water/methanol/n-butanol (1:1:1) ; water/n-butanol/glacial acetic acid (1:1:1). The extracts were added together and made up to 100 mls in a volumetric flask. The % fixation was determined using the following equation -

$$\text{Fixation (\%)} = 100 - \frac{100 (\text{O.D}_t)}{(\text{O.D}_s)}$$

O.D_t - optical density of the extract from crosslinked wool

O.D_s - Optical density of extract from uncrosslinked wool.

The extracted wool was washed with cold water and oven dried.

3.5.5.4 Diffuse Reflectance Spectra

Spectra were recorded as for the FBA's.

3.5.5.5 Light fastness Tests

Wool samples were exposed to blue scale 3 and 5 using the Xenotest according to ISO standard procedure.

3.6 REFERENCES

1. W.F Beech. 'Fibre Reactive Dyes', Logos, London 1970.
2. M. Zahradnik. 'The Production and Application of Fluorescent Brightening Agents', Chichester, Sussex, John Wiley and Sons, 1982.
3. J.A Maclaren and B Milligan. 'Wool Science - The Chemical Reactivity of the Wool Fibre', Marrickville, Science Press, (1981), p 169.
4. D.M Lewis. J.S.D.C (1982), 165.
5. D.M Lewis. Melliand Textilberichte, 67 , (1981), 717-723.
6. I.Steinken, I.Souren, U.A Henhofen and H.Zahn. Textil-Praxis, 36 , (1984), 1146 .
7. Chemistry in Britian, July, (1990) 650.
8. E.Pryde and J.Wimbush. 'The Quantitative Analysis of a New Wool Fibre Protective Agent By Reverse Phase Ion Pair HPLC', IWS lab report TR 419, (1985).
9. A.Pryde and M.T Gilbert. 'Applications of High Performance Liquid Chromatography', Chapman and Hall, London, p 48-50.
10. N.Nakajo. 'Prevention of the Yellowing of Protein Fibre', Japanese Patent 1197, March 1951.
11. J.E Tucker. 'Reduction of Sunlight Yellowing of Wool Fabric Treated With FBA's', Text Res Jour, 39, No.9, (1969), 830-835.

12. C.S.I.R.O Div Text Ind (Aust), 'Treatment of Woven and Knitted Wool Fabric With Thiourea - Formaldehyde to Retard Photoyellowing', Report G 16 (1968).
13. C.Kaneko, A.Sugimoto and S.Tanaka. Synthesis (1974), 876.
14. D.Gupta, R.Soman and S.Dev. Tetrahedron, 38, (1981), 3013-3018.
15. T.Ohtani. Chem Abs, 83, (1975), 96423
16. A.Warburg and S.Schohen. Arch Biochem, 21, (1949), 363.
17. G.O Schenk and H.Wirth. Naturwisserschafften, 40, (1953), 141.
18. J.P Dubose, C.Mercia and J.Bourdon. Bull Chem Soc Fran, 9, (1979), 3284-3290
19. R.S Davidson, G.M Ismail and D.M Lewis. JSDC 103, (1987), 308.
20. I.H Leaver. Text Res Jour, 48 (10), (1978), 610-615.
21. W.J Burke. J Am Chem Soc, 69, (1947), 2136-2137.
22. L.A Fedorov. 'nmr Spectroscopy of Azo Dyes', Russ Chem Revs, 57 (10), (1988), 941-946.
23. A.Streitweiser and C.Heathcock. 'Introduction to Organic Chemistry', 2 nd edition, Collier Macmillan Publishers, London, (1981), 543-544.
24. N.S Allen. 'Developements in Polymer Photochemistry Vol 1', Applied Science Publishers Ltd, London, (1980), Chapter 6.
25. H.C.A Van Beek, P.M Heertjen and K.Schaafsma. Rec Trav Chim Pays-Bas, 92, (1973), 1189.

26. R.B Coles and C.H Nicholls. JSDC, 92 , (1976),
166.
27. K. Issleib, W.Kitzrow and I.S Lutsenko, Phosphorous,
5 (4), (1975), 281-283
28. J.F Mckellar and N.S Allen. 'Photochemistry of Man
Made Fibres', Applied Science Publishers, London,
(1981), 1979.
29. P.R Brady, D.E Rivett and I.W Stapleton, Proc. 7th
Int. Wool Tex. Res. Conf., Tokyo, Vol iv, (1985),
421
30. C.Walling and E.S.Huyser, Org Rxns, 13 , (1963), 218.

CHAPTER 4

SYNTHESIS AND THE PHOTODECARBONYLATION OF N-FORMYLATED AROMATIC AMINES AND INDOLES

4.1 INTRODUCTION

There is extensive literature to support the view that tryptophyl residues are readily photodegraded ^{1,2,3,4}. Of the many products produced N-formylkynurenine (NFK) appears to be particularly important. The most critical properties of NFK are its near UV absorption and intrinsic photosensitising properties ⁵. It has been shown that in the presence of NFK, bovine carbonic anhydrase, several amino acids and nucleosides are photooxidised and it was proposed that two mechanisms are involved. These are a type I mechanism for tryptophan (trp) photo oxidation involving electron transfer quenching of NFK (T_1) by trp to give NFK radical anion which reacts with O_2 to give superoxide anion and a type II process in which singlet oxygen is the reactive species. The chemistry of NFK has been investigated with a view to ascertaining its role in producing singlet oxygen, the superoxide anion and its conjugate acid the hydroperoxy radical ^{6,7}. All these species can lead to further protein degradation.

Often the analysis of photodegraded proteinaceous material reveals the presence of kynurenine and the question arises as to whether NFK has been decarboxylated by a photochemical route or hydrolysis has occurred ⁸. Table 4.1 shows how susceptible NFK is to hydrolysis.

During peptide synthesis optimum conditions have to be employed to retard the chemical oxidation and the

Condition	pH	Reaction time	% Hydrolysed
H ₂ O	6.6	72 hrs RT	16
H ₂ O	6.6	reflux 1 hr	58
2M NaOH	12.0	10 mins RT	≈100
15% Na ₂ CO ₃ - CH ₃ CO ₂ H	7.2	10 mins RT	19

Table 4.1. Stability of NFK in various solvents.

Extracted from Ref.8.

degradation of tryptophyl residues. Essentially, a simple reversible modification of the indole nuclei is required. Previero ⁹ has found that Trp is formylated at the indolic nitrogen in formic acid/hydrogen chloride solution. Under the conditions employed no modification of the other amino acids occurred and no cleavage of peptide bonds took place. It was proposed that the high yield of specific formylation could be used for the spectrophotometric determination of tryptophan in proteins. As in the case of formylated tryptophan, hydrolysis occurs under very mild alkaline conditions. Several laboratories have reported that N¹ⁿ-formyl tryptophan is less susceptible to chemical oxidations than tryptophan during peptide coupling ¹⁰. There have been no reports if this simple modification imparts any photoprotection to

the indole nucleus. The photochemistry of Nⁿ-acyl indoles has been explored ¹¹ with a view to synthesising tryptophan derivatives containing an acyl group in the aromatic moiety. The study did not examine N-formylindoles and this leads to the question of whether decarbonylation or aromatic ring formylation will predominate with these compounds. Previous work on formanilide ¹² has shown that 254 nm irradiation will promote decarbonylation and the authors consequently proposed the use of formanilides as photosensitive protecting groups for anilines.

This chapter is concerned with the photochemical study of N-formylated indoles and formanilides. Of particular interest in the compounds studied is the number and various types of carbonyl groups present and how they may affect the photochemistry. When only an amidic carbonyl is part of the chromophore then the nature of the transition, whether $n-\pi^*$ or $\pi-\pi^*$ is difficult to ascertain. Compounds in which a ketone carbonyl is associated with the chromophore will have S₁ and T₁ states possessing (n,π*) character. NFK also has an aliphatic carboxylic acid group but this chromophore absorbs little at wavelengths > 230 nm and is not likely to be photoactive. The S₁ and T₁ states of the amidic carbonyl will be at higher energy than the corresponding ones of the ketone carbonyl and so compounds containing both groups (2-N-formylaminoacetophenone, NFK, N',N^α-diformylkynurenine, 1-N-formylaminoanthra-9,10-quinone)

have the possibility of exhibiting chemistry from two different singlet states and possibly two triplet states.

4.2 RESULTS

N¹ⁿ-formyl-3-methylindole, N¹ⁿ-formyltryptophan methyl ester hydrochloride, N-formylkynurenine, N'N^α-diformylkynurenine and 1-formylaminoanthra-9,10-quinone were synthesised by known procedures to give pure products in modest to excellent yields. A Uv / Vis spectrum of the sample formylindoles showed a hypsochromic shift of between 30 and 70 nanometres of the main absorption bands when compared to the parent amines. Most noticeable was 1,N-formylaminoanthra-9,10-quinone in which the λ max changed from 470 to 400nm. NFK when synthesised by the method of Dalgliesh ¹³ was established as pure by the lack of a peak at 360 nm corresponding to kynurenine. The UV spectra of N-formylated indoles were similar to those of N-acylated indoles and show a bathochromic shift of the main peak of 10 nm. This general effect is observed when indoles and N-substituted indoles are compared ^{14,15}. 2-N-Formylaminoacetophenone is an easily prepared model compound for NFK. The changes in its absorption spectrum attendant upon irradiation of 254 and 300 nm are shown in Figure 4.1. It can be seen that irradiation at 254 nm leads to elimination of the band at 320 nm and the appearance of a

300 nm

254 nm

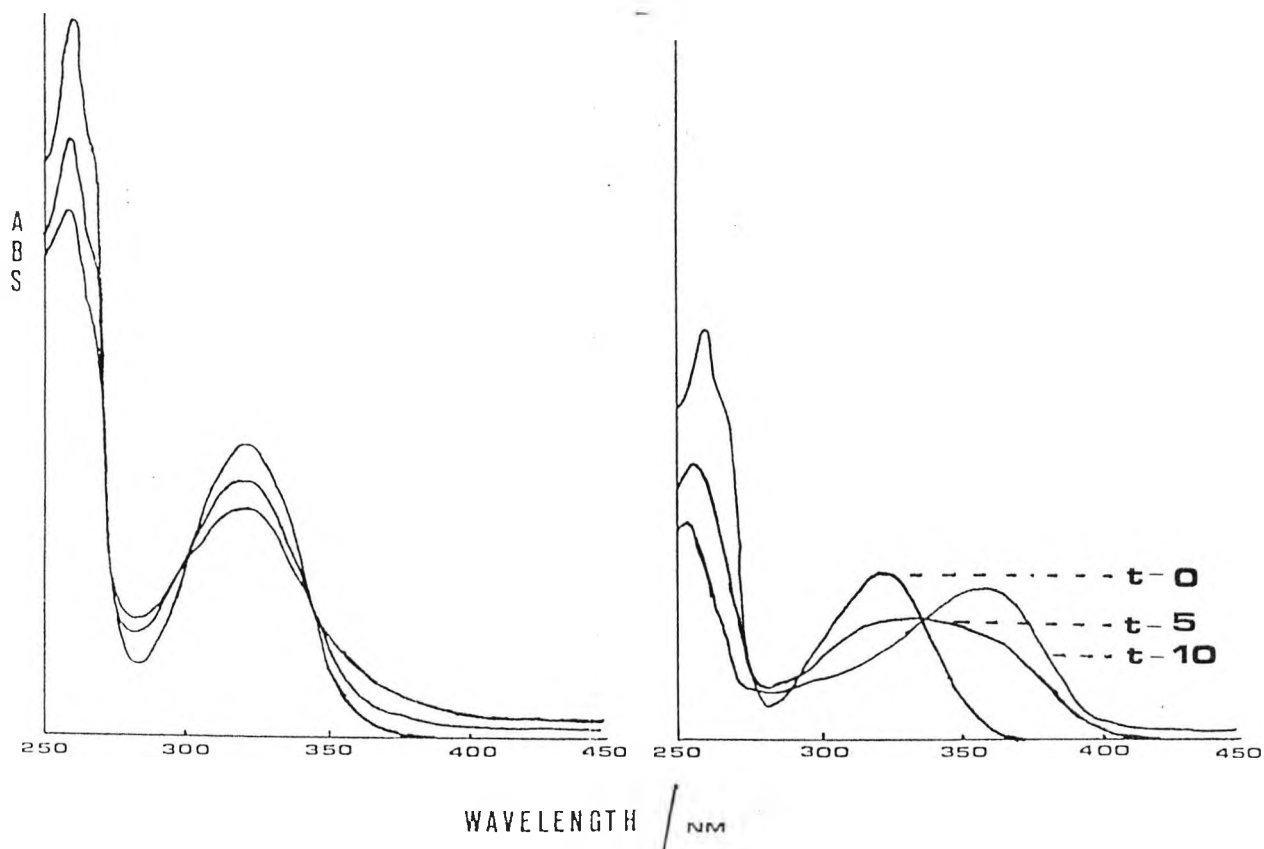


Figure 4.1. Changes in UV absorption of 2,N-formylaminoacetophenone dissolved in acetonitrile. Spectra are recorded after irradiation time $t = 0, 5, 10$ mins at 254 nm and $t = 0, 30, 60$ mins at 300 nm.

band at 360 nm associated with 2-aminoacetophenone. With longer wavelength irradiation, such changes are not seen and only the slow formation of unidentified degradation products takes place. In all cases identity of the major photoproducts was ascertained by gas liquid chromatography (GLC) or high performance liquid chromatography (HPLC) using known compounds to determine

retention times. Similar, but not as clear cut results were obtained for NFK, the spectra for which are shown in Figure 4.2. HPLC showed unambiguously that

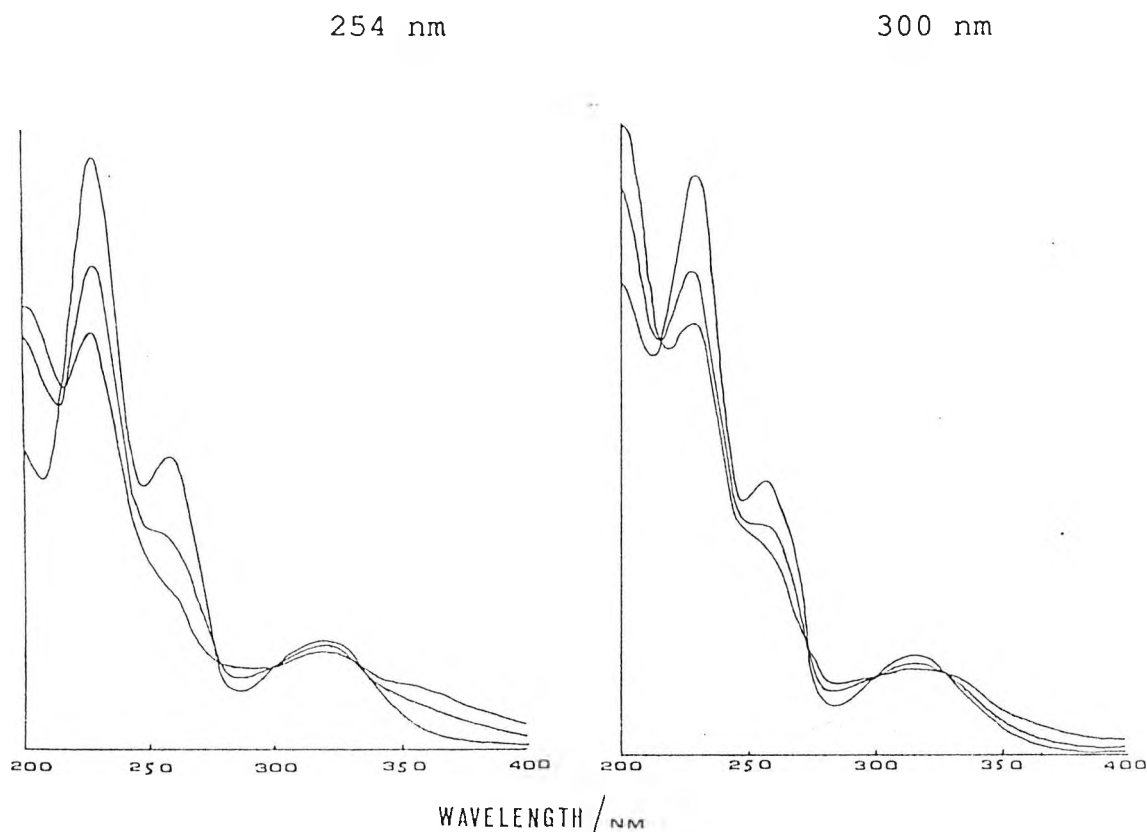
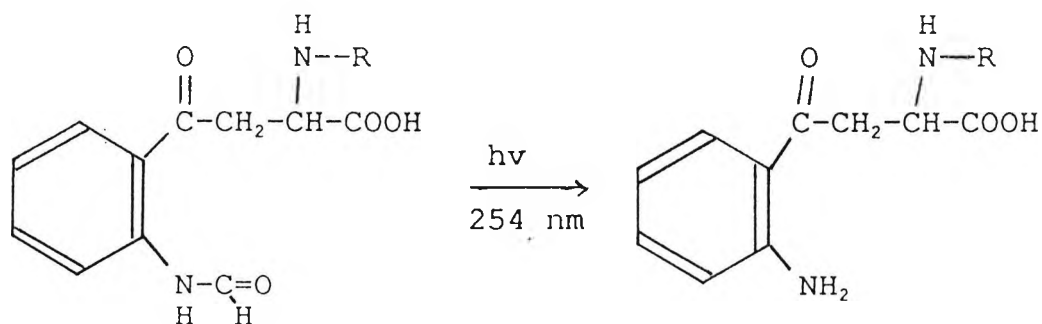


Figure 4.2. Changes in UV absorption of NFK dissolved in water. Spectra were recorded at $t=0, 30, 60$ mins.

kynurenine was a major product on 254 nm irradiation but use of wavelengths ≈ 300 nm gave rise to a variety of products. The UV spectra from N',N^{α} -diformylkynurenine photolysis reaction were similar to those for NFK. Analysis of the chromatogram showed the appearance of three main products when irradiated at 254 nm. Neither

kynurenine or NFK were observed in the reaction mixture. However, it is a reasonable assumption that



Scheme 4.1. Photochemical decarbonylation of NFK to kynurenine

decarbonylation occurs from the N' position. N-formylaminoanthra-9,10-quinone on photolysis at 254 nm

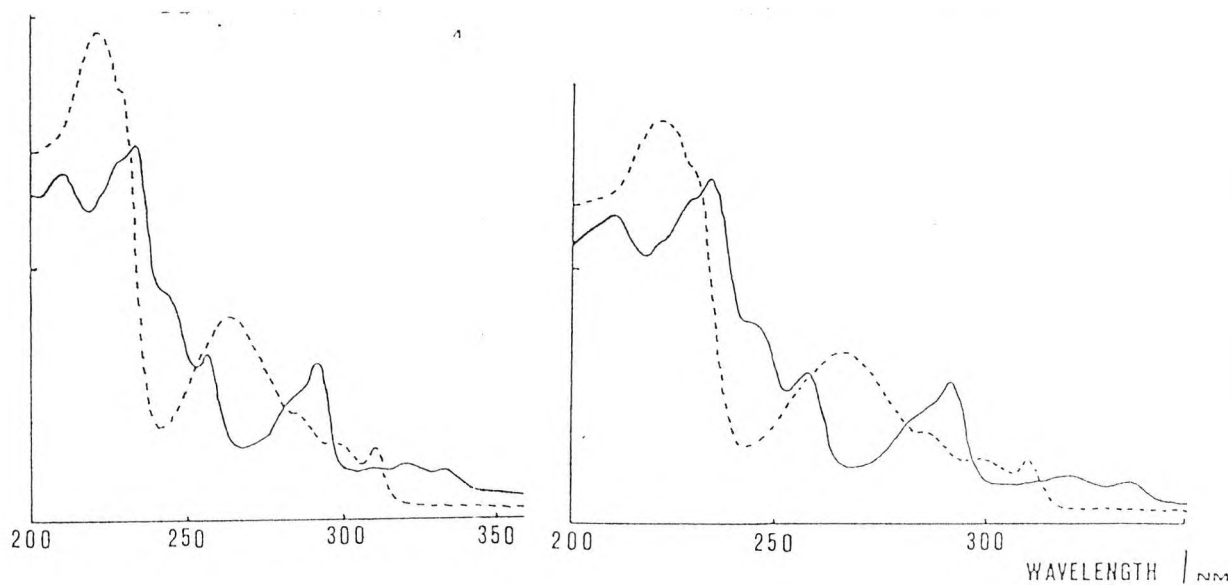
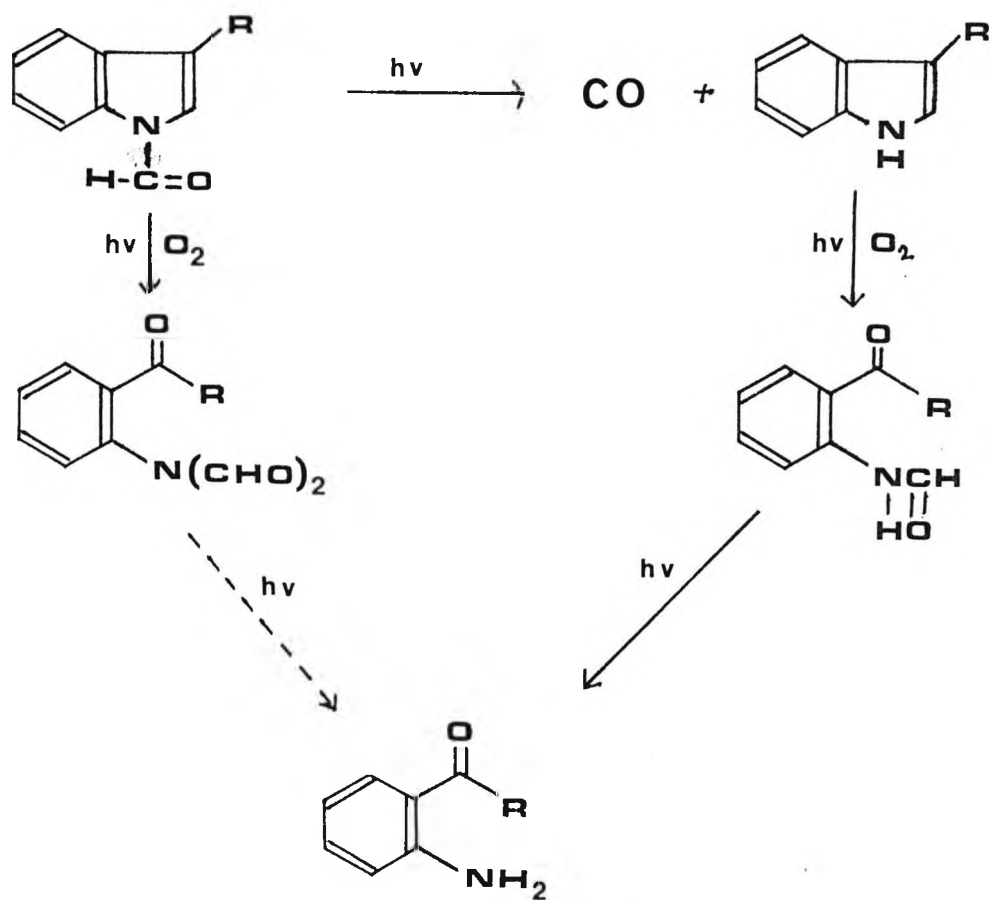


Figure 4.3. Changes in UV absorption of N-formylcarbazole (----) dissolved in acetonitrile when irradiated for 5 mins at either wavelength.

gives 1-aminoanthra-9,10 quinone together, with as yet, an unidentified highly polar product. No noticeable reaction was observed during a photolysis period of 1 hour at ≈ 300 nm irradiation.

In Figure 4.3. spectra are shown for the reaction of N-formylcarbazole. On irradiation at either wavelength this compound gives carbazole in high yield. Even though formanilide only absorbs light ≥ 300 nm very weakly it effectively decarbonylates on irradiation at 300 nm. Indolic compounds are interesting in that the irradiation



Scheme 4.2. Possible photochemical reaction pathways for formylated indoles

in the presence of oxygen may lead to oxidative cleavage of the heterocyclic ring or decarbonylation. The possibilities are depicted in Scheme 4.2. In Figure 4.4 we see the ≈ 300 nm photolysis of N^{in} -formyltryptophan methyl ester hydrochloride. In spectrum A the maxima at 290 and 300nm have undergone a hypsochromic shift of 10 nm after 5 mins irradiation and now correspond to an indolic absorption. Also observable is a new peak

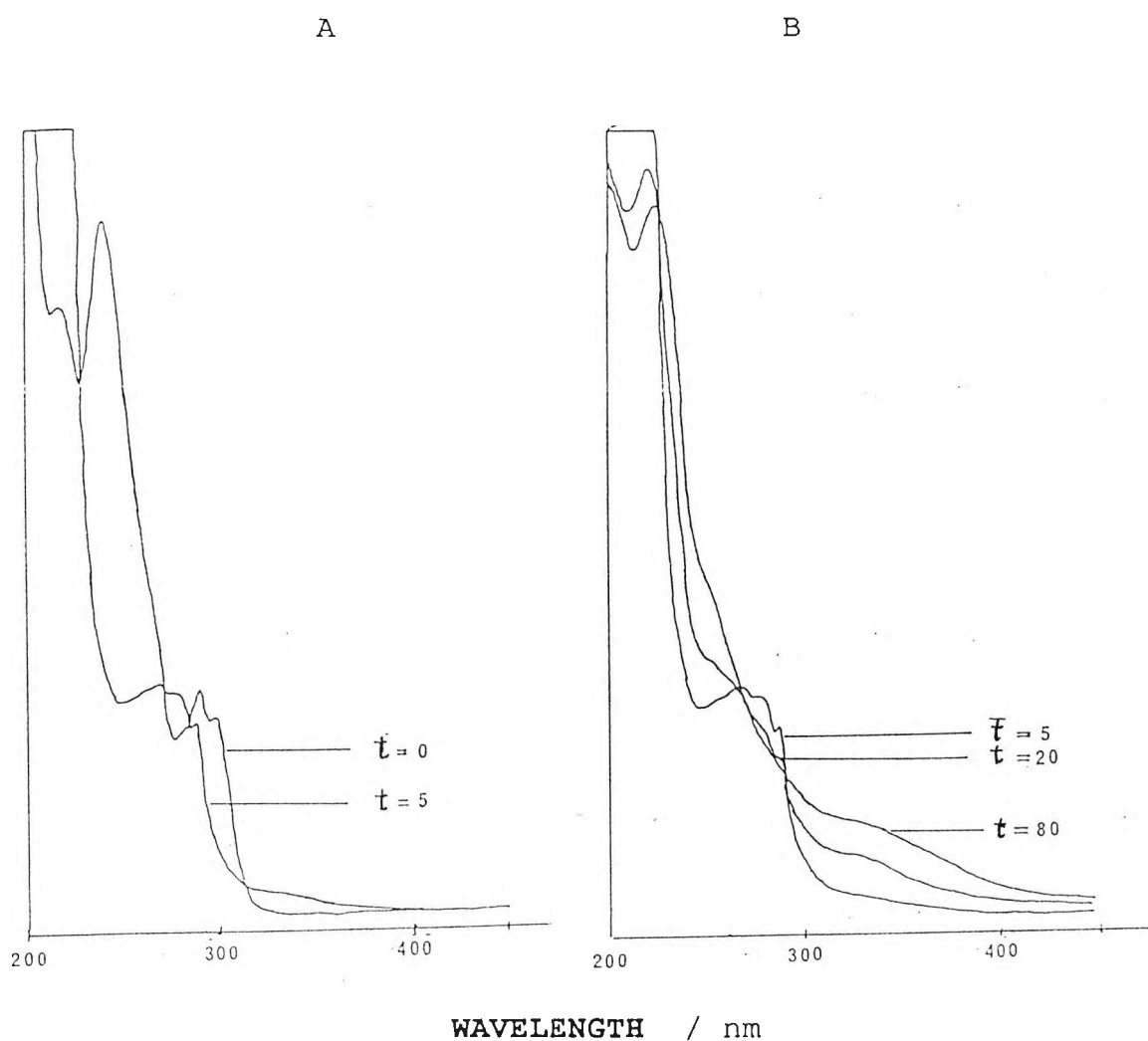


Figure 4.4 : 300 nm photolysis of N^{in} -formyltryptophan methyl ester and hydrochloride in water, Spectra taken in A after $t= 0, 5$ mins and in B after $t= 5, 20, 80$ mins.

appearing between 300 and 360 nm. Spectrum B shows further photolysis and it is readily seen that the indolic absorption bands (280 nm and 290 nm) gradually lose their fine structure and disappear to be replaced by a broad structure less band extending into the visible region. The experimental observations indicate that decarbonylation proceeds faster than heterocyclic ring cleavage. Irradiation with 254 nm light produces similar spectra albeit shorter irradiation times are required. The above results are mirrored by N-formyl-3-methylindole.

To determine a reaction mechanism the kinetics were examined using different photolysis conditions. A photostable internal standard (IS) was used and assuming that the peak height or peak area obtained during chromatographic analysis is proportional to concentration then a kinetic study can be performed. Equation (1) is

$$-\frac{d[A]}{dt} = k_1 [A] \dots\dots (1)$$

the simplest rate law for a first order reaction After rearrangement, integration and further rearrangement

$$\text{Ln} \frac{([A]_t)}{([A]_0)} = -k_1 t \dots\dots (2)$$

- where - $[A]_0$ = initial concentration
- $[A]_t$ = concentration at time t
- k_1 = rate constant
- t = time

equation (2) is formed. A plot of $\ln ([A]_t/[A]_o)$ vs t will give a straight line if first order kinetics are followed. The results for formanilide photolysis in oxygenated and deoxygenated solution at 254 and 300 nm irradiation are shown graphically in Figure 4.5. The graphs show that oxygen has no effect on the rate of decarboxylation and first order kinetics are followed.

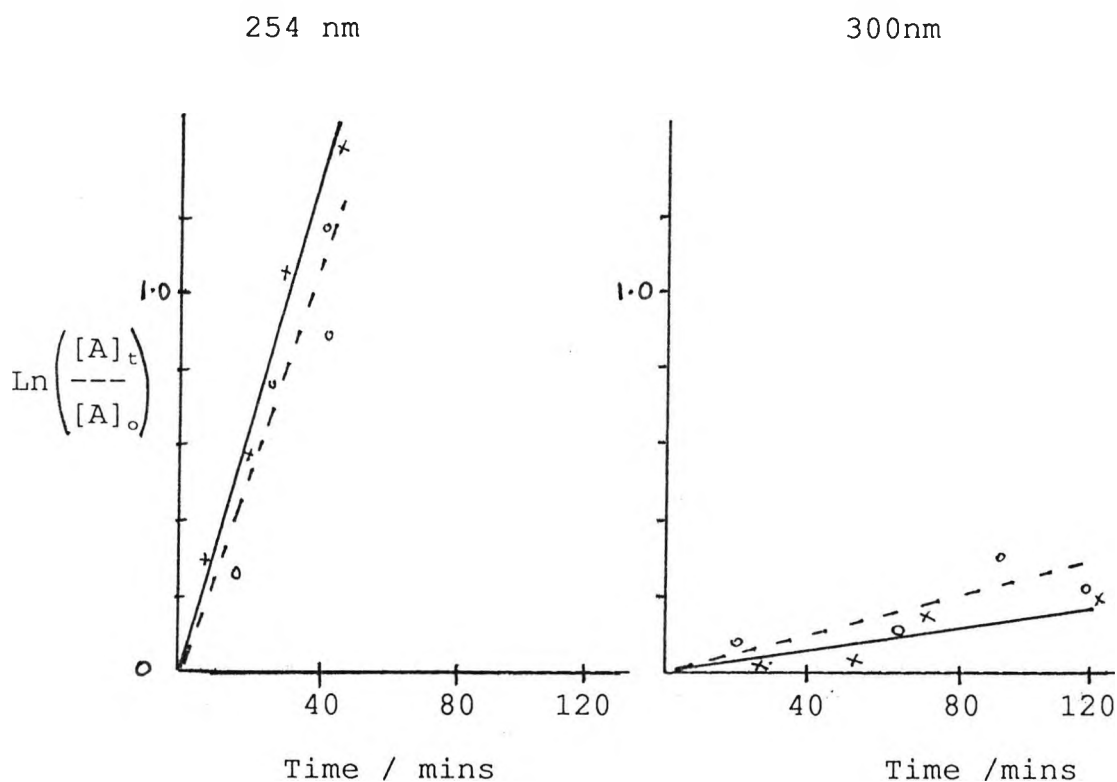


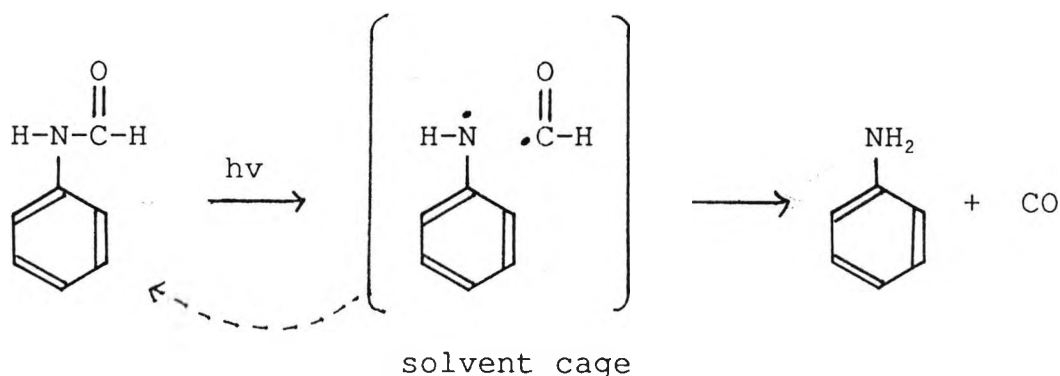
Figure 4.5. Relative rates of reaction for formanilide decarboxylation in oxygenated (----) and degassed (—) solutions.

Not surprisingly, the rate of decarboxylation was greater at 254 nm than 300 nm irradiation. Another kinetic study using 2-formylaminoacetophenone as substrate yielded similar results. Finally, the presence

of water was found to have no effect on the reaction rate. Thus under 254 nm irradiation, 1-N-formylaminoanthra-9,10-quinone decarbonylated at the same rate when in acetonitrile and 10% aqueous acetonitrile.

4.3 DISCUSSION

The results, in accord with previous work ¹² show that N-formyl derivatives of primary aromatic amines decarbonylate upon irradiation to give the parent amine. A simple mechanism (Scheme 4.2) which fits the observed



Scheme 4.2 : Photolysis of formanilides

data is that absorption of a photon causes homolytic fission of the amidic C-N bond to give a formyl and anilino radical. The radicals can either recombine to reform the starting material or the anilino radical abstracts a hydrogen atom to give aniline and carbon monoxide. Formation of carbon monoxide provides a driving force for the reaction. It is not clear how rapidly amides such as formanilide undergo intersystem

crossing and therefore one cannot say whether these reactions are predominantly singlet or triplet in nature. Furthermore, it is conceivable that the α - cleavage reaction competes effectively with intersystem crossing. However, it has been shown earlier that oxygen has no effect on the reaction rate and this is indicative of singlet state chemistry but cannot rule out participation by a short lived triplet state. The observation that N-formyl-3-methylindole and N¹ⁿ-formyltryptophan methyl ester hydrochloride decarbonylates faster than photo oxygenation occurs suggests that in these compounds also, decarbonylation competes effectively with either ISC or triplet energy transfer to oxygen and the reaction of the singlet oxygen so produced with the indole. Introduction of a carbonyl into the chromophore modifies the photochemical reactivity. This in part may be due to the aromatic carbonyl group screening light from the N-formyl group. More importantly it introduces singlet and triplet states of lower energy (Figure 4.6) and

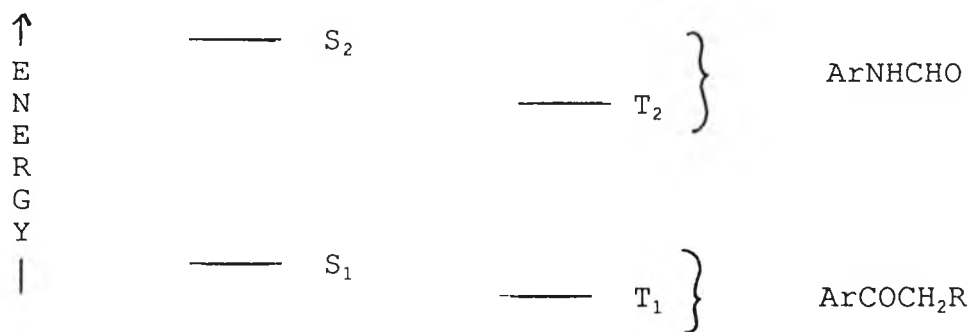


Figure 4.6. Relative energy levels of N-formylamines and aromatic ketones.

efficiently promotes ISC. Hence, irradiation of these compounds at 300 nm only populates a lower S_1 state which rapidly undergoes ISC. Decarbonylation does not occur from the T_1 state so other photochemical reactions can compete, for example, triplet energy transfer to oxygen and thermal deactivation to the ground state. When two ketone carbonyls are present e.g. N-formylaminoanthra-9,10-quinone ISC will occur with almost unity and this is seen in the lack of reactivity when irradiated at 300 nm. Irradiation at 254 nm populates the upper excited level of the amide from which decarbonylation can compete with internal conversion to lower excited states.

4.4 CONCLUSION

In conclusion, the evidence presented suggests that NFK decarbonylates from an upper excited state (either S_2 or T_2) and that the efficiency of this process is wavelength dependent being most efficient at wavelengths < 300 nm. This has important ramifications for biological systems where the transformation of NFK to kynurenine is observed. The results show that this cannot be a photochemical reaction and is therefore likely to be an enzymatic process. NFK when irradiated with light > 300 nm should as previously reported, sensitise the formation of singlet oxygen which is the case for normal triplet $n-\pi^*$ states of aromatic carbonyl compounds ¹⁸.

N-formylation of indole nuclei does not impart any photoprotection and no evidence of aromatic formylated indoles via a photo-Fries rearrangement was found.

4.5 EXPERIMENTAL

The starting materials were obtained from Aldrich except kynurenine (Sigma chemicals) and used without further purification. All melting points are uncorrected. ¹H nmr spectra were recorded with a Joel JMN-MH 100 instrument using TMS and DSS as internal standards. IR spectra were run on a Perkin-Elmer 983 instrument. Mass spectra were recorded on a Kratos MS 30 Electron Impact Instrument, linked to a Kratos DS 50 data system. Microanalysis was performed on a Carlo Erba Model 1106 Elemental Analyser. Uv / Vis absorption spectra were obtained on a Perkin-Elmer 402 and Philips PU 8700 spectrophotometers.

4.5.1 Synthesis of N-Formylated Compounds

4.5.1.1 Nⁱⁿ-formyl-3-methylindole ¹⁷

A solution of 3-methylindole (5.0 g, 38 mmol) in formic acid (50 mls) was heated under reflux for 90 mins. The acid was removed under reduced pressure. Sodium bicarbonate (10 %, 30 mls) was added to the remaining liquid which was then extracted with ethyl acetate (30

mls x 3). The extracts were combined, washed with water (30 mls x 2) and dried over anhydrous potassium carbonate. Removal of the solvent under reduced pressure gave a straw coloured liquid which was purified by vacuum distillation. The portion distilling at 180°C / 8 m bar was collected as a straw coloured liquid which solidified on cooling. Crystallisation was achieved by dissolving the solid in acetone (5 mls), adding hexane (20 mls) and storing at 0°C overnight. The crystals were collected at 10°C and air dried. Yield 2.3 g (43 %). Melting point 30-31°C

Analysis

IR (KBr disc) : 1708 cm⁻¹ (C=O str, formyl group).

¹H nmr : (solvent CDCl₃, ref TMS) δ 9.1 (1H, b d, formyl group), δ 8.3 (1H, b s, C-7 proton), δ 7.5 - 7.2 (4H, m, aromatic and enamine), δ 2.3 (3H, s, methyl).

Mass spec m/e (R.I) : 159 (43), 131 (12), 130 (54).

Uv / Vis : (Solvent CH₃CN) λ max - 288, 296 (shoulder) nm, (ε = 4000).

Elemental Analysis for C₁₀H₉NO

Calculated C- 75.44 H- 5.69 N- 8.79

Found C- 75.15 H- 5.62 N- 8.79

4.5.1.2 Nⁱⁿ-formyltryptophan methyl ester hydrochloride⁹

Tryptophan methyl ester hydrochloride (0.5 g, 2.0 m mol) was dissolved in formic acid (10 mls). Hydrogen

chloride gas was introduced until a saturated solution was obtained. This mixture was left for 75 minutes at room temperature. The solution turned from colourless to purple during this period. Excess formic acid was removed under reduced pressure to leave a purple liquid. Dropwise addition of ethanol (98 %) precipitated a white solid which was collected by filtration, washed with acetone and oven dried at 50°C. Yield 0.30 g (55 %). Melting point 181-182°C.

Yields of 90 % were achieved when the reaction was scaled up.

Analysis

IR (KBr disc) : 3100 - 2900 cm^{-1} (NH_3^+ str, primary amine), 1752 cm^{-1} (C=O str, sat ester), 1710 cm^{-1} (C=O str, formyl group).

^1H nmr : (solvent D_2O , ref TMS) δ 9.5 (1H, b s, formyl proton), δ 7.9 - 7.7 (5H, m, aromatic and enamine), δ 4.7 (1H, t, $J=8$ Hz α -CH), δ 4.0 (3H, s, methyl ester), δ 3.6 (2H, d, $J=8$ Hz methene CH_2).

Mass spec m/e (R.I) : 246 (17), 159 (42), 158 (50), 131 (11), 130 (100), 88 (35).

Uv / Vis : (solvent H_2O) λ max - 280, 288, 296 (shoulder) nm, ($E = 4000$).

<u>Elemental Analysis</u>	for	$\text{C}_{13}\text{H}_{15}\text{ClN}_2\text{O}_3$		
Calculated	C-	55.22	H- 5.34	N- 9.90
Found	C-	54.70	H- 5.51	N- 9.73

4.5.1.3 N-formylcarbazole

A solution of carbazole (10 g, 60 m mol) was heated under reflux in formic acid for 75 mins. The solution changed from colourless to green to black after about 15 mins reaction time. Excess reagent was removed under reduced pressure to leave a green solid. The solid was recrystallised twice from ethanol to give off white crystals. Yield 9.4 g (80 %). Melting point 92-94°C

Analysis

IR (KBr disc) : 1700 cm^{-1} (C=O str, formyl).

^1H nmr : (solvent CDCl_3 , ref TMS), δ 9.7 (1H, s, formyl proton), δ 8.1 - 7.4 (8H, m, aromatics),

Mass spec m/e (R.I) : 195 (79), 167 (100), 140 (11), 139 (13).

Uv / Vis : (solvent CH_3CN) λ_{max} - 222, 264, 298, 310 nm.

Elemental Analysis for $\text{C}_{13}\text{H}_9\text{NO}$

Calculated	C- 79.98	H- 4.64	N- 7.17
Found	C- 79.89	H- 4.60	N- 7.14

4.5.1.4 Formanilide

Formanilide was purchased from Aldrich and used without further purification.

4.5.1.5 2-Formylaminoacetophenone

Acetic anhydride (1.02 g, 10 m mol) was added to formic acid (0.50 g, 11 m mol) at 4°C and left to stand for 30 minutes. In one portion 2-aminoacetophenone (1.35 g, 10 m mol) dissolved in formic acid (10 mls) was added and the solution left for 2 hours at room temperature. Water (30 mls) was added and the mixture extracted with chloroform (3 x 25 mls). The organic phase was washed with water (3 x 30 mls) and dried over magnesium sulphate. The chloroform was removed under reduced pressure to leave a brown liquid which crystallised when the flask interior was scratched. The residual mass was recrystallised from acetone/hexane to give a white crystalline solid. Yield 1.1 g (67 %), melting point 78 - 80°C.

Analysis

IR (KBr disc) : 3250 cm^{-1} (N-H str, sec amide), 1681 cm^{-1} (C=O str, amide), 1645 cm^{-1} (C=O str, aromatic ketone).

^1H nmr : (solvent CDCl_3 , ref TMS), δ 8.9 - 8.3 (2H, b d, amidic and formyl), δ 8.1 - 7.3 (4H, m, aromatic), δ 2.7 (3H, s, methyl group).

Uv / Vis : (solvent CH_3CN) λ max - 259, 321 nm, ($E=4000$).

Mass spec m/e (R.I) : 163 (23), 148 (11), 135 (57), 121 (100), 92 (43).

Elemental Analysis for $\text{C}_9\text{H}_9\text{NO}_2$

Calculated	C- 66.24	H- 5.55	N- 8.58
Found	C- 66.24	H- 5.64	N- 8.63

4.5.1.6 N'-Formylkynurenine ¹⁷

Formic acid (0.15 g, 3.3m mol), and acetic anhydride (0.13 g, 1.2 m mol) were mixed together at 5°C and stood for 30 minutes. The formylating agent was then added dropwise at 5°C to kynurenine (0.25 g, 1.2 m mol) dissolved in formic acid (2 mls). The reaction was stirred at room temperature and followed by HPLC (for conditions see below) until complete. The reaction mixture was added dropwise into ether (50 mls) which deposited a fawn coloured powder. The powder was collected by filtration and washed with acetone and dried in a vacuum dessicator. Yield 157 mgs (60 %), melting point 163°C.

Analysis

IR (KBr disc) : 3400 - 2600 cm^{-1} (NH_3^+ str, aliphatic amine), 1710 cm^{-1} (C=O str, carboxylic acid), 1660 cm^{-1} (C=O str, formyl), 1640 cm^{-1} (C=O str, aromatic ketone).

Mass spac m/e (R.I) : 236 (0.7), 219 (18), 191 (36), 147 (16), 146 (75), 145 (72), 144 (33), 118 (25), 117 (40), 105 (10), 104 (73), 91 (28), 90 (27).

Uv / Vis : (solvent H_2O) λ max - 320 nm, ($E = 3100$).

Elemental Analysis for $\text{C}_{11}\text{H}_{12}\text{N}_2\text{O}_4$

Calculated	C- 55.93	H- 5.85	N- 11.86
Found	C- 55.43	H- 6.05	N- 11.57

4.5.1.7 N',N^α-diformylkynurenine

Formic acid (0.25 g, 1.2 m mol) was mixed with acetic anhydride (0.25 g, 2.5 m mol) and then added to kynurenine (0.25 g, 1.2 m mol) dissolved in formic acid (5 mls). After about 5 minutes a white solid dropped out of solution. The reaction was left to stir for a further 2 hours and then added to water (2 mls). The white solid was collected by filtration, washed with acetone and recrystallised from ethanol / water. Yield 100 mgs (31 %). Mpt 140-142 °C

Analysis

IR (KBr disc) : 1749 cm⁻¹ (C=O str, carboxylic acid), 1701 cm⁻¹ (C=O str, aromatic formyl), 1650 cm⁻¹ (C=O str, aliphatic formyl), 1613 cm⁻¹ (C=O str, aromatic ketone).

Uv / Vis : (solvent H₂O) λ max - 320 nm. (E = 3100).

Mass spec m/e (R.I) : 264 (3), 236 (4), 219 (7), 191 (18), 173 (13), 162 (16), 149 (11), 148 (43), 146 (70), 145 (25), 120 (62).

Elemental Analysis for C₁₂H₁₂N₂O₅

Calculated	C- 54.50	H- 4.55	N- 10.61
Found	C- 54.64	H- 4.76	N- 9.94

4.5.1.8 1-N-Formylaminoanthra-9,10-quinone

Formic acid (1.0 g, 22 m mol) was mixed with acetic

anhydride (2.02 g, 20 m mol) and added to 1-aminoanthra-9,10-quinone (4.6 g, 20 m mol) dissolved in formic acid (50 mls). A brown solid dropped out of solution and was collected by filtration. Recrystallisation from ethanol yielded a brown powder. Yield 4.6 g (92 %). m_{pt} 167-169°C

Analysis

IR (KBr disc) : 1714 cm^{-1} (C=O str, aromatic ketone), 1688 cm^{-1} (C=O str, formyl), 1642 cm^{-1} (C=O str, aromatic ketone adjacent formyl).

1H nmr : (solvent $CDCl_3$, ref TMS), δ 9.3 (1H, b s, amidic N-H), δ 8.9 (1H, s, formyl C-H), δ 8.6 - 8.0 (7H, m, aromatic).

Uv / Vis : (solvent CH_3CN) λ max - 375, 393 nm, ($\epsilon = 3500$).

Mass spec m/e (R.I) : 251 (15), 223 (100), 195 (13), 167 (15), 137 (16).

Elemental Analysis for $C_{15}H_9NO_3$

Calculated	C- 71.71	H- 3.61	N- 5.57
Found	C- 71.88	H- 3.50	N- 5.81

4.5.2 Photolysis Experiments

The solvents were oxygenated with a stream of oxygen or deoxygenated by bubbling nitrogen for 10 minutes.

A typical photolysis run was carried out as follows. In a quartz cuvette (1 cm^3), a solution was made up to an Optical Density (O.D) of 1 - 2 in spectroscopic grade

solvents. A Uv / Vis spectrum was recorded and the cuvette placed in a circular array of 10 x 8 watt 254 nm germicidal lamps or 10 x 8 watt lamps having a maximal emission of 300 nm. The sample was irradiated for 1 minute and a second spectrum recorded. This process was repeated to obtain spectra taken after irradiation times $T = 0, 1, 2, 5, 10, 20, 30$ and 60 minutes.

4.5.3 Chromatographic Conditions

4.5.3.1 High Performance Liquid Chromatography (HPLC)

The solutions were made up to a concentration of 1×10^{-4} mol l^{-1} and irradiated as above. Aliquots of 20 μ ml were removed by syringe at the designated time and analysed.

HPLC was performed on a Waters model 510 liquid chromatograph equipped with a Cecil Uv / Vis detector and a Fisons Vitatron printer. The column was a C_{18} 5 μ m Hypersil (25 x 0.45 cm) reverse phase. The eluent was degassed prior to use under vacuum in an ultrasound bath. In all cases the eluent was methanol / water and the ratios are given in the following table. The flow rate was varied for each experiment and these are given in Table 4.2.

With these conditions the formylated compound is well separated from the parent amine and the analysis time is

about 25 minutes.

Compound	Eluent (MeOH / H ₂ O)	Flow Rate (ml min ⁻¹)
N-formylkynurenine	1 : 4	1.0
N-formylaminoacetophenone	1 : 1	0.6
N',N ^α -diformylkynurenine	4 : 1	1.0
N-formylamino-1-anthra-9,10-quinone	2 : 1	0.6

Table 4.2 : HPLC conditions for the formylated compounds

4.5.3.2 Gas Liquid Chromatography (GLC)

Solutions were made up to a concentration of 1×10^{-2} mol l⁻¹ and irradiated as above. Aliquots of 5 or 10 μ ml were removed by syringe for the analysis.

GLC was performed on a Perkin-Elmer Sigma 5 gas chromatograph fitted with a Flame Ionisation Detector (F.I.D). The column (Internal diameter 2 mm, length 2 m) contained liquid phase S.E 30. The flow rate was 20 mls min⁻¹. The oven and injector temperatures were varied for each sample and are given in Table 4.3.

Compound	Oven Conditions (°C)	Injection Temp (°C)
Formanilide	110 for 1min 110-180 at 10°/ min 180 for 5 mins	225
N-formylcarbazole	180	220
N-formylaminoacetophenone	145	200
N ¹ⁿ -formyl-3-methylindole	150	200

Table 4.3 : GLC conditions for the formylated compounds

4.5.4 Kinetic Studies

Solutions were prepared as above and a photostable internal standard added (see Table 4.4). Irradiations were performed as described earlier and analysed using either HPLC or GLC under the conditions depicted above. The ratio of analyte to internal standard peak height served as the analytical parameter. From this measurement the concentration at irradiation time T was determined for either the appearance of the product or disappearance of the formylated starting material. The compounds analysed under different conditions are listed in table 4.4.

Compound	Conditions	Detection Method	Internal Standard
2-formylamino acetophenone	Irradiated at 254 and 300 nm in oxygenated + deoxygenated soln.	GLC + HPLC	Phenyl methyl sulphone
Formanilide	Irradiated at 254 and 300 nm in oxygenated and deoxygenated soln	GLC	Phenyl sulphone
1-formylamino anthra-9,10-quinone	Irradiated at 254 and 300nm in CH ₃ CN and 10% aqueous CH ₃ CN	HPLC	Phenyl methyl sulphone

Table 4.4 ; Formylated compounds and the conditions under which kinetic studies were performed.

4.6 REFERENCES

1. J.Dillon, R.Chiesa and A.Spector, Photochem. Photobiol, 45, (1987), 147 - 150.
2. C.Pigault and D.Gerard, Photochem. Photobiol, 50, (1989), 23 - 28.
3. J.A.MaClaren and B.Milligan, 'The effects of Radiation and Electric Discharge'. Wool Science. Science Press. Marrickville, (1981), Chapter 13, 219 - 234.
4. C.H.Nicholls, 'Photodegradation and Photoyellowing of Wool'. Developements in Polymer Photochemistry Vol 1. ed N.S.Allen, Applied Science Publishers Lmted, London, 1980, 125 - 144.
5. P.Walrant and R.Santus, Photochem. Photobiol, 19, (1974), 411 - 417, and 20, (1974), 455-460.
6. K.Mandal, S.K.Buse and B.Chakrabarth, Photochem. Photobiol, 43, (1986), 515 - 523.
7. U.P.Andley and B.Clark, Photochem. Photobiol, 50, (1989), 97 - 105.
8. M.Nakagawa, Y.Yokoyama, S.Sato, and T.Hito, Tetrahedron, 41, (1985), 2125 - 2132.
9. A.Previero, M.A.Coletti-Previero and J.C. Cavadore, Biochim Biophys Acta, 147, (1967), 453 - 461.
10. H.Gross and J.Meienhofer, The Peptides Vol 5, Academic Press, New York, (1981), 245 - 247.
11. M.Somei and M.Natsume, Tet Letts, 27, (1973), 2451 - 2454.

12. B.K.Barnett and T.D.Roberts, J Chem Soc Chem Comm, (1972), 758.
13. C.E. Dalgleish, J Chem Soc, (1952), 137 - 141.
14. B.G. Edward, Arch Biochem Biophys, 21, (1949), 103.
15. J.Derkosch, O.E. Polansky, E.Ringer and G.Derflinger, Monatsh Chem, 92, (1961), 1131.
16. P.W. Atkins, Physical Chemistry, 2nd edition, Oxford University Press, London, (1982), 927 - 928.
17. M.Kashimura and Y.Kigugawa, Chem Pharm Bull, 31 (8), (1983), 2892 - 2894.
18. A.A.Gorman and M.A.Rodgers, J Am Chem Soc, 108, (1986), 5074 - 5078.

CHAPTER 5

SYNTHESIS, REACTIONS AND PHOTOPHYSICAL STUDIES
OF AZLACTONES

5.1 INTRODUCTION

More than a century has passed since Plochl reported the acetic anhydride mediated condensation of benzoylglycine with benzaldehyde. However, it was Erlenmeyer who first established the correct structure and named the product an Azlactone, a term still encountered ¹.

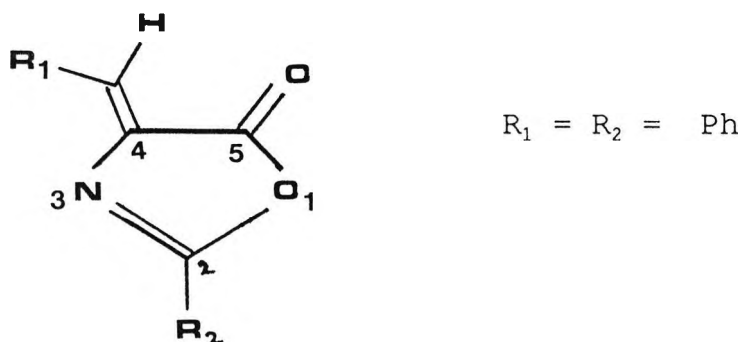


Figure 5.1 : Structure of unsaturated azlactones

The general structure and numbering system is given in Figure 5.1. A more systematic nomenclature is 4-'aryl' methylene-2-'aryl'oxazol-5-one, thus the compound shown above is 4-phenylmethylene-2-phenyloxazol-5-one. The classical synthesis works well with aromatic aldehydes but poor yields are obtained for aliphatic aldehydes, however, improvements have been reported ². Since the early work of Erlenmeyer several reviews on the synthesis and reactivity of Azlactones have appeared ^{1,3,4,5,6}.

Over the past few decades azlactones have emerged as an important class of synthetic intermediate particularly for the synthesis of amino acids and related

compounds ^{7,8,9}. Vigorous research has widened their horizons as synthons ¹⁰. Their easy availability and diverse reactions open the possibility for using them as building blocks in dye, heterocyclic, natural product and polymer chemistry ¹¹. During the last ten years little has been published on the use of azlactone as dyes. One report describes the synthesis of several pyrenyl derivatives and their application to polyester ¹². Unfortunately, no spectral data was given. To the authors knowledge unsaturated azlactones have not been investigated in view of studying their photophysical properties.

Colour chemistry is presently undergoing a period of intense interest in specialty dyes whose absorption and emission characteristics can be tailored to specific applications. Novel uses include photochemotherapy, photovoltaic dyes, dyes for optical disc recording and data storage, laser dyes, dyes for liquid crystal displays and electrophotographic processes ^{13,14}. When both R_1 and R_2 (Figure 5.1) are aromatic a chromophore is formed and by varying these groups it will be possible to alter the spectral properties.

This chapter describes the synthesis of various azlactones which are classified according to the type of aromatic substituents. To produce some original compounds new benzoylglycines and an aromatic aldehyde are synthesised. The first class of azlactone is a

series of donor-acceptor compounds. The second consists of polycyclic aromatics at position R_1 and the final azlactones have a ferrocenyl group at the same position. Their spectral characteristics are studied and the transitions giving rise to long wavelength Uv / Vis absorption bands are assigned. A selection of known reactions to other heterocyclic and acyclic compounds was undertaken. The new compounds were investigated spectroscopically bearing in mind the properties of the original azlactones and the myriad of novel application just mentioned.

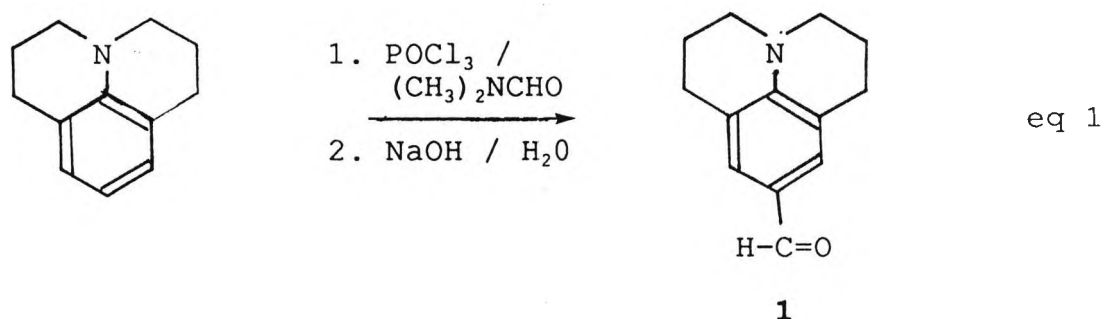
Rather than name each compound when it is discussed a reference number is allocated. Similarly, the chromophores are generally described by mention of the groups at R_1 and R_2 in the basic structure and the whole molecule is not reproduced.

5.2 RESULTS

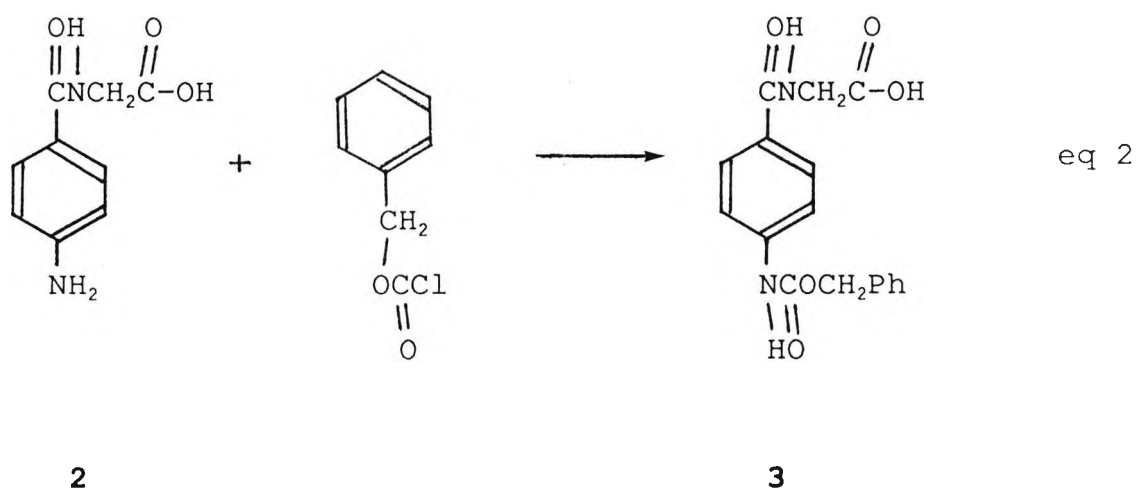
5.2.1 Arylglycine and Aldehyde Synthesis

To investigate the spectroscopic properties of azlactones it was deemed necessary to have various aromatic groups at positions 2 and 4. Introduction of the aryl group at position 4 is from an aromatic aldehyde. Activated arenes are readily formylated under Vilsmeier-Haack conditions ¹⁵. Using this method julolidine-9-

carboxaldehyde was obtained in 55% yield (eq 1). An aryl group at position 2 is derived from the initial

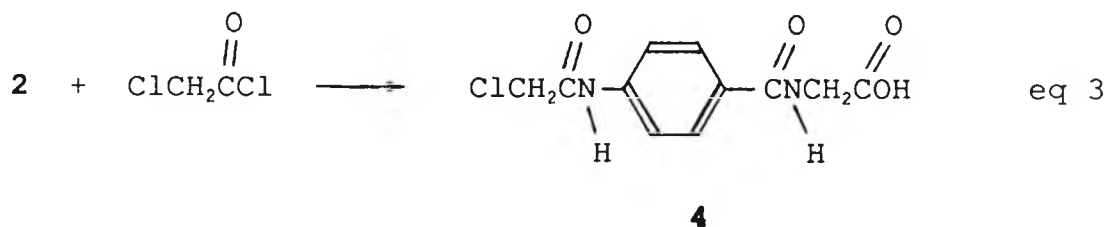


benzoylglycine and relatively few of these compounds are known. The synthesis of aroylglycine derivatives can be achieved by two main strategies :- (1) the reaction of glycine with substituted aroyl halides and (2) modification of existing aroylglycines. Both methods were used to obtain new aroylglycines. A readily available starting material was 4-aminobenzoylglycine **2**.

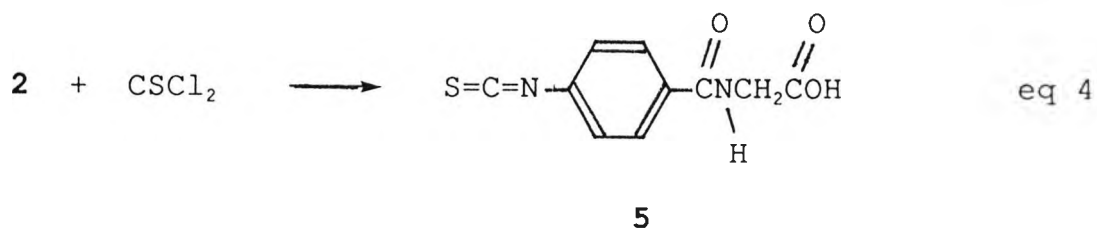


Under typical Schotten-Baumann conditions **2** reacts with benzyloxylchloride to give the amine protected aroylglycine **3** as white crystals in 67% yield (eq 2).

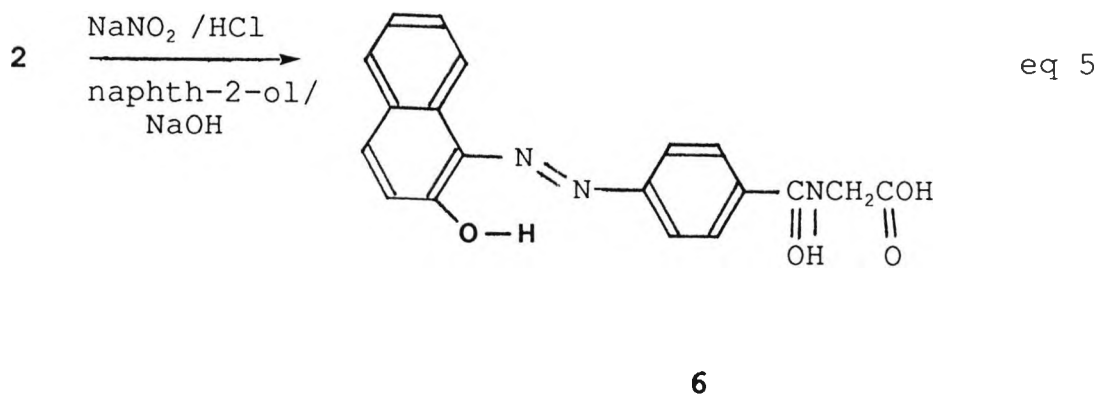
Similar conditions were used to react chloroacetylchloride with **2** to give **4** (eq 3) in



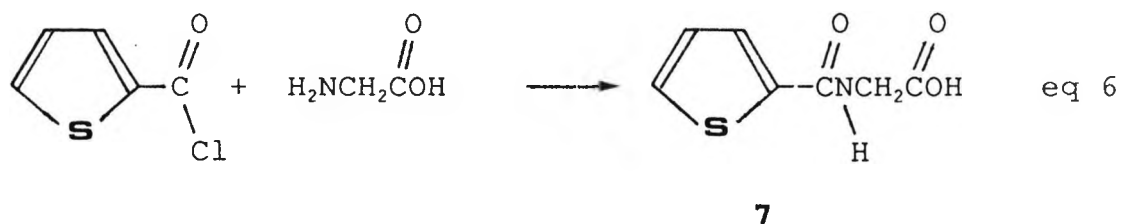
modest yield (40%). Reaction of the hydrochloride of **2** with thiophosgene in aqueous acetone gave the pure isothiocyanate **5** in almost quantitative yield (eq 4).



Under acid conditions **2** readily formed a diazo salt which was coupled in basic media with naphth-2-ol. The azo dye **6** was obtained pure in a 40% yield (eq 5).



The second strategy was to react an aromatic acid chloride with glycine under Schotten-Baumann conditions.



Thus, thiophene-2-carboxylchloride was reacted with glycine in aqueous acetone to yield thiophen-2-oylglycine **7** in an excellent 85% yield (eq 6).

5.2.2 Azlactone Synthesis and Structure

In broad terms, the azlactones synthesised can be divided into three classes with respect to the aromatic moiety at position 4. The simplest class has a phenyl nucleus allied to an electron donor or acceptor group and these are listed in Table 5.1. Compounds **8-13** were synthesised by method A (see experimental) in moderate to good yields. Both **8** and **9** are well characterised compounds ¹⁶. Unsaturated azlactones are more stable than their saturated counterparts and can generally be purified by recrystallization. In most cases the solvent of choice was either ethanol or glacial acetic acid. The methyl groups in **8** and **11** contain active hydrogens which allows the chromophore to be modified (see later). A second series of azlactones contained a fused ring

R ₁	R ₂	Compound no.	Yield (%)
Ph	CH ₃	8	60
Ph	Ph	9	45
Ph	Thiophenyl	10	45
p-O ₂ N-Ph	CH ₃	11	41
p-(Et) ₂ N-Ph	p-O ₂ N-Ph	12	59
julolidine	p-O ₂ N-Ph	13	54

Table 5.1 :- Azlactone substituents at positions R₁ and R₂ (figure 5.1)

system at position C-4 and various substituted arenes at C-2. Pyrene (Py) was the polycyclic moiety used in all

R ₁	R ₂	Compound no	Yield (%)
Py	CH ₃	14	40
Py	Ph	15	35
Py	Thienyl	16	36
Py	p-S=C=N-Ph	17	17
Py	p-O ₂ N-Ph	18	42
Py	PhCH ₂ CONH-Ph	19	56
Py	ClCH ₂ CONH-Ph	20	30
Py	azo dye 6	21	15
Anth	Ph	22	59

Table 5.2 : Substituents and yields of fused ring azlactones

cases except for one anthracenyl compound. These products are listed in Table 5.2 with their yields. As before the major synthetic methodology followed scheme A (see experimental). Purification was achieved by recrystallization and again, the yields were only modest.

The third class of azlactones incorporate a ferrocenyl (Fer) group at C-4 and can be regarded as organometallic heterocycles. The yields and substituents at C-2 are given in Table 5.3. Modest yields were obtained when the classical method was followed but could be improved

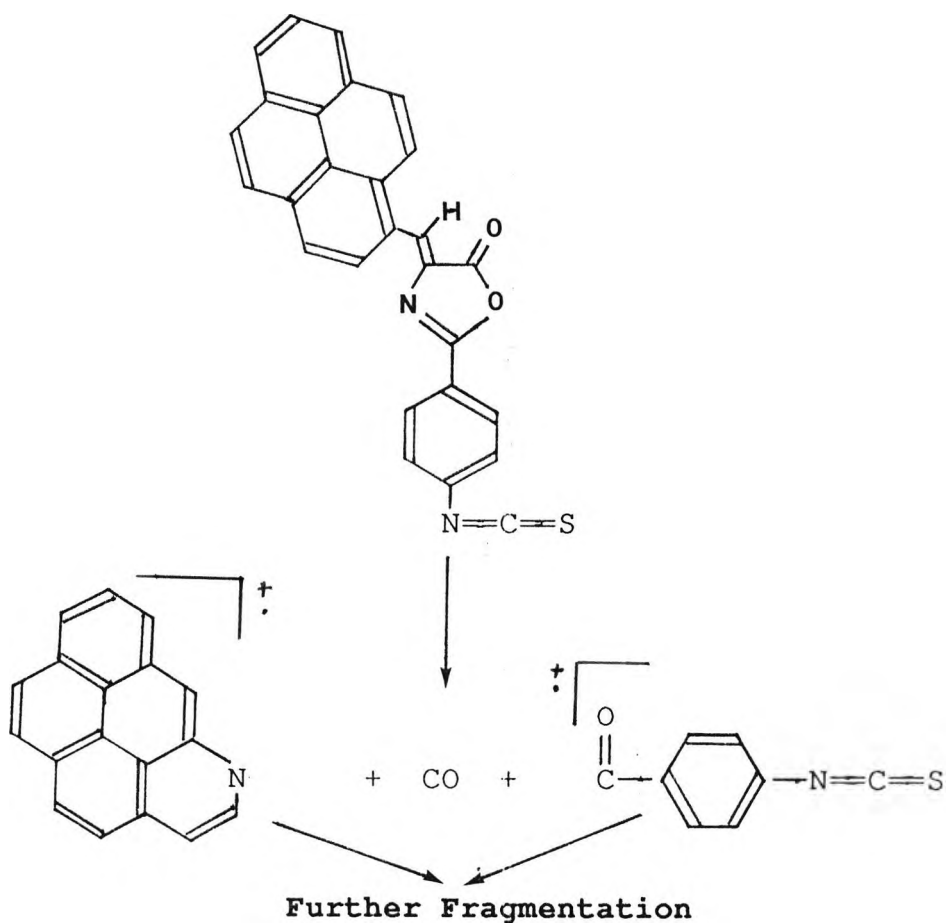
R ₁	R ₂	Compound no	Yield (%)
Fer	Ph	23	41 (method A)
			65 (method B)
Fer	p-O ₂ N-Ph	24	46
Fer	thienyl	25	15

Table 5.3 : Substituents and yields of ferrocenyl azlactones

for **23** using a milder procedure (method B). This is probably due to better isolation and purification procedures employed. Recrystallization was best completed by the slow evaporation of an acetone solution. When high boiling point liquids such as DMF were used the compounds decomposed to a black insoluble uncharacterised powder.

5.2.3 Azlactone Spectral Properties

In accordance with previous literature ¹⁷ the ir spectra of the azlactones (**8-25**) exhibited a carbonyl stretching frequency at 1810-1750 cm^{-1} . In most cases two bands were found in this region. A further characteristic peak at 1640 cm^{-1} was assigned to the heterocyclic ring C=N stretching frequency. The mass spectra of all the azlactones also feature similarities. A molecular ion was identified in all three classes and the primary fragmentation pathway involved heterocyclic ring destruction. This is more clearly shown in Scheme 5.1 where **17** is used as an



Scheme 5.1 Primary fragmentation pathway of azlactones

example. The oxazolone is cleaved at bonds **a,b** and **c** to give carbon monoxide, a substituted aromatic aldehyde and a nitrogen heterocycle. It is noticeable that a double bond (C=N) is cleaved whilst other carbon-heteroatom bonds remain intact.

The proton nmr spectra of **8,9** and **10** were identical to those reported in a previous study ¹⁸. Hence, a singlet at δ 7.2 was ascribed to the alkene hydrogen. The other spectra recorded (**14** and **23**) also displayed this signal and were therefore assigned a (Z)-configuration in agreement with literature data ¹⁹. Unfortunately, the other compounds were not sufficiently soluble in common deuterated solvents for their spectra to be determined. The absorption and emission spectra vary according to both R₁, R₂ and their substituents. This observation is confirmed by referring to the sample absorption spectra

Compound	Absorption max /nm (E x 10 ⁴)	Fluorescence max /nm
8	328 (0.81)	-----
9	380 (1.74)	Not Fluorescent
10	375 (1.19)	440 (very weak)
12	515 (3.01)	Not Fluorescent
13	545 (2.53)	Not Fluorescent

Table 5.4 - Absorption and emission maxima for compounds 8-13 in acetonitrile.

given in Figures 5.1, 5.2, 5.3 and 5.4. Table 5.4 lists the relevant data for compounds **8-13**. When a methyl group is at position 2 the maximal absorption is in the uv region. Moving from a methyl to a phenyl group increases the conjugation such that **9** now absorbs in the visible. A similar change occurs when an unsubstituted thiophene group replaces the phenyl. Introducing electron donor and acceptor substituents moves the absorption maxima to longer wavelengths. The spectrum of **12** in Figure 5.1 is a good illustration of this compound class. Between 200 - 400 nm there is a spectral window in which very little absorption occurs compared to the main absorption band. In the examples above the main absorption band undergoes a bathochromic shift of ≈ 140 nm compared to the unsubstituted phenyl analogue. It is of interest to note that the julolidine dye (**13**) absorbs at a slightly longer wavelength than the diethylamino analogue (**12**). The extinction coefficients all have the same order of magnitude. Only compound **10** emitted a weak fluorescence, the others were non fluorescent in solution.

This leads to the question of whether azlactones can be made into fluorophores. To test the idea a fluorescent group was inserted into a series of azlactones. The absorption and emission characteristics are given in Table 5.5. A pyrenyl nucleus at position 4 moves the absorption maxima into the visible, even with a methyl group at C-2. The maximal absorption band has

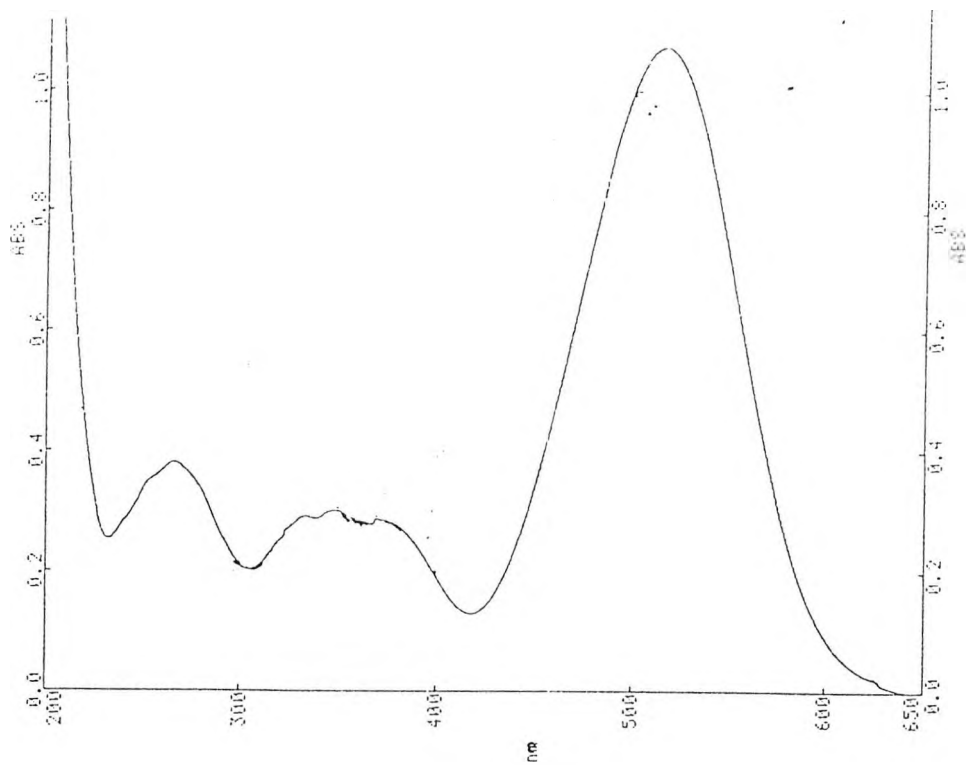


Figure 5.1 Uv / Vis spectrum of compound 12 in acetonitrile.

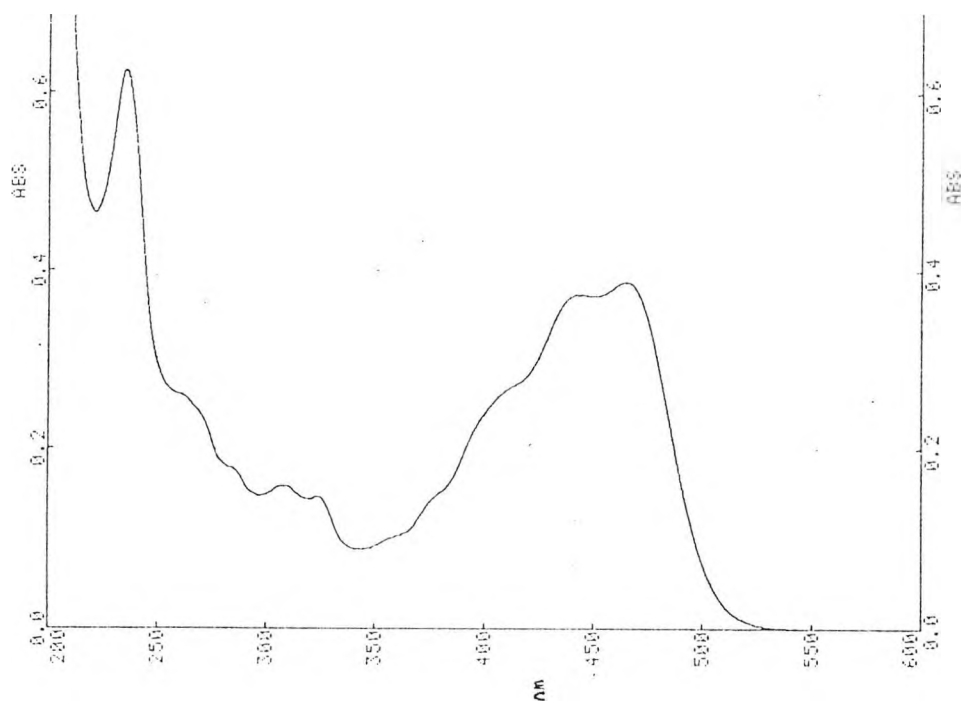


Figure 5.2 Uv / Vis spectrum of compound 15 in acetonitrile

shifted ≈ 110 nm compared to the earlier simple phenyl analogue (9). When the methyl is replaced by a phenyl the absorption maxima is moved by 30 nm to longer wavelength. This spectrum, displayed in Figure 5.2

Cmpd	Absorption max		Fluorescent max /nm	Stokes Shift /nm
	/nm	($E \times 10^4$)		
14	437	(1.75)	510	73
15	467	(3.23)	540	73
16	475	(2.52)	545	70
17	480	(2.09)	555	75
18	485	(2.90)	635	150
19	474	(1.89)	535	61
20	485	(2.13)	555	70
21	533	----	550	17
22	436	(0.50)	Not Fluorescent	----

Table 5.5 - Absorption and emission data for the polycyclic azlactones 14-22 in acetonitrile.

is representative of the pyrenyl derivatives. A spectral window between 250 -360 nm is found. The phenyl substituents are all electron withdrawing and have exerted a further slight bathochromic shift of up to 20 nm. A misfit of this series is compound 21 which absorbs at 533 nm. This dye is essentially two chromophores joined together and so the predicted absorption was

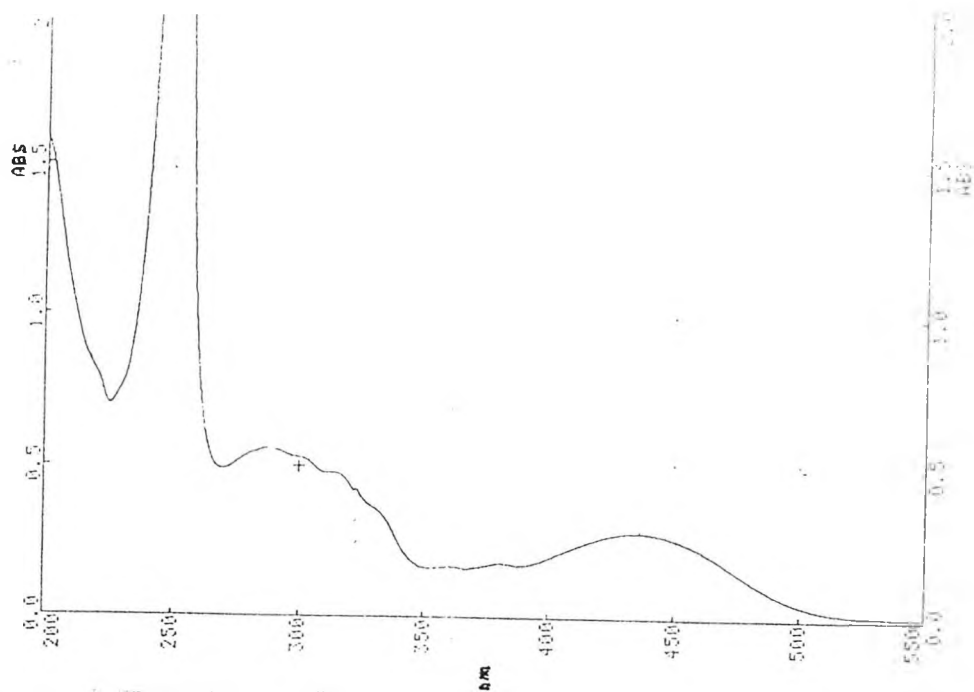


Figure 5.3 Uv / Vis spectrum of azlactone 22
in acetonitrile.

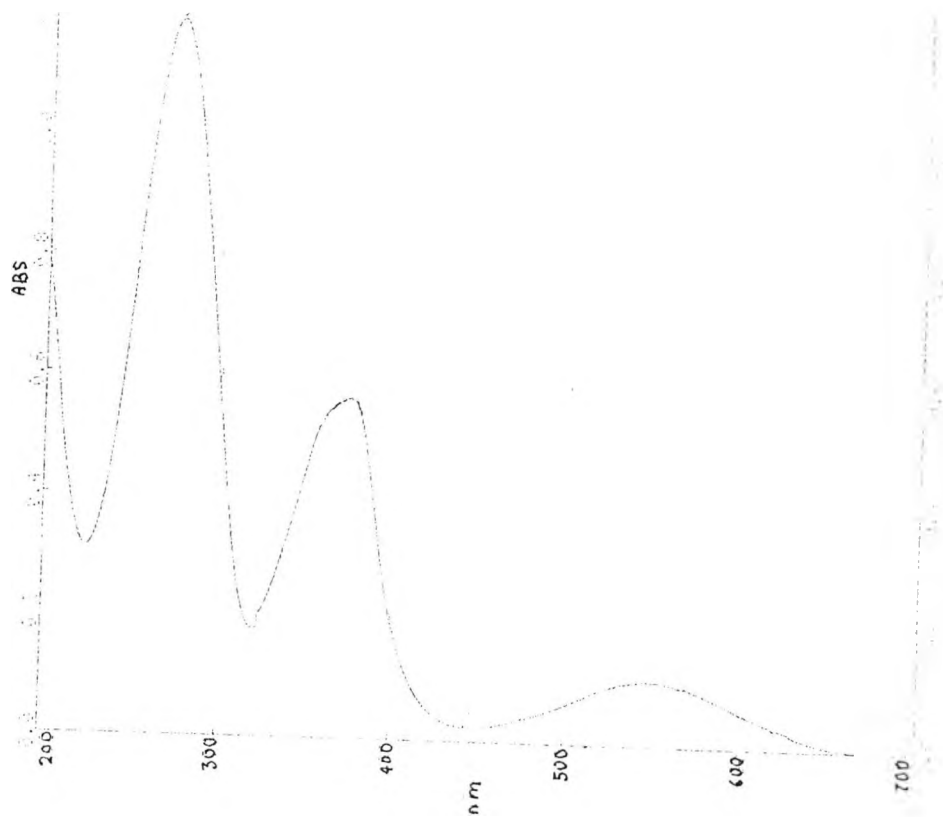


Figure 5.4 Uv / Vis spectrum of azlactone 23
acetonitrile

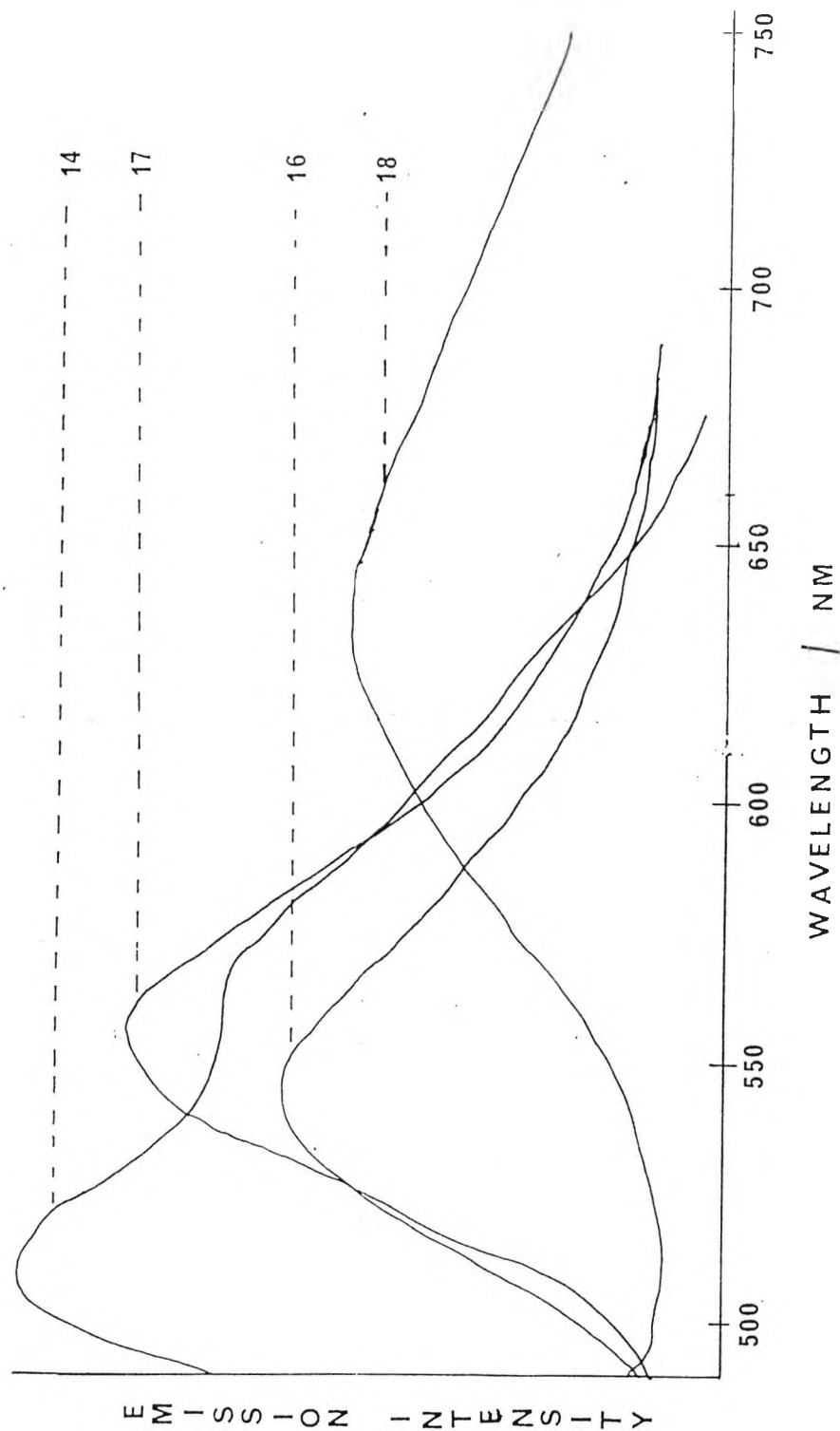


Figure 5.5 Solution fluorescence spectra of pyrenyl compounds 14,16,17 and 18 in acetonitrile. The instrument settings are the same for 14,16 and 17 but three times more sensitive for 18.

anticipated to be at much longer wavelength. All the pyrenyl dyes have comparable extinction coefficients. The anthracenyl azlactone absorbs at shorter wavelength than its pyrenyl counterpart and has a vastly smaller extinction coefficient. The uv/vis spectrum of this compound is displayed in Figure 5.3. To some extent all the pyrenyl azlactones are fluorescent. Samples **14,15,16,17,19** and **20** show comparable Stokes shifts of \approx 60-75 nm and are strongly fluorescent.

Interestingly, **18** has approximately double the Stokes shift of the above and an emission maxima at 635 nm. Its spectrum is a broad band starting at 530nm and tailing off into the near I.R at 810 nm. The spectra do not show any fine structure that is associated with pyrene. Compound **21** fluoresces very weakly and has a small Stokes shift. Unexpectedly the anthracenyl compound was not fluorescent. The fluorescence spectra of **14,16,17** and **18** are given in Figure 5.5.

The heterocyclic organometallic azlactone **23** first prepared by Pauson ¹⁷ has a completely different uv/vis spectra. The spectrum is given in Figure 5.4 and its absorption maxima is presented in Table 5.6. Compared to the previous samples the maximal absorption bands have small extinction coefficients. There is no spectral window identified with these compounds. The spectrum consists of three well separated bands of diminishing intensity.

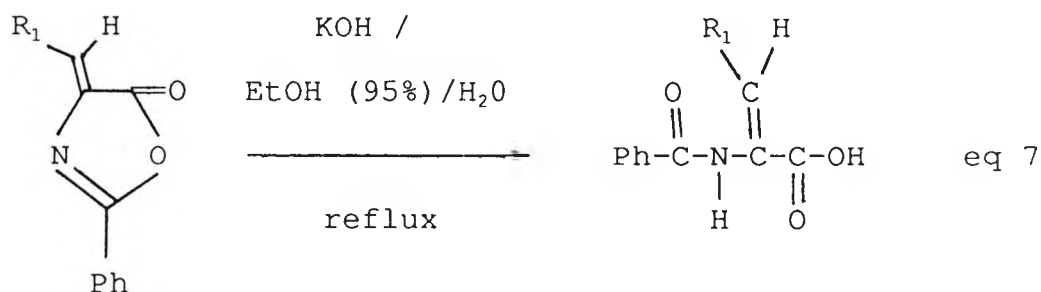
Compound	Absorption max / nm (E x10 ⁴)
23	545 (0.28)
24	600 (0.31)
25	555 (0.20)

Table 5.6 : Absorption maxima for the heterocyclic organometallic azlactones in acetonitrile.

5.2.4 Reactions of Azlactones

5.2.4.1. Hydrolysis

With careful control of the reaction conditions azlactones can be hydrolysed by acids and base to give didehydroamino acids or esters ^{16,22}. This methodology has proved a favourite route to unsaturated amino acids ²³. The base hydrolysis of **9** and **22** occurred readily in aqueous ethanol (eq 7) to give compounds **26** and **27**



respectively. Compound **26** is a prime substrate to test the efficiency of optically active ligands in transition

metal catalysed asymmetric homogeneous hydrogenations^{24,25}. More forceful conditions were required for **15** which was heated under reflux in basic aqueous DMF to give **28**. The yields are given in Table 5.7.

R ₁	Compound	Yield (%)
Ph	26	88
Anth	27	66
Py	28	30

Table 5.7 : Yields of hydrolysed azlactones

Not surprisingly, the I.R. of these three compounds were very similar. The most prominent peaks are at 1690 and 1640 cm⁻¹ which appear as a doublet. They can be assigned to the carbonyls associated with the conjugated carboxylic acid and a secondary amide respectively. The ¹H nmr data is consistent with the structure. It is interesting to note that alkene proton is shifted downfield into the aromatic signals at $\approx\delta$ 6.8 - 7.2. The downfield shift is consistent with the aromatic nucleus trans to the carboxylic acid functionality. In this configuration two of the functional groups are deshielding. The mass spectral fragmentation pathway can be explained by the loss of CO, an aromatic aldehyde and the formation of a nitrogen heterocycle (cf. azlactone).

The azlactone chromophore destruction is readily

confirmed by reference to the uv/vis spectra. All three maxima have moved to shorter wavelength (Table 5.7a). The anthracenyl spectrum (**27**) is comparable to its parent azlactone other than a 50 nm hypsochromic shift of the main absorption band. There are no similar events with **28**. Here the main band is replaced by a long shoulder from 420 - 470 nm with a low extinction coefficient and a new intense peak at 365 nm. The anthracenyl compound is weakly fluorescent and has an emission maxima at 465 nm. Excitation of **28** at two different wavelengths can result in two distinct fluorescence maxima. Irradiation into the band at 365 nm initiates a weak emission signal at 450 nm. A second

Compound	Absorption max /nm ($E \times 10^4$)	Fluorescence max /nm
26	281 (----)	-----
27	386 (0.50)	465
28	365 (1.05)	450
	shoulder at 475 (----)	540

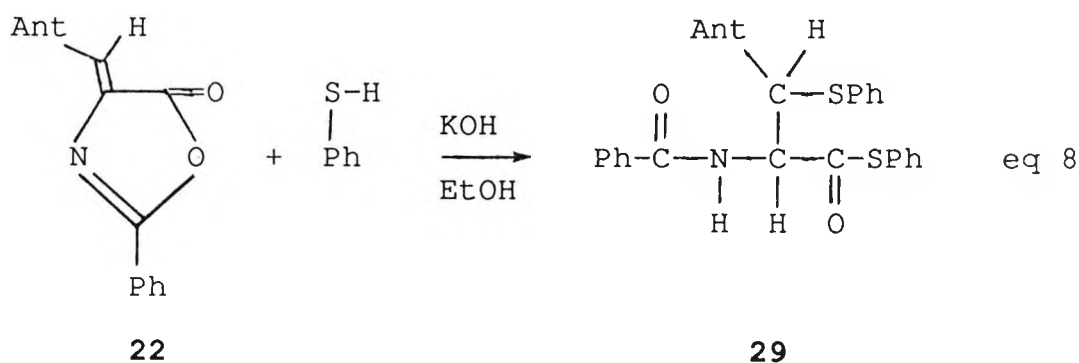
Table 5.7a : Absorption and emission data for didehydroamino acids 26-28 dissolved in acetonitrile.

very weak signal at 540 nm is found after excitation of the shoulder at 460 nm. There is no fine structure found in any of the emission spectra. The Stoke shift values

of both compounds were comparable over a 80 - 85 nm range. An excitation spectra of the signal at 540 nm only gave a peak at 470 nm and there was no band around 360 nm. A similar spectra of the signal at 450 nm only gave a peak at 380 nm.

5.2.4.2. Reaction with Nucleophiles

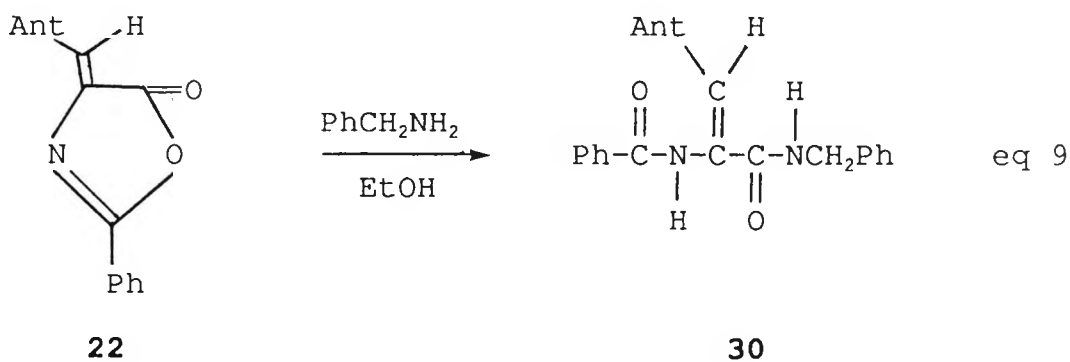
The base catalysed reaction of thiophenol with **9** in boiling ethanol has been reported to give a disubstituted addition product ²⁶. Application of similar conditions to **22** also furnished an analogus adduct **29**. The proposed structure is given in eq 8. Supporting evidence



from the IR data are two carbonyl peaks at 1704 and 1643 cm^{-1} which have been assigned to a thiolester and a secondary amide respectively. The ^1H nmr signals are a complex series of multiplets which have not been analysed in detail. No molecular ion was found in the mass spectrum. The base peak was allotted to an anthracenyl radical cation ($\text{C}_{15}\text{H}_{11}^+$). This was formed after the loss of two thiophenol radicals to give a cyclic intermeadiate

via an intramolecular rearrangement. The uv / vis spectrum was transformed into a structured spectrum identical to anthracene. Subsequently, the fluorescence spectrum was indistinguishable from an authentic anthracene sample (see Figure 5.6).

The reaction of azlactones with amines can lead to different products depending on the conditions ^{10,11}. In refluxing ethanol **22** reacts with one mole equivalent of benzylamine (eq 9) to give the amide **30**. Both amide



carbonyls are found at the same wavelength of 1637 cm^{-1} . The ^1H nmr spectrum shows a complex splitting pattern in the aromatic region. The absorption spectrum has an intense band at 260 nm ($E = > 5 \times 10^4$), a weaker maxima at 381 nm ($E = 0.81 \times 10^4$) and a shoulder at 400 nm ($E = 0.73 \times 10^4$). It is similar to the acid sample above. An emission signal with a maxima at 460 nm was found. Experimentally it was observed that the amidic compound (**34**) fluoresces about four times more strongly than the free acid when excited at 400 nm. A 60 nm stokes shift for this compound proved identical to the acid. The fluorescence spectra for the anthracenyl compounds are

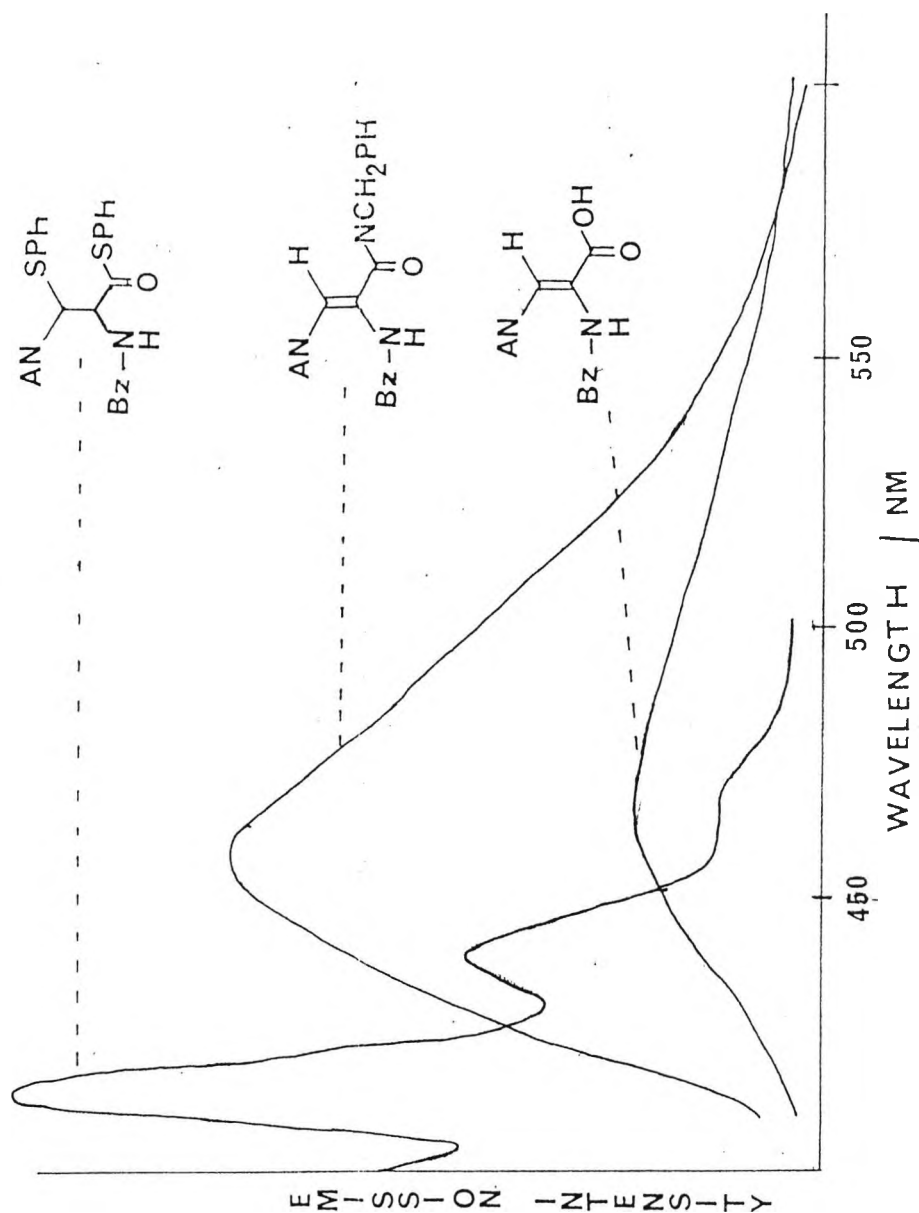
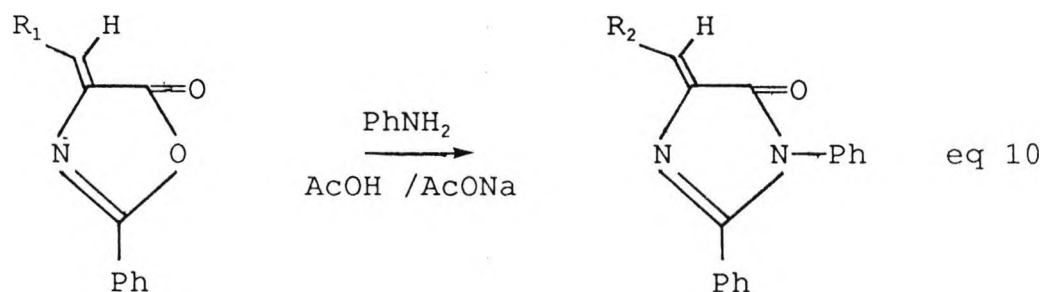


Figure 5.6 Solution fluorescence of the reaction products formed with the anthracenyl azlactone and thiols, amines and water. The instrument settings for the aminated and hydrolysed compounds are \approx ten times more sensitive than the thiol adduct.

shown on Figure 5.6.

The reaction of azlactones with primary aromatic amimes in glacial acetic acid with the presence of catalytic sodium acetate leads to 1,2-diaryl-4-arylmethylene-2-imidazolin-5-ones (eq 10) ^{27,28}. These reaction conditions



R - anthracene and pyrene

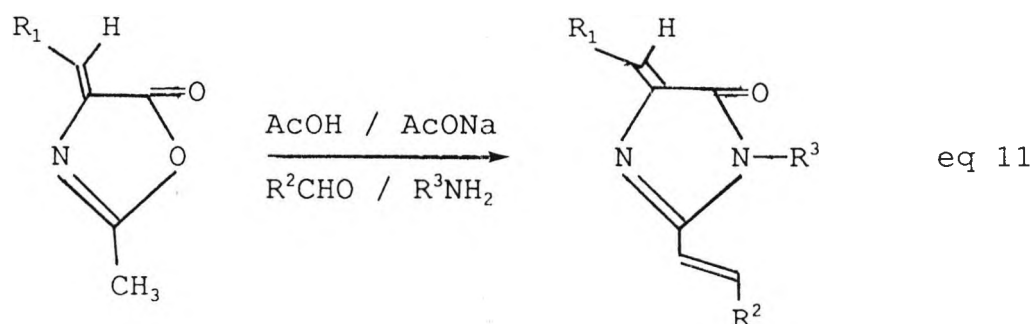
when applied to azlactones **15** + **22** gave the new imidazolin-5-ones **31** + **32** in modest yields. A peak at 1710 cm^{-1} assigned to the amide carbonyl and the C=N signal at 1640 cm^{-1} indicated imidazolin-5-one formation. Mass spectra of both compounds (**31**+**32**) showed molecular ions, but the fragmentation pathway differs from the

Compound	R ₁	R ₂	Absorption max		Fluorescence	
			/nm	(E x10 ⁴)	max	/ nm
31	Py	Ph	470	(1.29)	535	
32	Anth	Ph	410	(1.26)	Not Fluorescent	

Table 5.8 - Absorption and emission maxima for imidazolin-5-ones in acetonitrile.

azlactones and ring opened products. The absorption and emission are given in Table 5.8. There is no significant difference between the long wavelength imidazolin-5-one absorption and emission maxima compared to the parent azlactone. However, a new band at 370 nm (E^{-10^4}) has appeared and these two spectra do not have a window. Experimentally the fluorescence quantum yield of the imidazolin-5-one (**31**) was found to be identical to the azlactone (**15**).

The methyl group at position 2 of an azlactone contains active hydrogen atoms and in the presence of anhydrous zinc chloride can react with aldehydes to give styryl derivatives ²⁹. When the heterocycle is changed to an imidazolin-5-one the protons become more acidic such that a styrylimidazolin-5-one can be constructed with a base like sodium acetate ³⁰. The synthesis can be carried out by mixing an azlactone, an aromatic aldehyde and an amine together in refluxing glacial acetic acid (eq 11). Four



new compounds synthesised by this methodology are listed in Table 5.9. The yields were modest to good. As described above the heterocyclic ring is readily characterised by two I.R peaks at 1710 and 1615 cm^{-1} .

Again these are assigned to the amidic carbonyl and a ring C=N respectively. A trans configuration is ascribed to the styryl bond on the basis of strong peaks between 960 - 980 cm^{-1} . Unfortunately, this was not confirmed

R_1	R_2	R_3	Compound	Yield (%)
Ph	Ph	Ph	33	46
p-O ₂ N-Ph	p-(Et) ₂ N-Ph	p-O ₂ N-Ph	34	45
Ph	Pyr	Ph	35	31
Pyr	Pyr	Ph	36	71

Table 5.9 : Styrylimidazolin-5-ones synthesised .

by ¹H nmr due to the insolubility of these compounds in common deuterated solvents. All four compounds gave strong molecular ions in the mass spectra and a complex fragmentation pathway. The absorption and fluorescence

Compound	Absorption max /nm (E x10 ⁴)	Fluorescence max / nm	Stokes shift /nm
33	410 (1.35)	530	120
34	551 (in DMF)	---	---
35	500 (1.96)	600	100
36	500 (2.00)	580-620	80-120

Table 5.10 : Absorption and emission properties of the styrylimidazolin-5-ones in acetonitrile.

characteristics are recorded in Table 5.10. Introduction of a double bond increases the absorption maxima by approximately 30 nm compared to the parent azlactone. An intense band at ≈ 120 nm lower than the longwavelength maxima is also found. The most striking observation is an appearance of a strong emission spectrum for **33** and its large stokes shift. Compound **34** is insoluble in acetonitrile presumably because two nitro groups are present and so an absorption spectrum was run in DMF. The uv / vis spectra of **35** and **36** are very similar with absorption bands at 500 and 386 nm. Subsequently, the fluorescence spectra were also alike having similar emission maxima and quantum yields. Unusually, the maxima are plateau profiled and this is noticeable for **36** where the range is 40 nm.

5.2.5 Application of Azlactones

5.2.5.1 Protein Labelling

The synthetic ease with which a reactive group can be incorporated into the dye chromophore encourages an investigation of these compounds as possible labels. Consequently, the antibody Immunoglobulin G (Human IGG) was stirred with compound 17 in 50 % DMF / Phosphate buffer solution and separated on Sephadex. Bands in the uv/vis spectrum corresponding to aromatic amino acid absorption at 280 nm and a dye maxima at 482 nm clearly

show that some dye has been bound to the protein (Figure 5.7). However further peaks at 360 nm and more

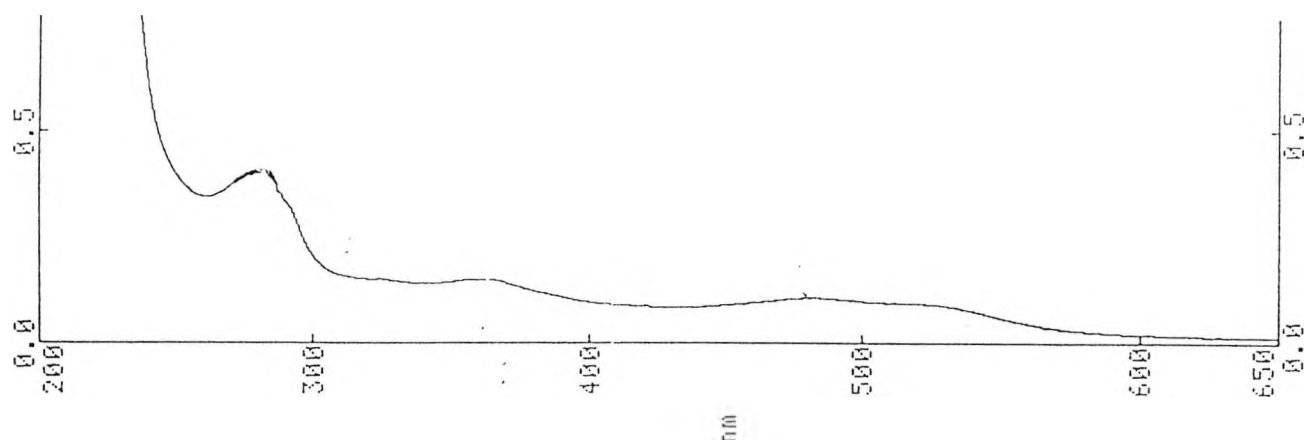


Figure 5.7 : Absorption spectra of protein labelled with compound 17 in phosphate buffer.

surprisingly at 525 nm indicate other reactions are occurring. The solution was diluted to give an optical density of 0.1 at 480 nm and excitation at this wavelength leads to a broad fluorescence emission from

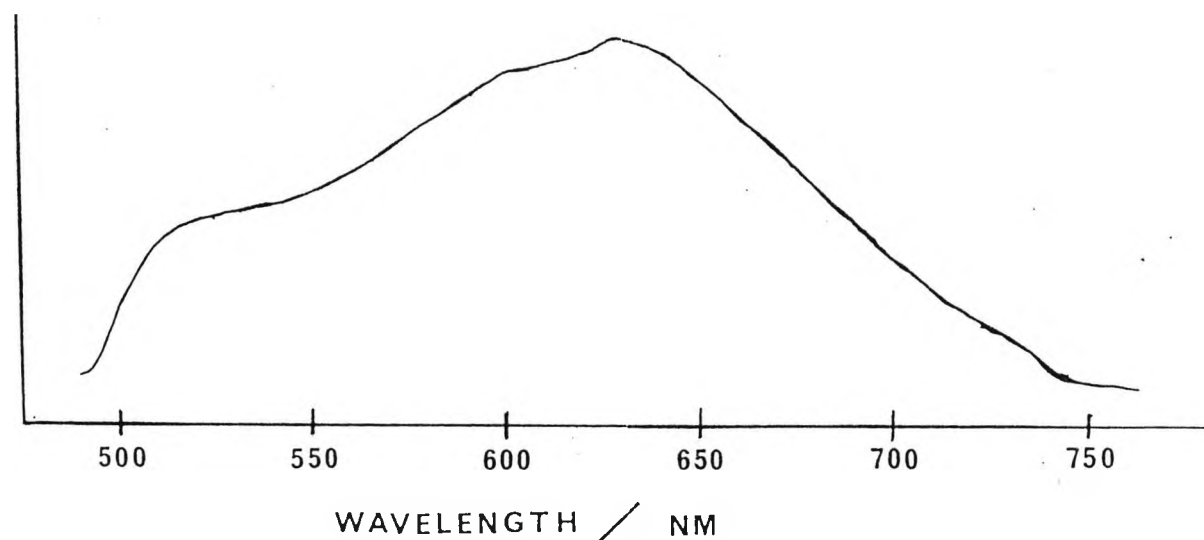


Figure 5.8 : Fluorescence spectrum of protein labelled with dye 17 in phosphate buffer. Excitation wavelength - 480 nm.

500 -740 nm. A shoulder from 520 - 560 nm is followed by a maxima at 630 nm which trails off to 740 nm (Figure 5.8) . If the excitation wavelength is changed to 525 nm a broad structureless emission with a maxima at 630 nm remains. These results indicate that a species other than dye - protein adducts are formed.

5.2.5.2 Dyes for Polyester

The traditional use of dyes is to colour fabrics. All the azlactones synthesised are water insoluble thus preventing their application to wool. A substrate amenable to dyeing from non aqueous media is polyester and hence a range of dyes were applied to this fibre. An application range of 0.05 - 0.5 % OWF gave different colour depths. There was no difference to the absorption maxima in the solid state from that in solution. As most of the dyes were fluorescent in solution it was surmised that the same effect would be observed from the solid state. This was the case and Table 5.11 compares the emission characteristics. It is interesting to note the appearance of structureless fluorescence bands from dyes **12** and **22** in the solid state. In fact, the peak from **12** tails off into the wavelength region between 700 - 780 nm. Examples of the solid state fluorescence are given in Figure 5.10. The Stokes shift for **18** decreases by 40 nm in the solid state because the peak 'sharpens'. The other dyes emission data in the solid

state mirror their solution properties.

Dye	In Solution		Solid State	
	emission	Stokes	emission	Stokes
	max /nm	shift /nm	max /nm	shift /nm
12	Not fluorescent		635	110
15	540	75	550	85
17	555	75	550	70
18	635	150	595	110
20	555	75	550	70
22	Not Fluorescent		530	80
35	535	75	545	85
37	530	120	530	120

Table 5.11 : Comparison of emission data for azlactones in solution and in the solid state

The stability to light of the dyes applied to polyester was assessed by their lightfastness results. From Table 5.12 it is clear that the pyrenyl azlactones (15,17,18 and 20) were the most stable and had a high degree of lightfastness. The two imidazolinones (35 and 37) were moderately stable whilst the anthracenyl (22) and substituted phenyl azlactone (12) exhibiting charge transfer readily degraded.

Dye	Lightfastness
12	< 1
15	3 - 4
17	4 - 5
18	4 - 5
20	4 - 5
22	< 1
35	3
37	2 - 3

Table 5.12 : Lightfastness results for the dyes applied to polyester

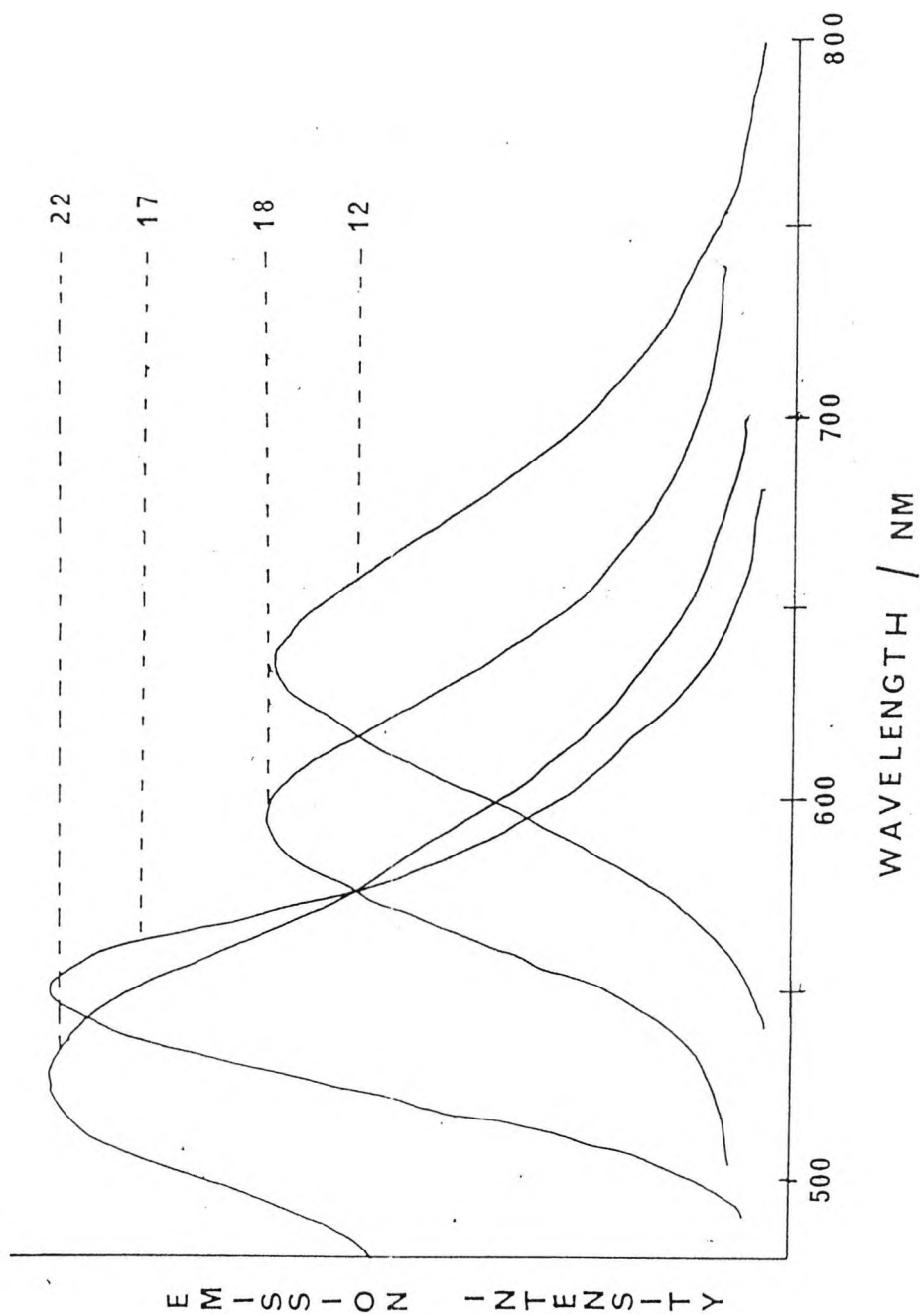


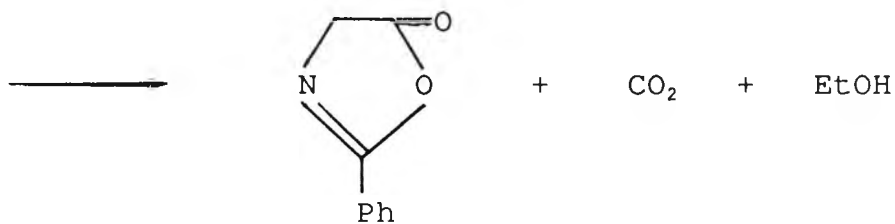
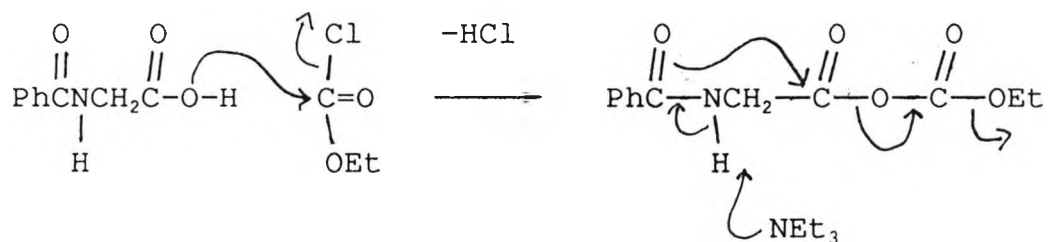
Figure 5.10 Solid sample fluorescence of azlactones 12, 17, 18 and 22 applied to polyester at a concentration of 0.05 % OWF. The excitation wavelengths are at the absorption maxima.

5.3 DISCUSSION

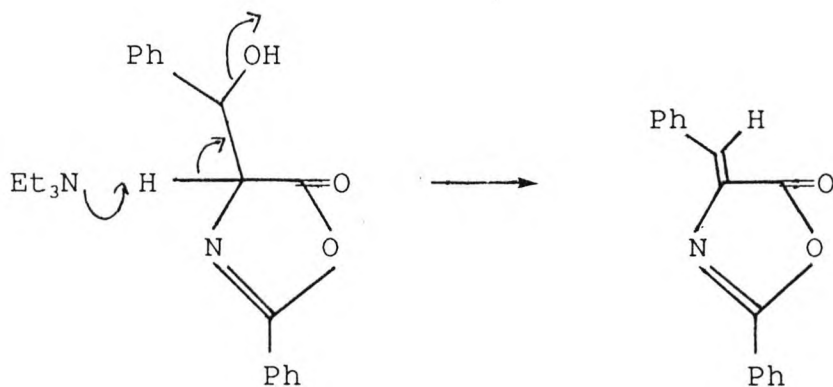
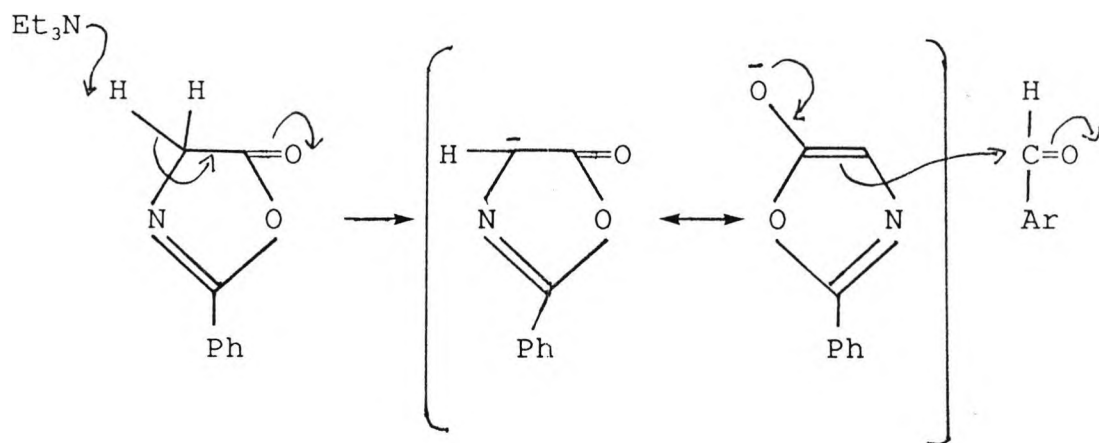
5.3.1 Azlactone Synthesis and Spectra

Two methods were used to synthesise the azlactones under conditions of differing severity. The classical procedure in which acetic anhydride / sodium acetate was the cyclising medium being method A. However, it was unsuitable for sensitive aldehydes and alcohol functionalities. Hence a second milder technique, method B, involving the cyclodehydration of N-arylglycines with ethyl chloroformate and triethylamine in benzene was employed in certain cases. Even though each method utilizes different reagents the reaction mechanisms are identical. This point is illustrated by inspecting the mechanism for method B which is given in Scheme 5.2.

The first stage is conversion of the carboxylic acid to an anhydride ester by reaction with the acyl chloride. This activates the acid to nucleophilic substitution by forming a good leaving group. A base, triethylamine, removes the amidic hydrogen initiating intramolecular cyclisation to the saturated oxazol-5-one, carbon dioxide and ethanol. Formation of carbon dioxide provides a large driving force for the reaction and its removal enables cyclisation to proceed quantitatively. Both methods allow isolation of the saturated azlactone intermediate but purification is much easier when milder conditions are used. The α - hydrogens in the saturated



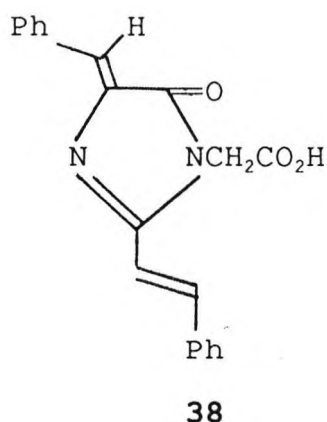
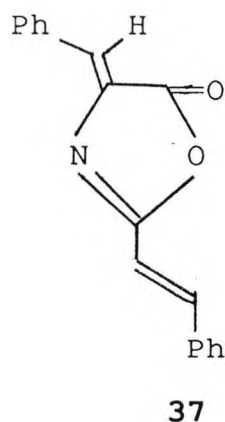
saturated oxazol-5-one



Scheme 5.2 : Mechanism for the formation of azlactones.

ring are acidic and in the presence of base can be removed to form an enolate anion which readily reacts with aromatic aldehydes. A β -hydroxyoxazol-5-one is the principle product which cannot be isolated because it readily dehydrates to the unsaturated azlactone. It has been observed that the direct use of 2-phenyloxazol-5-one in the Erlenmeyer reaction gave much improved yields with aliphatic aldehydes and ketones³¹. The simple oxazol-5-one, **8**, has a main absorption band in the uv region and it is ascribed to a $n-\pi^*$ transition of the carbonyl perturbed by intramolecular charge transfer from the arylmethylene to the polarised carbonyl group on the basis of the extinction coefficient²⁹.

A yellow product was isolated from the synthesis of **8**, however, it has been shown that pure **8** is white²⁰. The coloured contaminants are the styryloxazol-5-one **37**



formed by further condensation of the active methyl group with excess benzaldehyde²⁰ and the styrylimidazolin-5-one **38**²¹. A simple imidazolin-5-one analogue

(R₁ = P-HO-Ph, R₂-ME) predicted as a protein chromophore in the jellyfish 'aequorea' ³² was found to be non-fluorescent in all solvents and conditions ³³.

Extra conjugation results when the methyl is replaced by an aromatic group. The long wavelength absorption for **9** and **10** now tail into the visible. As above, the transition is assigned to a charge transfer perturbation of the carbonyl. This transition must be slightly lower in energy than the possible $\pi-\pi^*$. The lack of fluorescence is thus readily explained.

Adding donor - acceptor groups to the basic chromophore (**9**) moves the main absorption band to longer wavelength by 135 nm. In this case the heterocyclic ring is acting as a conjugating bridge between the donor (diethylamino) and acceptor (nitro) groups (Figure 5.11). The visible

Donor ——— Conjugating bridge ——— Acceptor

Figure 5.11 : Schematic representarion of a simple donor - acceptor chromogen

bands thus produced correspond to a migration of electron density from the diethylamino to the nitro group (Figure 5.12). A more complex scenario may be appearing for the heterocycle than just acting as a conjugating bridge. Because the nitrogen atom exhibits strong electronegativity, it can act as a site for charge

accumulation in the excited state and thus the bridge

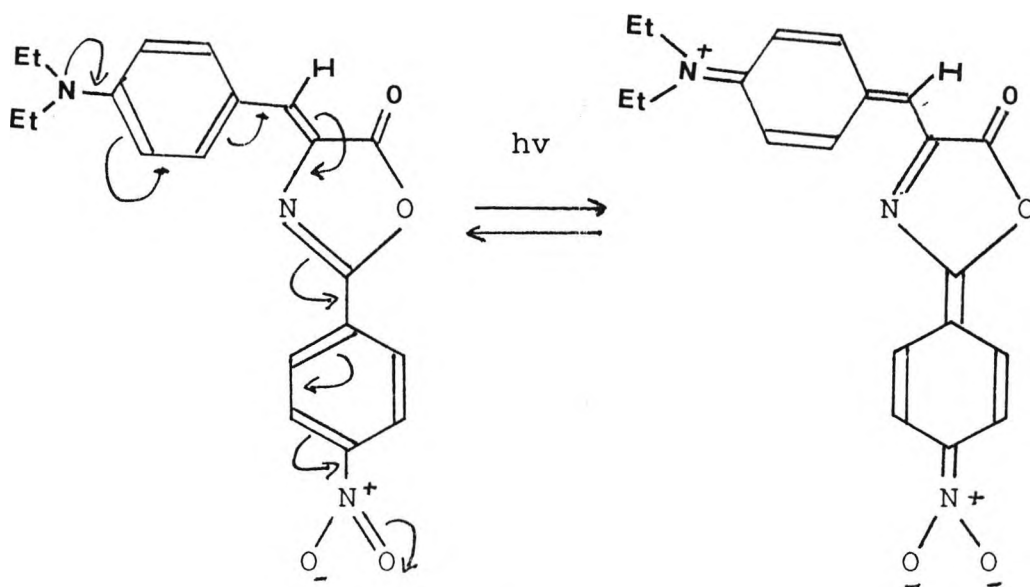


Figure 5.12 : Migration of charge density upon irradiation in donor - acceptor oxazol-5-ones.

its self plays the role of an electron acceptor ³⁴. Alternatively the colour can be explained by reference to simple MO theory. Here the colour determining electron transition is described as a transition between between the highest occupied MO (HOMO) and the lowest unoccupied MO (LUMO). The presence of donor - acceptor groups diminishes the energy difference between the frontier orbitals. Thus as the HOMO - LUMO energy difference decreases, so also does the spectral excitation energy and the absorption band shifts to longer wavelengths (Figure 5.13). The diethylamino group is a very good donating group but to gain a maximum effect the nitrogen lone pair must be orientated to obtain optimum overlap with the aromatic nucleus. As the nitrogen rotates then this overlap diminishes and so the donating

capacity decreases. The julolidine structure has a fused

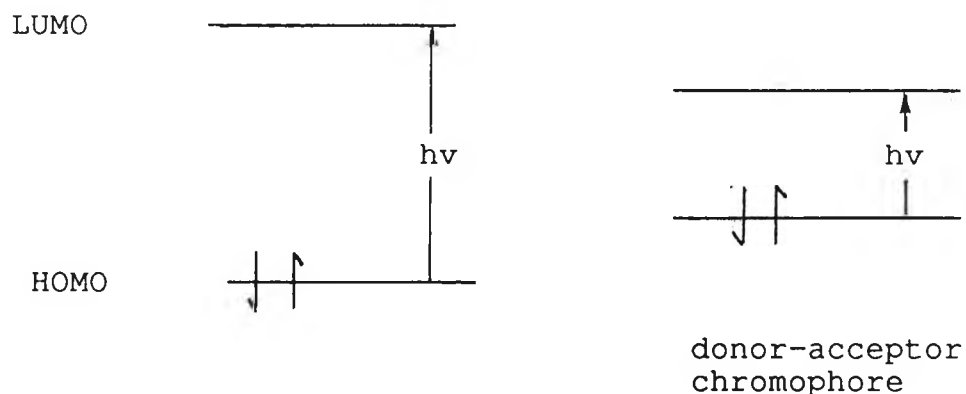


Figure 5.13 : HOMO-LUMO energy separations of donor-acceptor chromophores

ring configuration which prevents rotation and enforces efficient overlap between the nitrogen lone pair and the aromatic electron system (Figure 5.14). This readily explains the further 30 nm bathochromic shift on going

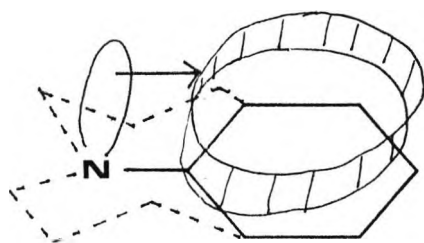


Figure 5.14 : The julolidine fixed configuration gives maximal overlap between the lone pair and aromatic system.

from compound **12** to **13**. Neither **12** or **13** are fluorescent in solution due to back electron transfer providing an efficient non radiative relaxation pathway to the ground state. The singlet - triplet energy difference is very

small (section 1.3.3) in donor acceptor compounds and so intersystem crossing can readily occur. Parker has reported that some intramolecular charge transfer compounds fluoresce weakly at room temperature (quantum yield = 10^{-3}) but have comparatively intense fluorescence and phosphorescence in rigid media at low temperature ³⁵.

Introduction of a pyrene nuclei into the chromophore moves the absorption maxima to longer wavelength than the simple phenylmethylen compound because it effects increased conjugation. These compounds have a large extinction coefficient and the bands are assigned as singlet $\pi-\pi^*$ transitions. There may be some charge migration to the nitrogen atom in the excited state but this is doubtful because attaching strong electron accepting groups to the arene has little effect on the absorption spectra. Possible $n-\pi^*$ states associated with the heterocycle and substituents on the phenyl group will be at higher energy than the $\pi-\pi^*$ state.

The seemingly highly conjugated dye **21** was expected to have a maxima at much longer wavelength. It is best to think of this dye as two different chromophores joined together but are not conjugated and both absorb over a similar wavelength range. For example, azo dyes in the absence of strong donor-acceptor groups exhibit long wavelength absorption from nitrogen $n-\pi^*$ transitions ³⁶. Pyrene is a good electron acceptor but the hydroxyl group is a poor donor and so we can predict that the primary

transition is a $n-\pi^*$. The pyrenyl / phenyl azlactone moiety has a $\pi-\pi^*$ transition and so the dye is only 'weakly' conjugated. A slight bathochromic shift compared to the other pyrenyl compounds may be due to the slight conjugation increase or a charge transfer transition.

The fluorescence emission is from the lowest excited singlet state arising from a $\pi-\pi^*$ transition. Disappearance of pyrenyl fine structure is due to the increased azlactone vibrational and rotational energy levels. The explanation above gives an insight as to the meagre emission for compound **21**. It is believed that competition of the two chromophores for light, plus deactivation by the relatively long lived $n-\pi^*$ state reduces the fluorescence efficiency and Stokes shift. The long wavelength transition for **22** is not readily assigned. The extinction coefficient is too high for a $n-\pi^*$ transition and yet too low for a charge transfer or $\pi-\pi^*$ transition. The λ_{\max} undergoes a slight hypsochromic shift in a less polar solvent and this signifies one of the latter two possibilities. There is no fluorescence signal from either solvent and so the $\pi-\pi^*$ transition is ruled out. The extinction coefficient has a similar value to the azlactone **8**. Therefore the transition is tentatively assigned to a charge transfer perturbation of the polarised carbonyl. Further evidence is supplied from the λ_{\max} in TFA which moves to 484 nm. The nitrogen atom being protonated in this media becomes a

good electron acceptor.

The uv/vis spectra of **23-25** are best described by analogy to their parent compound ferrocene and so a brief incursion into its bonding and spectra is required. The bonding is usually treated by the linear combination of atomic orbitals approximation (LCAO-MO). Each cyclopentadienyl ring can give rise to five MO's which can be combined with the iron atom orbitals and a semi-quantitative energy level diagram drawn (Figure 5.15) ³⁷.

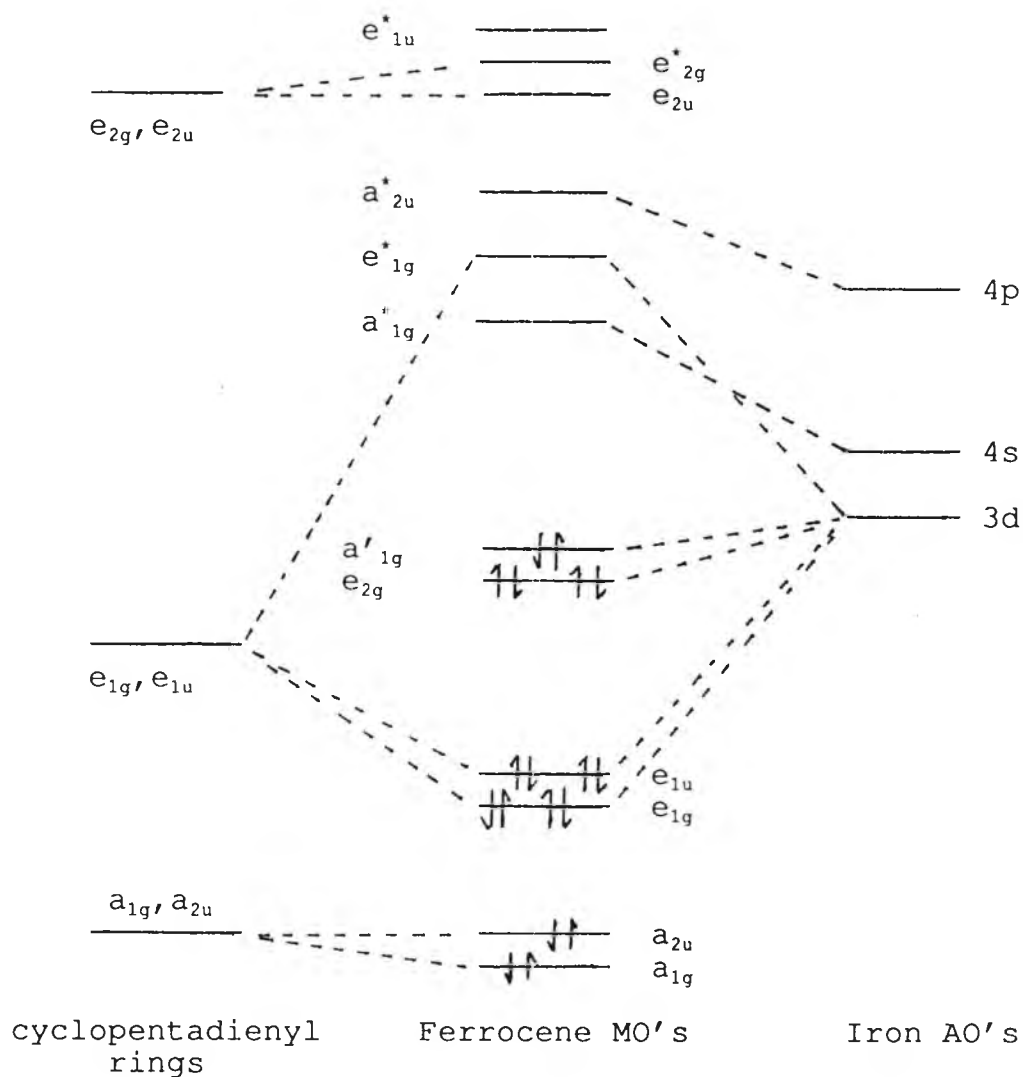


Figure 5.15 ; An approximate MO diagram for ferrocene.

On the left are the ring MOs and on the right are iron valence shell (3d, 4s, 4p) orbitals. In the centre are the MO's formed when the ring orbitals and iron valence orbitals interact. Figure 5.15 indicates that the main bonding is due to the e_{1g} and e_{1u} MO's with a minor contribution from the e_{2g} MO. The a'_{1g} is essentially a non bonding MO of predominantly iron character.

Ferrocene exhibits two low intensity bands in the uv / visible region at 435nm ($E = 80$) and 325 nm ($E = 49$). The two bands have been assigned as d-d interactions arising from spin allowed single electron transitions from $a'_{1g} - e^*_{1g}$ and $e_{2g} - e^*_{1g}$ MO's respectively. An intense peak at 200 nm ($E = 51,000$) was assigned as a Ligand - Metal charge transfer band arising from a $e_{1u} - e^*_{1g}$ single electron transition ³⁸.

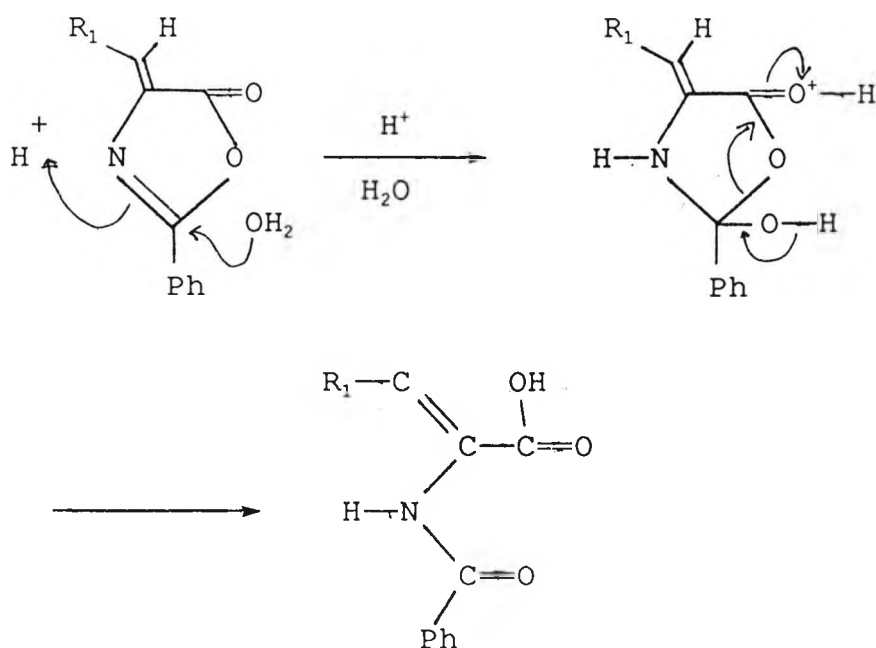
We can now move to **23** whose spectrum is shown in Figure 5.4 and use the above description to aid interpretation. The low intensity band at 545 nm ($E = 2850$) can be argued as a d-d transition even though the extinction coefficient is higher than expected. As the cyclopentadienyl ring conjugation increases then electron density around the iron decreases and so the MO energies are perturbed. Overall the MO order will remain unchanged but the $a'_{1g} - e^*_{1g}$ transition will be lowered in energy and thus an increase in λ_{max} found. When the energy levels become more compatible it can be expected that the ring orbitals and metal d orbitals will undergo greater mixing and a larger than usual extinction

coefficient is observed ³⁹. A second interpretation ascribes the long wavelength band as a d-d, or n- π^* transition which has been perturbed by a charge transfer from the ferrocenylmethylene to the polarised carbonyl. Evidence for this process is the slight hypsochromic shift on changing from a polar to non polar solvent. Furthermore a large red shift is observed when the arene at C-2 (compound 24) contains a strong electron acceptor. In this latter example, the visible band would correspond to migration of electron density from the ferrocenyl a'_{1g} molecular orbital to the nitro group.

A second band at 372 nm ($E = 15000$) was not credited to the d-d transition because of its large E value and a n- π^* interaction is ruled out for similar reasons. This band is postulated to arise from a π - π^* transition associated with the conjugated aromatic system. The intense uv band at 270 nm ($E = 31,700$) is designated a ligand - metal charge transfer transition analogous to ferrocene. These assignments are applicable to compounds **24** and **25**.

5.3.2 Reaction With Nucleophiles

The hydrolysis of azlactones under acid catalysis has been shown to occur at the C=N bond (Scheme 5.3) ⁴⁰. Under basic conditions the mechanism has not been investigated and attack could occur at either the C=N or C=O linkages.



Scheme 5.3 : Mechanism for the acid catalysed hydrolysis of azlactones.

The anthracenyl unsaturated acid, **27**, is weakly fluorescent and it is proposed that this arises from a singlet $\pi-\pi^*$ transition. Two carbonyl groups conjugated to the chromophore effect efficient intersystem crossing to the triplet state which accounts for the weak emission signal. The absorption peak at 365 nm of the pyrenyl compound **28** is assigned to a $\pi-\pi^*$ transition and excitation into this band gives an emission signal at 450 nm. Absorption bands which exhibit long wavelength 'tails' of low intensity can indicate the presence of impurities. The excitation spectra confirm that there are two distinct species. Therefore the tail is credited to a small amount of residual starting azlactone.

The adduct **29** formed in equation 7 arises from initial attack at the C=O centre by a thiophenol anion to give an α - β unsaturated thiolester (Figure 5.16). A second anion then adds to the activated double bond in a 1-4 fashion. The non isolatable enol tautomerises instantaneously to the final product. The spectroscopic properties of this molecule are readily identified with the isolated anthracenyl moiety.

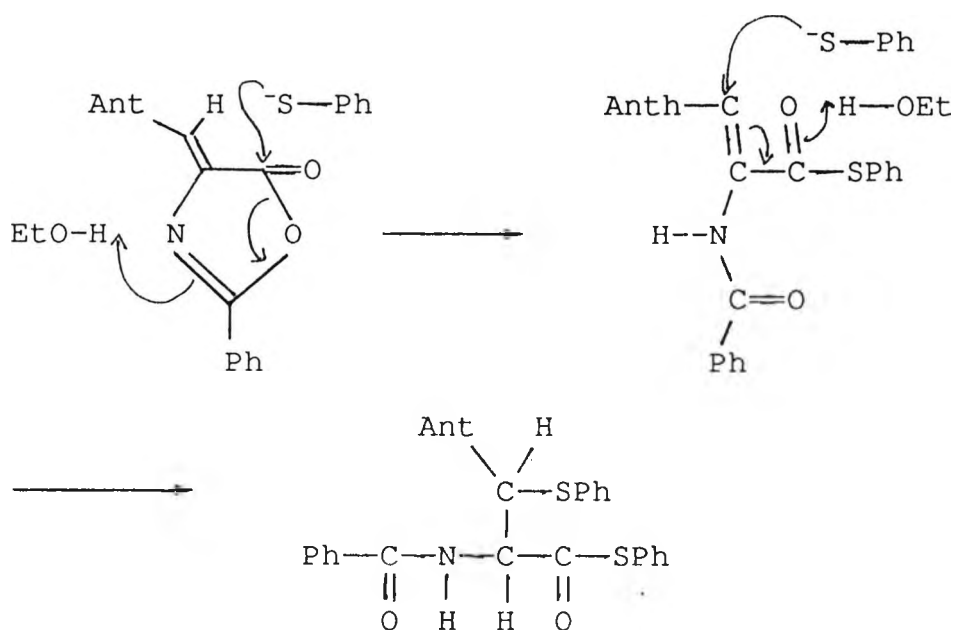
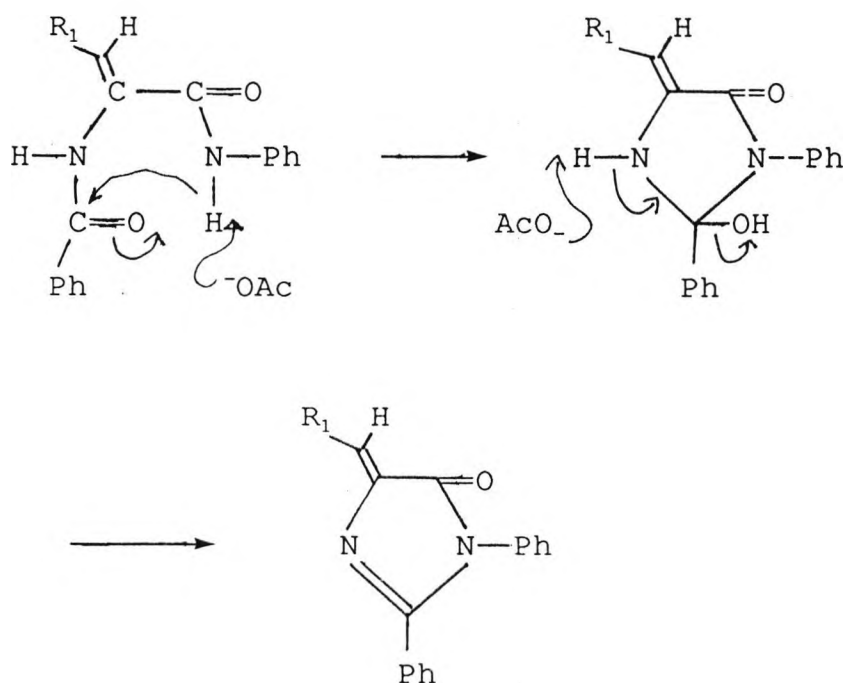


Figure 5.16 : Stepwise addition of thiophenol anion to 22.

The ring opened amide (**30**) has similar absorption characteristics to the acid and correspondingly a π - π^* transition describes the λ_{max} . Its emission signal is also thought to arise from the singlet (π, π^*) state. The increased fluorescence yield is due to the amide

promoting intersystem crossing less efficiently than the carboxylic acid function.

Formation of the imidazolin-5-ones is depicted in Scheme 5.4. The first step is nucleophilic attack by the amine on the C=O to give an amide. An acetate anion then removes the amidic hydrogen which instigates cyclisation. A saturated imidazolin-5-one is the cyclic intermediate which was not isolated because it undergoes spontaneous



Scheme 5.4 : Formation of imidazolin-5-ones. R¹=Py or Anth.

base catalysed dehydration to give the final product. Transformation to the amide has negligible effect on the low energy visible absorption properties because there is little change to the chromophore. Hence the electronic transitions and excited states are similar to the parent

azlactones which were discussed above. The new band at 370 nm has been assigned as charge transfer from the aromatic ring to the amidic carbonyl ²⁹.

In the synthesis of styrylimidazolin-5-ones (eq 11) the azlactone initially reacts with the amine as described above to furnish an imidazolin-5-one. The active methyl group then undergoes base catalysed condensation with the aromatic aldehyde. A non isolatable 6-hydroxyimidazol-5-one is the proposed intermediate which readily dehydrates to the styryl compound.

Compounds **33**, **35**, and **36** are designated to have a $\pi-\pi^*$ transition responsible for the long wavelength absorption. Subsequently, fluorescence is observed from this state. Parallel to **12**, a charge transfer absorption is credited to the maximal absorption band of **34**. It is unclear why two compounds (**35**, **36**) have plateau shaped emission spectra.

5.3.3 Application of Azlactones

5.3.3.1 Labelling of Proteins with Azlactones

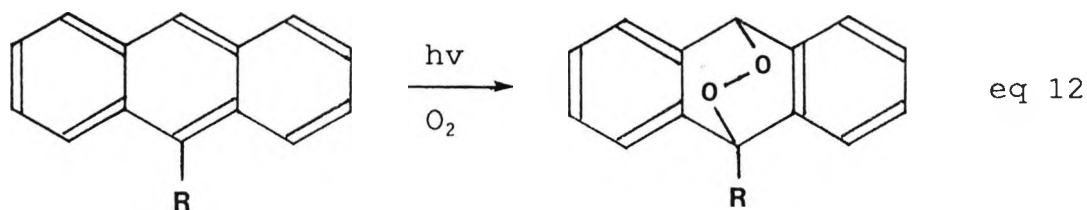
A maxima at 480 nm clearly shows that the some of the azlactone chromophore remains intact and is probably bonded to the antibody through a thiourea linkage. The peak at 360 nm corresponds to a ring opened product.

A major drawback of this scheme is the protein-thiourea-dye linkage dissociation into an isothiocyanate and amine. For this reaction to occur in solution requires catalysis by acids ⁴⁴. The dye can also react with an α -amino group and cyclise to a thiohydantoin and the photochemistry of this type of species should be considered. Two pyrene moieties bound to the protein may be in close proximity and so interact to form an excimer whose fluorescence maxima is at longer wavelength than the dye.

5.3.3.2 Dying Polyester with Azlactone and Related Compounds

The appearance of fluorescence from **12** in the solid state is because it has increased rigidity. This loss of rotation throughout the molecule maximises orbital overlap and makes charge transfer very efficient. In solution the three groups have to be aligned for efficient CT otherwise the transition can be imagined as a series of electron jumps from donor to acceptor. Thus in the solid state there is a direct single pathway for deactivation from S_1 to the ground state and this gives rise to the observed fluorescence signal. A similar argument is used for the anthracenyl compound **22**. The dyes whose solid state characteristics mirror their solution properties are assigned the same transitions and excited states as before.

The good light fastness of compounds **15,17,18**, and **20** is due to the inherent photostability of the pyrene nucleus. The nitro group in **18** seems to have little effect on the photostability of this dye. Little work has been reported on the photochemical reactions of azlactones ⁴¹. The dye, **22** which contains anthracene as the polycyclic aromatic has a very poor lightfastness. Anthracene is known to act as a sensitiser for singlet oxygen formation and this, when formed, adds to further anthracene molecules ⁴² (eq 12). This assertion is readily applied



to the anthracenyl dye and it can be seen that the chromophore is destroyed. The charge transfer dye **12**, is prone to photodegradation. It is probably because the nitro group is photoactive and the resulting photochemistry destroys the chromophore.

5.4 CONCLUSION

It has been shown that a wide variety of azlactones can be synthesised and purified by the simple methodology employed. The modest yields are generally the result of one experiment and have not been optimised.

The azlactones are readily characterised by their

spectroscopic data and elemental analysis. Both absorption and emission characteristics have been shown to depend on the aryl groups at position 2 and 4. The transitions and excited states responsible for the colour forming properties have been assigned. With respect to current trends in colour chemistry the dyes have not been thoroughly investigated. The ease with which the properties can be altered gives wide scope to their possible use in these areas. The inherent chemical reactivity of azlactones mitigates their use as fluorescent labels because of unwanted reactions. Even so, this raises the possibility of their use as probes. For example, the absorption and emission properties of 4-anthracenylmethylene-2-phenyloxazol-5-one changes dramatically and distinctly on its reaction with thiols, amines and water.

By varying the donor - acceptor groups a whole range of colours and hues should be accessible. The most noticeable observation was the appearance of fluorescence in the solid state. This merits an investigation into whether these dyes phosphoresce at room temperature in the same environment. To improve the light stability of simple donor - acceptor dyes it would be advisable to avoid nitro groups and move to more photostable moieties such as cyano residues.

An interesting proposition is to add donor groups to the pyrene nucleus and this should red shift their present

maxima. With judiciously chosen groups it may be possible to get an absorption or an emission signal in the near infra red. Their photochemical stability may qualify them as future laser dyes providing they are fluorescent.

The photostability of the ferrocenyl azlactones has not been investigated but it is expected that the iron will rapidly deactivate any excited state (S_1 or T_1) and thus give excellent lightfastness. Development of this chromophore should give photostable dyes.

There is no extensive change in the absorption or emission properties when the azlactone is changed to an imidazolin-5-one. Essentially the chromophore is unaltered. Chemically, the dye has been stabilised because the new 'amide' bond is less reactive than the original semi-anhydride. If the amine is bifunctional then further manipulation can be performed without touching the chromophore. This opens the area for a new class of labels. Reaction with thiols has not been investigated so their performance as probes for this functionality cannot be evaluated. The photostability of imidazolin-5-ones seems slightly poorer than oxazolones but still appears to be good. This is only from the comparison of two compounds and further work is necessary.

Styrylimidazolin-5-ones are easily prepared, and their

absorption maxima are at longer wavelength than the imidazolin-5-ones. The introduction of an alkene double bond induces fluorescence from these compounds. On the evidence of one compound the photostability is only average but this will probably improve if a pyrenyl group is present.

In conclusion, there is a rich diversity of novel compounds easily synthesised from readily available starting materials waiting to be investigated. Their application and commercial potential remains unrecognised and it can only be a matter of time before this situation is rectified.

5.5 EXPERIMENTAL

The starting materials were obtained from Aldrich and used without further purification. All melting points are uncorrected. ^1H nmr spectra were recorded with a Jeol JLM - MH 100 instrument using TMS and DSS as internal standards. IR spectra were run on a Kratos MS 30 electron impact instrument linked to a Kratos DS 50 data system. Microanalysis was performed on a Carlo Erba model 1106 Elemental Analyser. UV / VIS absorption spectra were obtained on a Philips PU 8700 spectrophotometer. Extinction coefficients were measured in spectroscopic grade solvents and are obtained in units of $\text{l mol}^{-1}\text{cm}^{-1}$. Solid sample uv /vis spectra were recorded

on a Perkin-Elmer Lambda 5 instrument using the Diffuse Reflectance attachment. Fluorescence spectra of deoxygenated solutions made up to an optical density of 0.1 at the excitation wavelength in spectroscopic grade solvents were recorded on a Perkin-Elmer MPF-4 spectrofluorimeter. Solid sample fluorescent spectra were recorded on the same instrument using a special fitment made at the City University. The sample was placed at 50° to the incident beam to avoid scattering.

The labelling experiment was performed by D. Chappell, a research worker at the City University. Application of the dyes to polyester and subsequent testing was carried out at ICI Colours and Fine Chemicals, Manchester.

5.5.1 Synthesis of Starting Compounds

5.5.1.1 Julolidine-9-carboxaldehyde (1)

In a 25 ml round bottomed flask, phosphorous oxychloride (2.54 g, 15 m mol) was added dropwise to dry DMF (2.5 g, 34 m mol). The resulting orange/ brown solution was left at room temperature for 30 mins. Julolidine (1.75 g, 10 m mol) was added as a solid and the mixture heated to 60°C under a stream of dry nitrogen for 15 mins. The green solution was allowed to cool to room temperature. Sodium hydroxide (3.0 g, 75 m mol) and water (20 mls) were

added and the solution heated at 50°C for 15 mins. A blue oily substance was deposited on the flask interior. The aqueous mixture was extracted with dichloromethane (DCM) (3 x 25 ml) to give a green solution. The organic phase was dried over sodium sulphate and filtered. Removal of the solvent under reduced pressure yielded a pale green solid which was recrystallised from Pet Ether (80-100) /acetone. The final product was very pale green crystals. Yield 1.10 g (55 %).

Analysis

Melting point 76 -78°C

IR (KBr disc) 3020 cm⁻¹ (C-H str, aromatic), 2690-2945 cm⁻¹ (C-H str, aliphatic), 1660 cm⁻¹ (C=O str aromatic carbonyl)

¹H nmr (solvent CDCl₃, ref TMS): δ 9.7 (1H, s, aldehydic proton), δ 7.3 (2H, s, aromatic), δ 3.3 (4H, t, J=5Hz, methylene group adjacent aromatic ring), δ 2.8 (4H, t, J=5Hz, CH₂ adjacent N), δ 2.0 (4H, quintet, central CH₂)

uv / vis (solvent EtOH) λ_{max} - 362 nm

Mass Spec m/e (R.I) : 201 (100), 200 (76), 170 (11), 144 (14), 130 (2), 115 (5).

Elemental Analysis: for C₁₃H₁₅NO

Calculated C-77.57, H-7.51, N-6.95

Found C-77.37, H-7.51, N-7.03

5.5.1.2 4-benzyloxyacetamidobenzoylglycine (3)

Benzyloxylchloride (2.3 g,, 14 m mol) in acetone (15 mls) was added dropwise to an ice bath cooled aqueous solution (20 mls) of 4-aminohippuric acid (2.0 g, 10 m mol) and sodium hydroxide (0.4 g, 10 m mol). The solution was allowed to warm up to room temperature and then stir for 1 hour. At 40° C acetone was removed under reduced pressure to produce a white solid. A further portion of water (20 mls) was added and the solid collected by filtration. The product was recrystallized from ethanol to give a white crystalline solid. Yield 2.20 g (67%).

Analysis

IR (KBr disc): 3313 cm^{-1} (N-H str, sec amide), 1726 cm^{-1} (C=O str, sat carboxylic acid), 1688 and 1631 cm^{-1} (C=O str, amide), 1187 - 1312 cm^{-1} (C-O str, carboxylic acid)

Mass spec m/e (R.I) : 328 (5), 284 (2), 146 (7), 137 (9), 119 (11), 91 (100).

Elemental Analysis - for $\text{C}_{18}\text{H}_{16}\text{N}_2\text{O}_5$

Calculated C-62.19 H-4.91 N-8.53

Found C-62.22 H-4.91 N-4.81

5.5.1.3 4-Chloroacetamidobenzoylglycine (4)

Chloroacetyl chloride (2.0 g, 17 m mol) was added in an identical way to the above sample and worked up similarly. The filter cake was recrystallised from EtOH/H₂O (1:4) to give a white powder. Yield 1.05 g (39 %).

Analysis

IR (KBr disc): 3279 and 3327 cm^{-1} (N-H str, sec amide), 2500-2950 cm^{-1} (O-H str, carboxylic acid), 1720 cm^{-1} (C=O str, sat carboxylic acid), 1640 cm^{-1} (C=O str, amides), 1182-1252 cm^{-1} (C-O str, carboxylic acid).

^1H nmr (solvent DMSO d_6 , ref TMS): δ 10.5 (1H, s, N-H between Ph and C=O), δ 8.7 (1H, t, $J=10$ Hz, N-H adjacent CH_2) δ 7.8 (4H, m, AA'BB' system, aromatics), δ 4.3 (2H, s, CH_2 from chloroacetamide), δ 4.0 (2H, d, $J=10$ Hz CH_2 from glycine)

Mass spec m/e (R.I): 272 (2), 270 (7), 226 (27), 225 (19), 198 (33), 196 (100), 121 (51), 120 (52).

Elemental Analysis for $\text{C}_{11}\text{H}_{11}\text{ClN}_2\text{O}_4$

Calculated	C-48.81,	H-4.09,	N-10.34
Found	C-48.79,	H-3.88,	N-10.08

5.5.1.4 4-Isothiocyanatobenzoylglycine (5)

Thiophosgene (1.4 g, 12 m mol) in acetone (5 mls) was added in one portion to 4-aminohippuric acid (2.0 g, 10 m mol) dissolved in 2M hydrochloric acid (20 mls) with constant stirring. The mixture was left to stir in a fume cupboard till no orange thiophosgene remained (about 2 hours). A cream colored solid dropped out of solution. The slurry was gently warmed to remove any remaining acetone. After cooling, the solid was collected by filtration and oven dried at 50°C . Elemental analysis of the crude product showed it was pure. However, if

desired, recrystallisation can be effected from acetone to give cream colored crystals. Yield 2.20 g (93 %).

Analysis

IR (KBr disc) : 3397 cm^{-1} (N-H str, sec amide), 2400-3100 cm^{-1} (O-H str, carboxylic acid), 2115 cm^{-1} (S=C=N str), 1745 cm^{-1} (C=O str, carboxylic acid), 1624 cm^{-1} (C=O str amide), 1200-1300 cm^{-1} (C-O str carboxylic acid).

^1H nmr (solvent $(\text{CD}_3)_2\text{CO}$, ref TMS) : δ 7.95 (2H, d, J=8 Hz, aromatic protons adjacent amide), δ 7.4 (2H, d, J=8 Hz, aromatics), δ 4.1 (2H, s, methylene protons)

Mass spec m/e (R.I) : 236 (12), 192 (28), 162 (100), 134 (33).

Elemental Analysis for $\text{C}_{10}\text{H}_8\text{O}_3\text{S}$

Calculated C-50.48 H-3.41 N-11.85

Found C-50.70 H-3.16 N-11.59

5.5.1.5 4-(2-Hydroxynaphthol-1-aza)-benzoylglycine (6)

Sodium nitrite (1.0 g, 14 m mol) was added slowly with constant stirring between 0-5°C to an ice cold mixture of p-aminohippuric acid (2.0 g, 10 m mol), hydrochloric acid (5 g, 137 m mol) and water (20mls). A brown solution of the diazonium salt formed which was kept below 5°C. The salt solution was added at 0-5°C to an aqueous solution (20 mls) of naphth-2-ol (1.45 g, 10 m mol) and potassium hydroxide (2.5 g, 45 m mol). When the two solutions were mixed a deep red solution formed and after about 2/3 rd

addition a solid precipitated. The red slurry was stirred at 0-5°C for 30 mins, collected by filtration and washed with water. The solid was recrystallized from glacial acetic acid to give red needle shaped crystals. Yield 2.2 g (63 %).

Analysis

IR (KBr disc) : 3424 cm^{-1} (N-H str, sec amide), 2550-3100 cm^{-1} (O-H str, carboxylic acid), 1727 cm^{-1} (C=O str, sat carboxylic acid), 1620 cm^{-1} (C=O str, amide), 1574 cm^{-1} (N=N str, azo), 1000-1300 cm^{-1} (C-O str and O-H bend, several bands).

UV / Vis (solvent CH_3CN) λ_{max} 229, 266, 307, 480 nm

Mass spec m/e (R.I) 350 (6), 349 (30), 331 (2), 275 (7), 171 (13), 143 (55), 120 (12), 115 (31).

Elemental Analysis for $\text{C}_{19}\text{H}_{15}\text{N}_3\text{O}_4$

Calculated C-65.32 H-4.32 N-12.02

Found C-63.92 H-4.46 N-11.71

5.5.1.6 Thiophen-2-oylglycine (7)

Thiophenecarboxyl chloride (1.5 g, 10 m mol) in acetone (10 mls) was added dropwise to a 2:1 aqueous acetone solution of glycine (2.0 g, 26 m mol) and sodium bicarbonate (0.5 g, 6 m mol). The solution was allowed to stir at room temperature for 1 hour. The acetone was removed under reduced pressure at 40°C to leave a colourless aqueous solution. Hydrochloric acid was

added to pH 2 and allowed to stand. After a few minutes white crystals began to form and the mixture was left at 4°C overnight. The crystals were collected by filtration and oven dried at 50°C. Yield 1.57 g (85 %).

Analysis

IR (KBr disc) : 3340 cm^{-1} (N-H str, sec amide), 1744 cm^{-1} (C=O str, carboxylic acid), 1690 cm^{-1} (C=O str, amide), 1164-1306 cm^{-1} (C-O str, carboxylic acid).

^1H nmr (solvent $(\text{CD}_3)_2\text{CO}$, ref TMS) : δ 8.0 (1H, b.s, amidic N-H), δ 7.7 (2H, apparent t, $J=4$ Hz, aromatic protons at C2 and C4) δ 7.15 (1H, t, $J=4$ Hz aromatic proton at C3), δ 4.1 (2H, d, $J=6$ Hz, methylene protons).

Mass spec m/e (R.I) 185 (1), 141 (36), 111 (100), 83 (10),

Elemental Analysis for $\text{C}_6\text{H}_7\text{NO}_3\text{S}$

Calculated C-45.39 H-3.80 N-7.56

Found C-45.45 H-3.68 N-7.52

5.5.2 Azlactone Synthesis

Method A

A mixture of aroylglycine (1.0 m mol), an aromatic aldehyde (1.1 m mol), anhydrous sodium acetate (0.5 m mol) and acetic anhydride (3.0 m mol) were heated gently with stirring until a solution was obtained (20 mins). The solution was heated under reflux for 1 hour. In the

case of ferrocene derivatives the reaction was carried out under dry nitrogen at 100 - 110°C. The solution was allowed to cool and stored at 4°C overnight. Water (20 mls) was added and the solid mass filtered under vacuum. After washing with copious amounts of water a pure product was obtained by recrystallisation from an appropriate solvent (see individual compounds). Generally the reaction can be performed on a larger scale.

Method B

Ethyl chlorocarbonate (11 m mol) was added to a stirred suspension of the aroylglycine (10 m mol) in dry benzene (25 ml / g of the acid) containing triethylamine (12 m mol). The mixture stirred at room temperature until the acid disappears and triethylamine hydrochloride crystals separate (usually about an hour). Triethylamine hydrochloride was filtered under suction and washed twice with dry benzene. An aromatic aldehyde was added to the combined benzene filtrates and the solution heated under reflux for 15 mins. The benzene was removed under reduced pressure and the residue recrystallised from a suitable solvent.

5.5.3 Donor - Acceptor Azlactones

5.5.3.1 4-benzylmethylene-2-methyloxazol-5-one (8)

Synthesised by method A and recrystallised from carbon tetrachloride to give a pale yellow crystalline solid. Yield 60 % . *M p t*

Analysis

IR (KBr disc): 3021 cm^{-1} (C-H str, aromatics), 1802 and 1776 cm^{-1} (C=O str, oxazolone ring), 1654 cm^{-1} (C=N str, oxazolone ring), 1160, 1172, 1239, 1264 cm^{-1} (C-O str, oxazolone ring).

^1H nmr (solvent $(\text{CD}_3)_2\text{CO}$, ref TMS) : δ 8.4 - 8.2 (2H, m, aromatics adjacent alkene), δ 7.7 - 7.5 (3H, m, aromatics), δ 7.2 (1H, s, alkene proton), δ 2.4 (3H, s, methyl group)

Mass spec m/e (R.I) : 187 (27), 159 (13), 118 (8), 117 (100), 116 (10), 90 (16), 89 (19).

Uv / Vis (solvent CH_3CN) λ max 328 nm ($E = 8500$)

Elemental Analysis for $\text{C}_{11}\text{H}_9\text{NO}_3$

Calculated	C-70.57	H-4.84	N-7.48
Found	C-69.94	H-4.63	N-7.28

5.5.3.2 4-benzylmethylene-2-phenyloxazol-5-one (9)

Synthesised by method A and recrystallised from ethanol to give pale yellow needle shaped crystals. Yield 45 % .

Analysis

IR (KBr disc) : 3040 cm^{-1} (C-H str, aromatic), 1794 and 1768 cm^{-1} (C=O str, oxazolone ring), 1650 cm^{-1} (C=N str,

oxazolone ring), 1296, 1164 cm^{-1} (C-O str, oxazolone ring).
 ^1H nmr (solvent CDCl_3 , ref TMS) : δ 8.1 - 7.9 (4H, m, aromatics), δ 7.4 - 7.2 (6H, m, aromatics), δ 7.0 (1H, s, alkene proton).

Mass spec m/e (R.I) : 249 (13), 105 (100), 77 (10)

Uv / Vis (solvent CH_3CN) : λ max 380 nm (E= 17400)

Elemental Analysis for . $\text{C}_{16}\text{H}_{11}\text{NO}_2$

Calculated C-77.09 H-4.44 N-5.61

Found C-76.89 H-4.31 N-5.58

5.5.3.3 4-Benzylmethylene-2-thienyloxazol-5-one (10)

Synthesised by method A and recrystallised from ethanol to give pale yellow crystals. Yield 45 %. M pt 150-152 $^\circ\text{C}$

Analysis

IR (KBr disc) : 3090 cm^{-1} (C-H str, aromatics), 1808 and 1782 cm^{-1} (C=O str, oxazolone ring), 1651 cm^{-1} (C=N str, oxazolone ring), 1185 cm^{-1} (C-O str, oxazolone ring).

^1H nmr (solvent CDCl_3 , ref TMS) : δ 8.1 (2H, m, phenyl protons adjacent alkene), δ 7.9 (1H, d of d, J=6 and 2 Hz, thiophene), δ 7.8 (1H, d of d, J=10 and 2 Hz, thiophene), δ 7.5 (3H, m, phenyls), δ 7.2 (2H, m, thiophene-C3 and alkene).

Mass spec m/e (R.I): 256 (2), 255 (14), 111 (100), 83 (7)

Uv / Vis : solvent CH_3CN max 375 nm (E= 11900).

Fluorescence max : (solvent CH_3CN , Excit -375) - 440 nm

Elemental Analysis for $C_{14}H_9NO_2S$

Calculated	C-65.86	H-3.55	N-5.48
Found	C-65.63	H-3.33	N-5.43

5.5.3.4 4-(4-nitrophenyl)methylene-2-methyloxazol-5-one (11)

Synthesised by method A and recrystallised from ethanol to give a pale yellow powder. Yield 41 %. $m.p.$ $> 200^\circ C$

Analysis

IR (KBr disc) : 3049 cm^{-1} (C-H str, aromatic), 2925 cm^{-1} (C-H str, alkyl), 1820 and 1791 cm^{-1} (C=O str, oxazolone ring), 1661 cm^{-1} (C=N str, oxazolone ring), 1517 and 1344 cm^{-1} (NO_2 str, conjugated), $1269, 1228, 1169\text{ cm}^{-1}$ (C-O str, oxazolone ring),

1H nmr (solvent DMSO d_6 , ref TMS) : δ 8.4 (4H, AB splitting pattern, $J=10$ Hz, aromatics), δ 7.4 (1H, s, alkene), δ 2.5 (3H, s, methyl)

Mass spec m/e (R.I) : 233 (15), 232 (100), 162 (17), 146 (8), 116 (17), 94 (26), 89 (33).

Uv / Vis : (solvent CH_3CN) λ_{max} 345 nm ($E = 9000$)

Elemental Analysis for $C_{11}H_7N_2O_4$

Calculated	C-56.90	H-3.47	N-12.06
Found	C-57.18	H-3.39	N-11.86

5.5.3.5 4-(4-diethylaminophenyl)methylene-2-(4-nitrophenyl) oxazol-5-one (12)

Synthesised by method A and recrystallised from glacial acetic acid to give shining green crystals. Yield 59 %
M pt > 230°C

Analysis

IR (KBr disc) : 2975 cm⁻¹ (C-H str, alkyl), 1783 and 1755 cm⁻¹ (C=O str, oxazolone ring), 1640 cm⁻¹ (C=N str, oxazolone ring), 1514 and 1328 cm⁻¹ (NO₂ str, conjugated), 1292, 1196, 1153, 1128 cm⁻¹ (C-O str, oxazolone ring).

Mass spec m/e (R.I) : 366 (6), 365 (29), 188 (13), 187 (100), 172 (13), 143 (10), 120 (5).

Uv / Vis : (solvent CH₃CN) λ max - 515 nm (E= 30,100)

Fluorescence max : (solvent CH₃CN, Excit λ-515), Not fluorescent

<u>Elemental Analysis</u>	for	C ₁₉ H ₁₉ N ₃ O ₄
Calculated	C-65.74	H-5.24 N-11.50
Found	C-65.62	H-5.12 N-11.45

5.5.3.6 4-(9-Julolidinyl)methylene-2-(4-nitrophenyl) oxazol-5-one (13)

Synthesised by method A and recrystallised from glacial acetic acid to give a green/black powder. Yield 54 % .
M pt > 230°C

Analysis

IR (KBr disc) : 2923 cm⁻¹ (C-H str, alkyl), 1757 cm⁻¹ (C=O

str, oxazolone ring), 1631 cm^{-1} (C=N str, oxazolone ring), 1530 and 1308 cm^{-1} (NO_2 str, conjugated), 1212, 1195, 1186, 1170, 1156 cm^{-1} (C-O str, oxazolone ring).

Mass spec m/e (R.I) : 389 (2), 359 (3), 211 (17), 120 (18).

Uv / Vis : (solvent CH_3CN) λ max 543 nm (E= 25,300).

Fluorescence max : (solvent CH_3CN , Excit λ = 543 nm), Not fluorescent

Elemental Analysis for $\text{C}_{22}\text{H}_{19}\text{N}_3\text{O}_4$

Calculated	C-67.85	H-4.91	N-10.79
Found	C-67.85	H-4.98	N-10.49

5.5.4 Fused Ring Azlactones

5.5.4.1 4-Pyrenylmethylene-2-methyloxazol-5-one (14)

Synthesised by method A and recrystallised from glacial acetic acid to give small brown needle shaped crystals. Yield 40 % . $m p t > 230^\circ\text{C}$

Analysis

IR (KBr disc) : 3233 cm^{-1} (C-H str, aromatic), 2925 cm^{-1} (C-H str, alkyl), 1784 and 1758 cm^{-1} (C=O str, oxazolone ring), 1649 cm^{-1} (C=N str, oxazolone ring), 1257, 1236, 1198, 1169 cm^{-1} (C-O str, oxazolone ring).

^1H nmr (solvent $(\text{CD}_3)_2\text{CO}$, ref TMS) : δ 8.4 - 8.0 (9H, m, pyrenyl), δ 7.2 (1H, s, alkene), δ 3.7 (3H, b s, methyl).

Mass spec m/e (R.I) : 312 (7), 311 (33), 242 (19), 241

(100), 213 (13).

Uv / Vis : (Solvent CH₃CN) λ max = 437 nm (E=17,500)

Fluorescence max : (solvent CH₃CN, Excit λ = 437 nm) 510 nm

Elemental Analysis for C₂₁H₁₄NO₃

Calculated C-81.01 H-4.20 N-4.49

Found C-80.42 H-4.20 N-4.54

5.5.4.2 4-Pyrenylmethylene-2-phenyloxazol-5-one (15)

Synthesised by method A and recrystallised twice from glacial acetic acid to give an orange powder. Yield 35 %

M_{pt} > 230 °C

Analysis

IR (KBr disc) : 3050 cm⁻¹ (C-H str, aromatic), 1784 and 1754 cm⁻¹ (C=O str, oxazolone ring), 1642 cm⁻¹ (C=N str, oxazolone ring), 1235, 1198, 1175 cm⁻¹ (C-O str, oxazolone ring).

Mass spec m/e (R.I) : 373 (16), 230 (42), 201 (26), 105 (100).

Uv / Vis : (solvent CH₃CN) λ max 467 nm (E= 32,300)

(solvent ethyl acetate) λ max 455 nm (E = 32,000)

Fluorescence max : (solvent CH₃CN, Excit λ - 470 nm) 540 nm

Elemental Analysis for C₂₆H₂₆NO₂

Calculated C-83.63 H-4.04 N-3.75

Found C-83.00 H-4.03 N-3.75

5.5.4.3 4-Pyrenylmethylenen-2-thienyloxazol-5-one (16)

Synthesised by method A and recrystallised from glacial acetic acid to give a red/orange powder. Yield 36 % .

Analysis

IR (KBr disc) : 3025 cm^{-1} (C-H str, aromatic), 1772 cm^{-1} (C=O str, oxazolone ring), 1641 cm^{-1} (C=N str, oxazolone ring), 1260, 1233, 1217, 1196 cm^{-1} (C-O str, oxazolone ring).

Mass spec m/e (R.I) : 380 (5), 379 (19), 240 (15), 181 (5), 111 (100).

Uv / Vis : (solvent CH_3CN) λ max 475 nm ($E = 25,200$),
(solvent ethyl acetate) λ max 465 nm ($E = 24,800$)

Fluorescence max : (Solvent CH_3CN , Excit λ 475 nm) 545 nm.

Elemental Analysis for $\text{C}_{27}\text{H}_{11}\text{N}_2\text{O}_2\text{S}$

Calculated C-75.97 H-3.45 N-3.69

Found C-75.50 H-3.51 N-3.85

5.5.4.4 4-Pyrenylmethylene-2-(4-isothiocyanatophenyl) oxazol -5-one (17)

Synthesised by method A and recrystallised from DMF to give an orange/red powder. Yield 17 % . $M_p > 200^\circ\text{C}$

Analysis

IR (KBr disc) : 3025 cm^{-1} (C-H str, aromatic), 2075 cm^{-1} (S=C=N str, isothiocyanate), 1781 cm^{-1} (C=O str, oxazolone ring), 1641 cm^{-1} (C=N str, oxazolone ring),

1291, 1232, 1196, 1177, 1166 cm^{-1} (C-O str, oxazolone ring).

Mass spec m/e (R.I) : 431 (16), 430 (13), 240 (20), 215

(10), 162 (100), 134 (21).

Uv / Vis : (solvent CH₃CN) λ max 480 nm (E= 20,900).

Fluorescence max : (solvent CH₃CN, Excit λ - 480 nm) 555 nm

Elemental Analysis for C₂₇H₁₄N₂O₂S

Calculated C-75.33 H-3.27 N-6.50

Found C-76.09 H-4.05 N-6.97

5.5.4.5 4-Pyrenylmethylene-2-(4-nitrophenyl)oxazol-5-one (18)

Synthesised by method A and recrystallised from DMF to give deep red crystals. Yield 42 % . M pt > 240°C

Analysis

IR (KBr disc) : 1784 cm⁻¹ (C=O str, oxazolone ring), 1642 cm⁻¹ (C=N str, oxazolone ring), 1516 and 1335 cm⁻¹ (NO₂ str, conjugated), 1234, 1196, 1176 cm⁻¹ (C-O str, oxazolone ring).

Mass spec m/e (R.I) : 419 (6), 418 (21), 241 (22), 240 (100), 150 (28), 120 (27), 104 (11), 92 (11), 91 (11).

Uv / Vis : (solvent CH₃CN) λ max - 485 nm (E= 29,000)

Fluorescence max : (solvent CH₃CN, Excit λ = 485 nm) 635 nm

Elemental Analysis for C₂₆H₁₄N₂O₂

Calculated C-74.63 H-3.37 N-6.69

Found C-74.38 H-3.13 N-6.56

5.5.4.6 4-Pyrenylmethylene-2-(4-benzyloxyacetamidophenyl)
oxazol-5-one (19)

Synthesised by method A and recrystallised from glacial acetic acid to give an orange/red powder. Yield 56 %.

M pt > 200 °C

Analysis

IR (KBr disc) : 3310 cm⁻¹ (N-H str, sec amide), 1780 and 1762 cm⁻¹ (C=O str, oxazolone ring), 1685 cm⁻¹ (C=O str, sec amide), 1630 cm⁻¹ (C=N str, oxazolone ring), 1285-1120 cm⁻¹ (C-O str).

Mass spec m/e (R.I) ; 522 (0.2), 415 (11), 414 (36), 241 (7), 240 (23), 147 (12), 146 (100), 118 (7), 108 (11).

Uv / Vis : (solvent CH₃CN) λ max 474 nm (E= 18,900),
(solvent ethyl acetate) λ max 460 nm (E = 18,800).

Fluorescence max : (solvent CH₃CN, Excit λ=475 nm) 535 nm

Elemental Analysis for C₃₄H₂₂N₂O₄

Calculated C-78.14 H-4.24 N-5.36

Found C-78.12 H-4.25 N-5.18

5.5.4.7 4-Pyrenylmethylene-2-(4-Chloroacetamidophenyl)
oxazol-5-one (20)

Synthesised by method A and recrystallised from DMF / glacial acetic acid to give a red powder. Yield 30 % .

M pt > 200 °C

Analysis

IR (KBr disc) : 3334 cm⁻¹ (N-H str, sec amide), 1765 and

1745 cm^{-1} (C=O str, oxazolone ring), 1698 cm^{-1} (C=O str, amide), 1635 cm^{-1} (C=N str, oxazolone ring), 1258, 1234, 1218, 1198, 1175 cm^{-1} (C-O str, oxazolone ring).

Mass spec m/e (R.I) : 466 (10), 464 (27), 240 (12), 198 (32), 196 (100), 121 (21), 120 (20).

Uv / Vis : (solvent CH_3CN) λ max 474 nm (E= 18,900)

Fluorescence max : (solvent CH_3CN , Excit $\lambda = 485$ nm) 540 nm

Elemental Analysis for $\text{C}_{28}\text{H}_{17}\text{ClN}_2\text{O}_3$

Calculated C-72.33 H-3.68 N-6.02

Found C-72.43 H-3.80 N-6.17

5.5.4.8 4-Pyrenylmethylene-2-(4-(naphth-2-ol-1-aza) phenyl) oxazol-5-one (21)

Synthesised by method A and recrystallised from DMF to give a red powder. Yield 15 % . mp $> 220^\circ\text{C}$

Analysis

IR (KBr disc) : 3042 cm^{-1} (C-H str, aromatic), 1782 cm^{-1} (C=O str, oxazolone ring), 1641 cm^{-1} (C=N str, oxazolone ring), 1254, 1232, 1175, 1160, 1148 cm^{-1} (C-O str, oxazolone ring),

Mass spec m/e (R.I) : 544 (2), 543 (5), 388 (3), 275 (13), 240 (2), 156 (2), 120 (13), 92 (2).

Uv / Vis : (solvent DMF) λ max - 535 nm.

Fluorescence max : (solvent DMF, Excit $\lambda = 530$ nm) 570 nm

Elemental Analysis for $C_{36}H_{21}N_3O_3$

Calculated	C-79.54	H-3.89	N-7.73
Found	C-78.27	H-3.93	N-7.73

5.5.4.8 4-Anthracenylmethylene-2-phenyloxazol-5-one (22)

Synthesised by method B and recrystallised from ethanol to give fine orange crystals. Yield 59 %. M pt 241-243 °C

Analysis

IR (KBr disc) : 3049 cm^{-1} (C-H str aromatic), 1796 cm^{-1} (C=O str, oxazolone ring), 1659 cm^{-1} (C=N str, oxazolone ring), 1261, 1186, 1173 cm^{-1} (C-o str, oxazolone ring).

Mass spec m/e (R.I) : 349 (15), 261 (6), 214 (2), 105 (100), 77 (25).

Uv / Vis : (Solvent CH_3CN) λ max 436 nm ($E = 5,000$),
(Ethyl acetate) λ max 405 nm, ($E = 4,500$).

(Trifluoroacetic acid) λ max 484 nm

Fluorescenc max : (Solvent CH_3CN , Excit $\lambda = 436$ nm) No Fluorescence signal.

Elemental Analysis for $C_{24}H_{15}NO_2$

Calculated	C-82.50	H-4.32	N-4.00
Found	C-82.39	H-4.27	N-4.08

5.5.5 Heterocyclic Organometallic Azlactones

5.5.5.1 4-Ferrocenylmethylene-2-phenyloxazol-5-one (23)

Synthesised by method A and recrystallised from pet-ether (40-60) to give a purple powder. Yield 41 %.

Synthesised by method B and purified by allowing the solvent to evaporate from an acetone solution to give shining purple crystals. Yield 65 % .

Analysis

Melting point 189-191°C

IR (KBr disc) : 3020 cm^{-1} (C-H str, aromatics), 1776 and 1760 cm^{-1} (C=O str, oxazolone ring), 1645 cm^{-1} (C=N str, oxazolone ring), 1254, 1227, 1147 cm^{-1} (C-O str, oxazolone ring).

Mass spec m/e (R.I) : 358 (11), 357 (43), 329 (4), 225 (5), 224 (19), 210 (12), 121 (26), 105 (100), 77 (25), 56 (16).

Uv / Vis : (Solvent CH_3CN) λ_{max} - 270 nm (E= 31,700), 372 nm (E= 15,000), 545 nm (E= 2850).

(solvent heptane) λ_{max} - 363 , 537 nm (E = 2800),

Elemental Analysis for $\text{C}_{20}\text{H}_{15}\text{NO}_2\text{Fe}$

Calculated	C-67.25	H-4.23	N-3.92
Found	C-67.12	H-4.49	N-3.65

5.5.5.2 4-Ferrocenylmethylene-2-(4-nitrophenyl)oxazol-5-one (24)

Synthesised by method A and recrystallised from ethanol to give a black powder. Yield 46 % . $m\text{ pt} > 200^\circ\text{C}$

Analysis

IR (KBr disc) : 3107 cm^{-1} (C-H str, aromatics), 1787 and 1767 cm^{-1} (C=O str, oxazolone ring), 1646 cm^{-1} (C=N str, oxazolone ring), 1518 and 1340 cm^{-1} (NO_2 str, conjugated), 1225, 1150 cm^{-1} (C-O str, oxazolone ring).

Mass spec m/e (R.I) : 403 (11), 402 (47), 225 (16), 224 (100), 121 (64), 120 (15), 104 (13), 76 (13).

Uv / Vis : (solvent CH_3CN) λ - 280 nm (E= 32,000), 395 nm (E= 16,000), 600 nm (E= 3,100).

Elemental Analysis for $\text{C}_{20}\text{H}_{14}\text{N}_2\text{O}_4\text{Fe}$

Calculated	C-59.72	H-3.50	N-6.96
Found	C-59.77	H-3.37	N-6.97

5.5.5.3 4-Ferrocenylmethlene-2-(2-thiophenyl)oxazol-5-one (25)

Synthesised by method A and recrystallised twice from ethanol to give a purple/black powder. Yield 16 %

Analysis

IR (KBr disc) : 3094 cm^{-1} (C-H str, aromatics), 1770 cm^{-1} (C=O str, oxazolone ring), 1643 cm^{-1} (C=N str, oxazolone ring), 1252, 1224, 1144 cm^{-1} (C-O str, oxazolone ring).

Mass spec m/e (R.I) : 364 (10), 363 (41), 225 (13), 224 (35), 210 (8), 121 (52), 111 (100).

Uv / Vis : (solvent CH_3CN) λ - 275 nm (E= 30,500), 370 nm (E= 16,100), 555 nm (E= 2,000).

Elemental Analysis for $C_{18}H_{13}NO_2SFe$

Calculated	C-59.52	H-3.60	N-3.85
Found	C-60.52	H-3.97	N-3.53

5.5.6 Hydrolysis of Azlactones

5.5.6.1 2-Benzoylamino-3-Phenylprop-2-eneoic acid (26)

4-Benzylmethylen-2-phenyloxazol-5-one (2.5 g 10 m mol) and potassium hydroxide (0.67 g, 12 m mol) were mixed with 95 % ethanol water (50 mls). The mixture was stirred at room temperature until the reactants dissolved to give a pale yellow solution. The solution was heated under reflux for 15 minutes. After cooling the organic solvent was removed under reduced pressure to leave a thick viscous oil. Water (35 mls) was added to give a pale yellow solution. Hydrochloric acid (50 %) was added and a white solid dropped out of solution which was collected by filtration and recrystallised from ethanol/water 1:1. The product was a white crystalline solid. Yield 2.35 g (88 %).

Analysis

Melting Point 229 - 231°C

IR (KBr disc) : 3296 cm^{-1} (N-H str, sec amide), 3065 cm^{-1} (C-H str, aromatics), 3200-2400 cm^{-1} (O-H str, carboxylic acid), 1689 cm^{-1} (C=O str, conjugated carboxylic acid), 1645 cm^{-1} (C=O str, amide), 1275 (C-O str, carboxylic

acid).

^1H nmr (solvent DMSO d_6 , ref TMS) : δ 9.6 (1H, b s, amide), δ 7.8 (2H, d d, $J=6$ and 2 Hz, aromatic protons adjacent amide), δ 7.6 - 7.1 (9H, m, aromatic and alkene).

Uv / Vis : (solvent CH_3CN) λ max 281 nm

Mass spec m/e (R.I) : 267 (11), 223 (3), 105 (100).

Elemental Analysis for $\text{C}_{16}\text{H}_{13}\text{NO}_3$

Calculated	C-71.82	H-4.91	N-5.28
Found	C-71.89	H-4.90	N-5.42

5.5.6.2 2-Benzoylamino-3-anthracenylprop-2-eneoic acid (27)

The reaction and work up was performed as above. However a small amount of residual material remained after water had been added. This was removed by filtration before acidification. The product was recrystallised from ethanol to give pale yellow crystals. Yield 66 % .
 M_p 225-227 °C

Analysis

IR (KBr disc) : 3309 cm^{-1} (N-H str, sec amide), 3050 cm^{-1} (C-H str, aromatics), 3000-2400 cm^{-1} (O-H str, carboxylic acid), 1693 cm^{-1} (C=O str, unsaturated carboxylic acid), 1642 cm^{-1} (C=O str, amide), 1261 cm^{-1} (C-O str, carboxylic acid).

^1H nmr (solvent $(\text{CD}_3)_2\text{CO}$, ref TMS) : δ 11.0 (1H, b s, amide), δ 9.5 (1H, s, acid proton), δ 8.5 (1H, s, C-10

anthracenyl proton), δ 8.1 - 7.9 (5H, m, aromatics), δ 7.6 - 7.2 (9H, m, aromatic and alkene).

Mass spec m/e (R.I) : 367 (6), 323 (15), 246 (13), 217 (15), 202 (37), 105 (100), 77 (50).

Uv / Vis : (solvent CH₃CN) λ max 386 nm (E= 5,200).

Fluorescence max : (solvent CH₃CN, Excit λ = 386 nm) 465 nm

Elemental Analysis for C₂₄H₁₇NO₃

Calculated C-72.58 H-5.37 N-4.97

Found C-72.52 H-5.40 N-5.00

5.5.6.2 2-Benzoylamino-3-pyrenylprop-2-enoic acid (28)

4-Pyrenylmethylene-2-phenyloxazol-5-one (0.5 g, 1.3 m mol), potassium hydroxide (0.1 g, 1.7 m mol), triethylamine (1ml), water (1ml) and DMF (30 mls) were heated gently under reflux for 1 hour. The solution was cooled and water (50 mls) added and the solid filtered. The filtrate was acidified with hydrochloric acid (50 %) and a yellow solid collected. The product was recrystallised from ethanol/water to give a yellow/orange powder. Yield 160 mgs (30 %). M pt > 250 °c

Analysis

IR (KBr disc) : 3448 cm⁻¹ (N-H str, amide), 3200 - 2450 cm⁻¹ (O-H str, carboxylic acid), 1680 cm⁻¹ (C=O str, unsaturated carboxylic acid), 1640 cm⁻¹ (C=O str, amide), 1279 cm⁻¹ (C-O str, carboxylic acid).

Mass spec m/e (R,I) : 391 (4), 373 (10), 348 (3), 347

(10), 242 (10), 241 (10), 215 (3), 105 (100), 77 (18).

Uv / Vis : (solvent CH₃CN) λ - 236 nm (E= 21,800), 278 nm (E= 10,000), 365 nm (E= 13,500), weak shoulder at 475 nm.

Fluorescence max : (solvent CH₃CN, Excit λ = 365 nm) 450 nm, (solvent CH₃CN, Excit λ = 475nm) 540nm.

Excitation max : (solvent CH₃CN, Emission λ - 540nm) 465nm, (solvent CH₃CN, Emission λ - 445 nm) 380 nm.

Elemental Analysis for C₂₆H₁₇NO₃

Calculated C-79.78 H-4.37 N-3.57

Found C-79.07 H-4.29 N-3.79

5.5.7 Reaction of Azlactones with Nucleophiles

5.5.7.1 3-anthracenyl-3-thiophenol-2-benzoylamino-1-thio phenolpropionate (29)

4-anthracenylmethylene-2-phenyloxazol-5-one (0.5 g 1.4 m mol), thiophenol (1ml), potassium hydroxide (0.11 g 2 m mol) and ethanol were heated gently under reflux for 2 hours. The solution was allowed to cool to room temperature and the yellow crystals collected. A product was obtained after recrystallisation from ethanol. Yield 330 mg (41 %). *m pt* 186 - 189 °C

Analysis

IR (KBr disc) : 3280 cm⁻¹ (N-H str, sec amide), 3051 cm⁻¹ (C-H str, aromatic), 1704 cm⁻¹ (C=O str, thiol ester),

1643 cm^{-1} (C=O str, amide).

^1H nmr (solvent CD_3Cl , ref TMS) : δ 8.2 - 8.1 (3H, m, aromatic), δ 7.8 - 7.7 (2H, m, aromatic), δ 7.4 - 7.0 (15H, m, aromatics), δ 6.8 - 6.5 (4H, m, aromatic), δ 5.3 (1H, d, $J=6$ Hz, β -CH proton), δ 4.4 (1H, d, $J=6$ Hz, α -CH)

Mass spec m/e (R.I) : 351 (4), 203 (6), 191 (100), 189 (10), 110 (21), 105 (14).

Uv / Vis : (solvent CH_3CN) λ - 334, 351, 368, 389 nm

Fluorescence max : (solvent CH_3CN , Excit $\lambda = 390$ nm) 415, 440, shoulder at 465 nm.

Elemental Analysis for $\text{C}_{36}\text{H}_{27}\text{NOS}_2$

Calculated C-75.89 H-4.77 N-2.45

Found C-76.21 H-4.81 N-3.02

5.5.7.2 2-Benzoylamino-3-anthracenylprop-2-ene-1-benzyl amide (30)

4-Anthracenylmethylene-2-phenyloxazol-5-one (0.7 g, 2.0 mmol) benzylamine (0.24 g, 2.2 mmol) and ethanol (25 mls) were heated under reflux for 1 hour. The reaction was followed by TLC (silica plates, eluent DCM) and shown to be virtually complete. The solution was allowed to cool and the solid filtered. This solid was found to be contaminated with a small amount of starting material. About 300 mgs of solid were dissolved in DCM and chromatographed over silica (30 x 2 cm), eluting initially with DCM. The first orange band was discarded.

The eluent was changed to acetone / DCM (1:1) and the next band to elute was collected. The solvent was removed under reduced pressure and the residue recrystallised from chloroform. Yield 255 mgs.

m pt 198 - 199 °C

Analysis

IR (KBr disc) : 3413, 3330 cm^{-1} (N-H str, sec amides), 3055 cm^{-1} (C-H str, aromatic), 2970 cm^{-1} (C-H str, alkyl), 1640 cm^{-1} (C=O str, amides), 1576 cm^{-1} (C=C str, alkene).

^1H nmr (solvent $(\text{CD}_3)_2\text{CO}$, ref TMS) : δ 8.6 (1H, s, anthracenyl C-10), δ 8.3 - 7.9 (6H, m, aromatics), δ 7.6 - 7.3 (13H, m, aromatic + alkene), δ 4.6 (2H, d, $J=6$ Hz, benzyl CH_2).

Uv / Vis : (solvent CH_3CN) λ max - 381 nm ($E=8,100$), shoulder - 400 nm ($E=7,300$).

(solvent ethyl acetate) λ max - 381 nm, shoulder - 400 nm

Fluorescence max : (solvent CH_3CN , Excit $\lambda = 400$ nm) 460 nm.

Elemental Analysis for $\text{C}_{31}\text{H}_{24}\text{N}_2\text{O}_2$

Calculated C-81.56 H-5.30 N-6.14

Found C-80.29 H-5.12 N-6.05

5.5.8 Conversion of Azlactones to Imidazolin-5-ones

5.5.8.1 1,2-diphenyl-4-pyrenylmethyleneimidazolin-5-one (31)

4-pyrenylmethylene-2-phenyloxazol-5-one (0.37 g, 1 mmol), aniline (0.10 g, 1.1 mmol), sodium acetate (0.1 g,

1.2 m mol), and glacial acetic acid (10 mls) were heated under reflux. The reaction can be followed by TLC (silica plates, acetone / hexane 2:8 as eluent). After 3 hours the starting material had been consumed and the solution was allowed to cool to room temperature. A solid was collected by filtration and recrystallised from glacial acetic acid to give an orange powder. Yield 192 mgs, (42 %). *mp* 226-228 °C

Analysis

IR (KBr disc) : 3025 cm^{-1} (C-H str, aromatic), 1710 cm^{-1} (C=O str, amide), 1645 cm^{-1} (C=N str, imidazolinone ring).

Mass spec m/e (R.I) : 448 (34), 373 (10), 240 (15), 215 (18), 180 (43), 105 (100), 93 (7), 91 (3), 77 (74).

Uv / Vis : (solvent CH_3CN) λ - 370 nm (E= 11,900), 447 nm (E= 13,200), 470 nm (E= 12,900).

Fluorescence max : (solvent CH_3CN , Excit λ = 470 nm) 535 nm

Elemental Analysis for $\text{C}_{22}\text{H}_{20}\text{N}_2\text{O}$

Calculated	C-85.69	H-4.49	N-6.24
Found	C-84.03	H-4.58	N-5.89

5.5.8.2 1,2-diphenyl-4-anthracenylmethylenimidazolin-5-one (32)

4-Anthracenylmethylen-2-phenyloxazol-5-one (0.5 g 1.43 m mol), aniline (0.20 g, 2.2 m mol), sodium acetate (0.25 g, 2.8 m mol), and glacial acetic acid were heated under reflux for 4 hours. The solution was allowed to cool to

room temperature and poured into water (50 mls). The solid was collected by filtration and recrystallised from methanol to give pale orange needle shaped crystals.

Yield 340 mgs (55 %). $M_p > 200^\circ C$

Analysis

IR (KBr disc) : 3047 cm^{-1} (C-H str, C-H aromatic), 1726 cm^{-1} (C=O str, imidazolinone ring), 1648 cm^{-1} (C=N str, indazolinone ring).

Uv / Vis : (solvent CH_3CN) λ_{max} - 410 nm ($E = 8,500$), (solvent ethyl acetate) λ_{max} - 380 nm ($E = 7,500$),

Fluorescence max ; (solvent CH_3CN , Excit $\lambda = 450$) ----- Not fluorescent.

Elemental Analysis for $C_{30}H_{20}N_2O$

Calculated	C-84.88	H-4.75	N-6.60
Found	C-83.76	H-4.68	N-6.36

5.5.8.3 4-Phenylmethylene-2-styryl-1-phenylimidzolin-5-one (33)

4-Phenylmethylene-2-methyloxazol-5-one (1.0 g, 5.3 m mol), aniline (0.6 g, 6.5 m mol), benzaldehyde (0.68 g, 6.5 m mol), sodium acetate (0.44 g, 5.0 m mol) and glacial acetic acid were heated under reflux for 4 hours. The reaction mixture was cooled and poured into water. The crude solid was collected by filtration and recrystallised from glacial acetic acid to give yellow/orange crystals. Yield 0.85 g (46 %).

Analysis

IR (KBr disc) : 3050 cm^{-1} (C-H str, aromatic), 1710 cm^{-1} (C=O str, imidazolinone ring), 1622 cm^{-1} (C=N str, imidazolinone ring), 969 cm^{-1} (C-H def, trans alkene).

Mass spec m/e (R.I) : 351 (25), 350 (100), 349 (64), 273 (19), 206 (39), 131 (41), 128 (15), 103 (20), 77 (97).

Uv / Vis : (solvent CH_3CN) λ - 293 nm (E= 17,000), 410 nm (E= 13,500).

Fluorescence max : (solvent CH_3CN , Excit λ = 410 nm) 530 nm

Elemental Analysis for $\text{C}_{24}\text{H}_{18}\text{N}_2\text{O}$

Calculated C-82.26 H-5.17 N-7.99

Found C-81.60 H-5.11 N-8.06

5.5.8.4 4-(4-Nitrophenylmethylene)-2-(4-diethylamino phenyl)styryl-1-(4-nitrophenyl)imidazolin-5-one (34)

4-(4-nitrophenylmethylene)-2-methyloxazol-5-one (232 mgs, 1 m mol), 4-nitroaniline (138 mg, 1 m mol), 4-diethylaminobenzaldehyde (177 mg, 1 m mol), sodium acetate (100 mg, 1.1 m mol) and glacial acetic acid were heated under reflux for 3 hours. After cooling to room temperature the black solid was collected by filtration, washed with water and acetone. The remaining solid was recrystallised from DMF, washed with water, acetone and oven dried at 50°C. A black powder was obtained. Yield 267 mgs (45 %). M pt > 230°C

Analysis

IR (KBr disc) : 2923 cm^{-1} (C-H str, alkyl), 1716 cm^{-1} (C=O str, imidazolinone ring), 1610 cm^{-1} (C=N str, imidazolinone ring), 1524 and 1331 (NO_2 str, conjugated), 939 cm^{-1} (trans alkene).

Mass spec m/e (R.I) : 512 (14), 511 (40), 496 (29), 481 (10), 466 (3), 391 (3), 252 (38), 278 (6), 185 (12), 163 (58), 155 (15), 149 (4), 115 (39), 108 (7).

Uv / Vis : (solvent DMF) λ - 296 , 393, 551 nm.

Elemental Analysis for $\text{C}_{26}\text{H}_{24}\text{N}_4\text{O}_3$

Calculated	C-64.92	H-5.04	N-14.02
Found	C-64.46	H-4.76	N-13.58

5.5.8.5 4-Phenylmethylen-2-styrylpyrene-1-phenyl imidazolin -5-one (35)

4-Phenylmethylen-2-methyloxazol-5-one (1.0 g, 5.3 m mol), pyrenecarboxaldehyde (1.23 g, 5.3 m mol), sodium acetate (0.01 g, 0.1 m mol), aniline (0.60 g, 6.4 m mol), and glacial acetic acid (50 mls) were heated under reflux for 3 hours. The reaction was shown by TLC (silica plates, hexane/acetone 8:2) to be virtually complete. The solution was cooled and the solid filtered, washed with water then acetone. The filter cake was recrystallised from DMSO to give a purple powder. Yield 0.78 g (31 %). M pt $> 200^\circ\text{C}$

Analysis

IR (KBr disc) : 3098 cm^{-1} (C-H str, aromatic), 1710 cm^{-1} (C=O str, imidazolinone ring), 1613 cm^{-1} (C=N str, imidazolinone ring), 942 cm^{-1} (trans alkene).

Mass spec m/e (R,I) : 475 (9), 474 (21), 397 (4), 94 (100), 78 (52), 77 (13).

Uv / Vis : (solvent CH_3CN) λ - 386 nm (E= 11,800), 500 nm (E=19,600).

Fluorescence max : (solvent CH_3CN , Excit λ - 500 nm) 600 nm

Elemental Analysis for $\text{C}_{34}\text{H}_{22}\text{N}_2\text{O}$

Calculated	C-86.07	H-4.64	N-5.91
Found	C-87.06	H-4.33	N-5.53

5.5.8.6 4-Pyrenylmethylene-2-styrylpyrene-1-phenyl imidazolin-5-one (36)

4-Pyrenylmethylene-2-methyloxazol-5-one (38 mg, 0.12 m mol), pyrenecarboxaldehyde anil ⁴³ (39 mg, 0.13 m mol), sodium acetate (18 mg, 0.2 m mol) and glacial acetic acid were heated under reflux for 9 hours. During this time the solution turned from yellow to red. The solution was allowed to cool and the purple solid collected. Recrystallization was effected from glacial acetic acid to give purple crystals. Yield 34 mg, (71 %). $M_p > 200^\circ\text{C}$

Analysis

IR (KBr disc) : 3020 cm^{-1} (C-H str, aromatic), 1700 cm^{-1} (C=O str, imidazolinone ring), 1620 cm^{-1} (C=N str, imidazolinone ring), 961 cm^{-1} (HC=CH def, trans alkene).

Mass spec m/e (R.I) : 599 (32), 598 (63), 597 (17),
482 (8), 428 (27), 330 (13), 255 (21), 239 (20), 215
(57), 94 (100), 78 (48).

Uv / Vis : (solvent CH₃CN) λ - 387 nm (E= 12,000), 500 nm
(E= 20,000).

Fluorescence max : (solvent CH₃CN, Excit λ = 500 nm)
580-620 nm.

<u>Elemental Analysis</u>	for C ₄₄ H ₂₆ N ₂ O		
Calculated	C-88.27	H-4.37	N-4.67
Found	C-87.52	H-4.37	N-4.48

5.6 REFERENCES

1. H.E Carter, Organic Reactions 3, (1946), 198.
2. H.E Carter, P.Handler and D.B Melville, J. Biol.Chem , 129, (1939), 359.
3. A.E Baltazze, Quart Revs, (London), 1955, 9 , 150.
4. R.C Elderfield, Heterocyclic Compounds Vol 5, John Wiley and Sons Ltd, New York, (1951), 336.
5. R.V Filler, Advances in Heterocyclic Chemistry, 4, (1965), 75.
6. R.V Filler and Y. Rao, Advances in Heterocyclic Chemistry, 21, (1977), 175.
7. E. Gross and J. Meienhoffer, The Peptides Vol 5, Academic Press, New York, (1981), p 245.
8. U. Schmidt, J. Hausler, E. Ohler and H.Poisel, Progress in the Chemistry of Organic Natural Products, Vol 37, Springer-Verlag, Wien, (1979), 263.
9. H. Stammer, Chemistry and Biochemistry of Aminoacids Peptides and Proteins Vol 6, John Wright and Sons Lmted, London, (1982), 33-74.
10. A.K Mukerjee and P.Kumar, Heterocycles, 16, (1981), 1995.
11. A.K Mukerjee, Heterocycles, 26, (1987), 1077.
12. British Patent 2,114,588.
13. J. Griffiths, JSDC, 104, (1988), 416-424.
14. F. Jones, Rev. Prog. Colouration, 19, (1989), 20.

15. A. Steitweiser and C. Heathcock, Introduction to Organic Chemistry 2nd edition, Collier MacMillan Publishers, London, (1981), 761.
16. A. Vogel, Practical Organic Chemistry 3rd edition, Vol 2, Longmans Green and Co Ltd, London, (1956), 908 - 910 .
17. P.L Pauson and J.M Osgerby, J. Chem. Soc. (1958), 656.
18. P. Kumar, H.D Mishra and A.K Mukerjee, Synthesis, (1980), 836.
19. A. Rao and R.V Filler, Synthesis (1975), 749.
20. K. Rufenacht, Helv. Chem. Acta. 37 , (1954), 1451.
21. R. Pflieger and J. Pelz, Chem Ber. 90, (1957), 89.
22. P.K Tripathy and A.K Mukerjee Synthesis (1984), 418.
23. U. Schmidt, A. Lieberknecht and J. Wild, Synthesis, (1988), 159.
24. S.L Blystone, Chem Revs, 89, (1989), 1663.
25. H. Brunner, Synthesis, (1988), 645.
26. A. Mustafa, A.H Elsayed Harhash and M. Kamel, J Am Chem Soc, 77, (1955), 3860.
27. A.M Islam, A.M Khalil and I.I El-Gawad, Aust J Chem, 26, (1973), 827.
28. A.M Islam, A.M Khalil and M.L. El-Houseni, Aust J Chem, 26, (1973), 1701.
29. M.Z Badr, H. Ahmed and H. El-Sherief, Bull Chem Soc Japan, 55, (1982), 2267-2270.

30. A.K Mukerjee and P. Kumar, *Can J Chem*, **60**, (1982), 317-322.
31. M. Crawford and W.T Little, *J Chem Soc*, (1959), 729.
32. O. Shimomura, *FEBS Lett*, **104**, (1979), 220.
33. F. McCapra, Z. Razavi and A.P Neary, *J Chem Soc Chem Comm*, (1988), 790.
34. J. Griffiths, *Colour and Constitution of Organic Molecules*, Academic Press, London, (1976), Chapter 6, 140.
35. C.A Parker, *Photoluminescence of Solutions*, Elsevier Publishing Co, England, (1968), p 32.
36. J. Griffiths, *Colour and Constitution of Organic Molecules*, Academic Press, London, (1976), Chapter 5, 117.
37. F.A Cotton and G Wilkinson, *Advanced Inorganic Chemistry* 5th edition, John Wiley and Sons Ltd, New York, (1988), 78-83.
38. Y.S Sohn, D.N Hendrickson and H. B Gray, *J Am Chem Soc*, **93**, (1971), 3603.
39. W.H Morrison, E.Y Ho and D.N Hendrickson, *Inorg Chem*, **14**, (1975), 500.
40. W. Steglich, V Austel, and A Prox, *Angew Chem Int Ed*, **7**, (1968), 726.
41. O. Buchardt, *The Photochemistry of Heterocyclic Compounds*, John Wiley and Sons, New York, (1976), 162
42. J. M Coxon and B. Halton, *Organic Photochemistry*, Cambridge University Press, William Clowes and Sons Ltd, London, (1974), p 158.

43. This compound was synthesised by refluxing pyrenecarboxaldehyde and aniline in EtOH for 30mins, removing the solvent and recrystallising the residue from EtOH. The product gave satisfactory spectroscopic data and elemental analysis.
44. S.Patai, *The Chemistry of Functional Groups, Isocyanates and Isothiocyanates*, John Wiley and Sons, New York, (1977), Part 2 , p 1003 - 1221.

APPENDIX 1

The lightfastness and Yellowness Index results for the FBA - polyamine adducts are listed fully in the following tables.

1. DCDAS + 1,2-Diaminoethane

Light fastness Tests

<u>FBA conc</u>	<u>FBA</u>		<u>FBA + Form</u>		<u>FBA + TUF</u>	
	St3	St5	St3	St5	St3	St5
0	3+	4-5	3+	4-5	3+	5
0.2	3	4-5	3+	4-5	3+	4-5
0.4	3	4-5	3+	4-5	3+	5
0.6	3	4	3+	4	3+	5
0.8	3	4	3+	4	3+	5
1.0	2-3	4	3	4	3	4-5

Yellowness Index

<u>FBA conc</u>	<u>FBA</u>	<u>FBA + Form</u>	<u>FBA +TUF</u>
0	10.8	10.2	10.2
0.2	12.4	11.7	11.6
0.4	12.6	12.2	12.5
0.6	12.2	12.2	11.8
0.8	12.9	12.5	12.4
1.0	14.3	13.4	12.3

DCDAS + 1,3-Diaminoethane

Lightfastness Tests

<u>FBA conc</u>	<u>FBA</u>		<u>FBA + Form</u>		<u>FBA + TUF</u>	
	St3	St5	St3	St5	St3	St5
0	3+	5	3+	5	3+	5
0.2	3	4-5	3	5	3	5
0.4	2-3	4	3	5	3	5
0.6	2-3	4	3	5	3	5
0.8	3	4	2-3	4-5	2-3	4
1.0	2-3	3-4	2-3	4	2-3	4

Yellowness Index

<u>FBA conc</u>	<u>FBA</u>	<u>FBA + Form</u>	<u>FBA + TUF</u>
0	14.7	13.6	13.8
0.2	14.7	12.8	12.1
0.4	10.2	7.7	9.0
0.6	9.2	6.4	6.1
0.8	17.8	14.3	13.7
1.0	18.0	13.2	13.6

DCDAS + Diethylenetriamine

Lightfastness Tests

<u>FBA conc</u>	<u>FBA</u>		<u>FBA + Form</u>		<u>FBA + TUF</u>	
	St3	St5	St3	St5	St3	St5
0	3+	3+	3+	5	3+	5
0.2	2-3	4	2-3	4	3	4-5
0.4	3	4	3	4-5	3	4
0.6	2-3	4	2-3	4	2-3	4
0.8	3	4	3	4	3	4
1.0	2-3	4	3	4	2-3	4

Yellowness Index

<u>FBA conc</u>	<u>FBA</u>	<u>FBA + Form</u>	<u>FBA + TUF</u>
0	11.9	11.1	10.8
0.2	10.3	8.5	8.4
0.4	11.7	10.0	8.7
0.6	11.5	9.2	8.3
0.8	12.0	11.0	8.6
1.0	13.8	10.7	9.8

DCDAS + Triethylenetetramine

Lightfastness Tests

<u>FBA conc</u>	<u>FBA</u>		<u>FBA + Form</u>		<u>FBA + TUF</u>	
	St3	St5	St3	St5	St3	St5
0	3+	4-5	3+	4-5	3+	5
0.2	3	4-5	3+	4-5	3+	5
0.4	2	4-5	2-3	4-5	2-3	4-5
0.6	1-2	4	2-3	3-4	2-3	4
0.8	1	4	2	3-4	2-3	4
1.0	1	3-4	2	3-4	2	3-4

Yellowness Index

<u>FBA conc</u>	<u>FBA</u>	<u>FBA + Form</u>	<u>FBA + TUF</u>
0	11.7	11.1	10.4
0.2	11.2	11.6	11.2
0.4	13.6	11.6	14.0
0.6	17.6	14.4	14.0
0.8	18.8	15.5	15.2
1.0	21.2	18.7	18.3

DCDAS + Tetraethylenepentamine

Lightfastness Tests

<u>FBA conc</u>	<u>FBA</u>		<u>FBA + Form</u>		<u>FBA + TUF</u>	
	St3	St5	St3	St5	St3	St5
0	3+	4-5	3+	5	3+	5
0.2	2-3	4-5	3	4-5	3	4
0.4	2	4	2-3	4	3+	4-5
0.6	1-2	4	2	4	2-3	4
0.8	1	4	2	3-4	2-3	4
1.0	1	3-4	2	3	2-3	3-4

Yellowness Index

<u>FBA conc</u>	<u>FBA</u>	<u>FBA + Form</u>	<u>FBA + TUF</u>
0	11.7	11.1	9.5
0.2	9.6	8.4	7.6
0.4	12.3	10.2	9.2
0.6	15.1	11.8	11.7
0.8	17.5	13.4	13.3
1.0	19.3	15.4	14.3